CONTRACTOR REPORT ARLCD-CR-81059

BLAST CAPACITY EVALUATION OF A STRENGTHENED STEEL BUILDING

FREDERICK E. SOCK
NORVAL DOBBS
W. STEA
KIRIT SHAH
AMMANN & WHITNEY, CONSULTING ENGINEERS
TWO WORLD TRADE CENTER
NEW YORK, NY 10048

PAUL PRICE
PROJECT LEADER
JOSEPH CALTAGIRONE
PROJECT ENGINEER
ARRADCOM

JANUARY 1982

US ARMY ARMAMENT RESEARCH AND DEVELOPMENT COMMAND
LARGE CALIBER
WEAPON SYSTEMS LABORATORY
DOVER, NEW JERSEY

The views, opinions, and/or findings contained in this report are those of the author(s) and should not be construed as an official Department of the Army position, policy or decision, unless so designated by other documentation.

Destroy this report when no longer needed. Do not return to the orginator.

The citation in this report of the names of commercial firms or comercially available products or services does not constitute official endorsement or approval of such commercial firms, products, or services by the U.S. Government.

REPORT DOCUMENTATION PAGE

READ INSTRUCTIONS BEFORE COMPLETING FORM

1. REPORT NUMBER: ARLCD-CR-81059
2. GOVT ACCESSION NO.:
3. RECIPIENT'S CATALOG NUMBER:

4. TITLE (and Subtitle): BLAST CAPACITY EVALUATION OF A STRENGTHENED STEEL BUILDING

5. TYPE OF REPORT & PERIOD COVERED: Final Report

6. PERFORMING ORG. REPORT NUMBER:

7. AUTHOR(s): Frederick E. Sock, Norval Dobbs, W. Stea, Kirit Shah, Ammann & Whitney (cont.)

8. CONTRACT OR GRANT NUMBER(s): DAAA 21-77-C-0134

9. PERFORMING ORGANIZATION NAME AND ADDRESS:
Ammann & Whitney, Consulting Engineers
Two World Trade Center
New York, New York 10048

10. PROGRAM ELEMENT, PROJECT, TASK AREA & WORK UNIT NUMBERS:
MMT-579429
Projects 5774291, 5794291

11. CONTROLLING OFFICE NAME AND ADDRESS:
ARRADCOM, TSD
STINFO Division (DRDAR-TSS)
Dover, NJ 07801

12. REPORT DATE: January 1982

13. NUMBER OF PAGES: 151

14. MONITORING AGENCY NAME & ADDRESS (if different from Controlling Office):
ARRADCOM, LCWSL
Energetic Systems Process Division (DRDAR-LCM-SP)
Dover, NJ 07801

15. SECURITY CLASS. (of this report): Unclassified

15a. DECLASSIFICATION/DOWNGRADING SCHEDULE:

16. DISTRIBUTION STATEMENT (of this Report):
Approved for public release; distribution unlimited.

17. DISTRIBUTION STATEMENT (of the abstract entered in Block 20, if different from Report):

18. SUPPLEMENTARY NOTES:
This project was accomplished as part of the U.S. Army's Manufacturing Methods and Technology Program. The primary objective of this program is to develop, on a timely basis, manufacturing processes, techniques, and equipment for use in production of Army materiel.

19. KEY WORDS (Continue on reverse side if necessary and identify by block number):
Blast overpressures
Strengthened steel building
Pre-engineered building
Personnel safety
Barricated intraline distance
MMT - blast effects
Acceptor structures
Steel structures
Frame structures

20. ABSTRACT (Continue on reverse side if necessary and identify by block number):
A series of dynamic tests were performed on a specially designed strengthened-steel building for use in Army Ammunition Plants. Test results indicated that the building can resist approximately 48.3 kPA (7.0 psi) of blast over-pressures.

Block 7 (cont.)

Paul Price, Project Leader, ARRADCOM
Joseph Caltagirone, Project Engineer, ARRADCOM

SUMMARY

The U.S. Army, under the direction of the Project Manager for Production Base Modernization and Expansion, is currently engaged in a multi-billion dollar program to modernize and expand its ammunition production capability. In support of this program, the Energetic Systems Process Division of the Large Caliber Weapons Systems Laboratory, ARRADCOM, with the assistance of Ammann & Whitney, Consulting Engineers, has, for the past several years, been engaged in a broad base program to improve explosive safety at these facilities. One segment of this program deals with the development of design criteria for explosion-resistant protective structures.

Development of these design criteria has, in the past, been primarily concerned with structures located in the high pressure region close to an explosion. The basic document to evolve from this effort is the tri-service manual, TM 5-1300, "Structures to Resist the Effects of Accidental Explosions (ref. 3). This manual contains comprehensive information on the principles of protective design, the calculation of blast loadings, dynamic analyses, and detailed procedures for designing reinforced concrete protective structures.

It is common practice in the explosives industry for process buildings associated with the same line to be separated by "intraline distances" which are meant to provide a high degree of protection against the propagation of explosions from building to building. Similarly, the minimum distance permitted between an inhabited building, not associated with the line in question, and an explosives location is the "inhabited building distance". These distances are published in the DARCOM Safety Manual (DRCR 385-100) and are based on the cubic root scaling of the explosive weight which defines areas of equal pressure. In all cases, however, the blast overpressures that an acceptor structure would experience in the event of an explosion in the "building next door" would be greater than the overpressures a conventional structure is designed to withstand, and serious injury to personnel within it is likely.

In this regard, explosive tests have been conducted to evaluate the blast capacity of strengthened steel buildings. The results of these tests, which are described below, have been used to verify and refine data contained in the ARRADCOM technical reports pertaining to the design of acceptor structures (refs. 2 and 3).

The specially designed steel building was constructed in accordance with ARRADCOM Drawing No. 132 (see Appendix B). The overall dimensions of the structure were 24.4 m (80 ft) long by 6.1 m (20 ft) wide by 3.7 m (12 ft) high. The building was subdivided into four bays in the longitudinal direction, each of which was approximately 6.1 m (20 ft) wide. The primary structural framework in the transverse direction consisted of three interior rigid frames and an exterior rigid frame at both ends. The column, girts, beams, girders and purlins were wide flanges with a minimum static yield stress of 248,200 kPa (36,000 psi). The walls and roof panels consisted of 18- and 20-gage cold-formed steel panels.

Instrumentation consisted of electronic deflection gages to record the movement of the structure, and pressure gages to measure the blast loads acting on the building as well as the free-field pressures. Photographic coverage, including both still photographs and motion pictures, was also used to document both pre-shot construction and post-shot test results.

A total of seven tests were performed, each utilizing approximately 900 kg (2,000 lb) of nitro-carbo-nitrate as the explosive source. The recorded peak free-field pressure for each of the last five tests was 22.06 kPa (3.20 psi), 24.13 kPa (3.50 psi), 36.61 kPa (5.31 psi), 46.82 kPa (6.79 psi) and 29.03 kPa (4.21 psi). Most of the instruments failed during the first two tests; however, damage incurred by the structure during these tests was minimal. Pressure buildup was recorded within the structure in each test. This buildup was attributed to leakage between seams of siding and roofing.

Minimal damage occurred in Test 3. The overlapping panel joints were opened approximately 3/8 inch halfway between Frames 2 and 3. In some places, the panel was slightly disengaged where it was fastened to the foundation and girts.

More extensive damage was apparent in the next four tests (Tests Nos. 4, 5, 6 and 7). This included buckling of panel siding and roof deck, web crippling of girts and purlins, and failure of bolts at one of the column bases.

Pressure measurements on the front wall of the building were consistent with theory; that is, the blast pressure acting on the front wall varied from approximately 1.2 to 1.6 times the incident pressure at the bottom to about 0.9 to 1.2 times the peak pressure at the top.

Test data provided by the deflection gages was quite extensive and was more than adequate to analyze the test results.

Based upon the overall results, the following observations can be made:

1. The specially designed strengthened steel building can be used as a protective structure.

2. Certain modifications have to be made to the current design procedures presented in References 2 and 3.

TABLE OF CONTENTS

TABLE OF CONTENTS
(continued)

TABLE OF CONTENTS
(continued)

TABLE OF CONTENTS
(concluded)

INTRODUCTION

Background

In the design of steel buildings to withstand the effects of High Explosive (HE) and other types of explosions, standard structural members can be utilized for structures located in pressure ranges of less than 10 psi. However, because of the transient nature and the relatively high intensity of the blast loads, certain procedures and criteria have to be met in order to increase the capacity of the structure to resist the applied loads.

Steel buildings consist of three general structural systems:

1. The walls and roof panels.

2. Supporting members such as girts, purlins, diagonal bracing and other members which can be treated as individual elements, and

3. The main structural frame.

Usually, the capacity of the frame members to resist blast loads greatly surpasses those of the supporting members and thus certain modifications have to be made in designing such structures.

In order to determine those areas where modifications are required and also furnish data for establishing reliable safety design procedures for buildings exposed to blast overpressures, a specially designed strengthened steel building was subjected to challenges provided by detonating charges at various locations around the building. Seven tests were done by the Energetic Systems Process Division of the Large Caliber Weapons Systems Laboratory, ARRADCOM, as part of its overall Safety Engineering Support Program for the Project Manager for Production Base Modernization and Expansion. This report which was prepared with the assistance of Ammann & Whitney, Consulting Engineers, describes and evaluates the results, and presents recommended changes to fully develop the blast capacity of a strengthened steel building. A brief comparison of this strengthened steel building and the pre-engineering building described in Contract Report ARLCD-CR-79004 (ref. 1) is also presented in this report.

Purpose and Objectives

The overall purpose of the test program was to evaluate the usefulness of strengthened steel buildings as protective structures at Army Ammunition Plants and to provide recommended design procedures whereby the full-blast capacity of the structures could be achieved. The objectives of the program and related analyses are summarized below:

1. To evaluate the blast capacity of the steel building as a unit.

2. To dertermine those areas where modifications are required over conventional design procedures for steel buildings.

3. To evaluate the computer programs and design procedures (and criteria) presented in References 2 and 3.

Format and Scope of Report

The following two sections describe the Test Program, including the Test Procedures and Results. These sections are followed by a section which evaluates the results and provide recommended changes for the building tested. The fourth section presents the results of an analytical evaluation of the structure and the fifth section compares the behavior of the test structure (the strengthened steel building) and the pre-engineered building described in Reference 1. Appendix A contains reproductions of a comparison of actual blast loads and theoretical blast loads as computed from Design Manual TM 5-1300, "Structures to Resist the Effects of Accidental Explosions" (ref. 4). The second appendix contains reproductions of the Engineering Drawings used for the tests.

For convenience, all measurements are presented in the SI Units (International System of Units) as well as the present system being used in the United States, where appropriate.

TEST DESCRIPTION

General

A specially designed strengthened steel building was subjected to blast tests at the U.S. Army Dugway Proving Ground (DPG) in Utah during the month of June 1979. A total of seven trials were conducted, subjecting the structure to the detonation of 2,000 pounds of high explosives at various distances from it and recording the resultant dynamic pressure, deflection and status deflection of the structure.

Instrumentation to record the structural response consisted of electronic self-recording deflection and pressure gages. In addition, both still and high-speed motion pictures were taken of each trial..

Description of Test Structure

The strengthened steel building was constructed in accordance with ARRADCOM Drawing Number 132. The overall dimensions of the structure were 24.4 m (80 ft) long by 6.1 m (20 ft) wide by 3.7 m (12 ft) high. The building was subdivided into four bays in the longitudinal direction, each of which was approximately 6.1 m (20 ft) wide. The primary structural framework in the transverse direction consisted of three interior rigid frames and an exterior rigid frame at both ends.

The columns, girts, beams, girders and purlins were wide flanges with a minimum static yield stress of 248,200 kPa (36,000 psi). The walls and roof consisted of 18- and 20-gage cold-formed steel panels having a minimum static yield stress of 227,527 kPa (33,000 psi). Engineering drawings showing the plans, section of test structure and location of explosions are provided in Appendix A.

Instrumentation

Deflection Gages

The test structure was provided with 15 deflection gages which were located as shown in Figures 1 and 2. All of the gages were linear displacement transducers which operated on the principle of change in inductance in the coils of a linear differential transformer with change in position of the core. The deflection gages measured the deflection-time histories of one end frame, the center frame, one longitudinal frame, two

girts, a purlin, and a roof and wall panel. A deflection gage schedule is provided in Table 1. The rigid end frame was provided with three gages. Two of these measured the horizontal deflections of one of the columns and the third measured the vertical deflection at the midspan of the girder. The center frame was instrumented in a similar manner and also provided with a fourth deflection gage to measure the horizontal deflections at a point on the outer column (D4 in fig. 1). In addition, deflection gages were provided to measure the horizontal deflections at the midspan of a lower girt (D11 in fig. 1), an upper girt (D12), and the section of wall panel spanning between upper and lower girts (D13 in fig. 1). The deflection gages used to measure horizontal frame displacements had a 0.25-m (10-in) stroke; vertical deflections were measured with gages having a 0.15-m (6-in) stroke and the horizontal deflections of the girts were measured with gages having a 0.30-m (1-ft) stroke. The deflections of the wall and roof panels were recorded with gages having a 0.10-m (4-in) stroke.

The gages were mounted to steel support frames which were welded to base plates cast into the foundation slab. Figures 3 and 4 show a typical gage mount and details of the gage support frames. The deflection rods (cores) were connected to steel rods (fig. 3) which were attached to the structure. Since the building was subjected to horizontal deflections in only one direction, the steel rods for all horizontal gages were rigidly attached to the structure as shown in Figure 4a. Such a connection could not be used for the vertical deflection gages because the horizontal deflections of the structure would have produced bending in the steel rods as they moved downward, thereby inhibiting the motion of the rod and possibly damaging the rod, the connection of the rod to the structure and the support framework. Therefore, the sliding connection shown in Figure 4b was used for all vertical deflection gages.

Pressure Gages

Pressure gages were used to record the blast loads acting on the exterior surfaces of the building, as well as the blast pressure leakage into the building and the free-field pressures. A total of 20 pressure gages were located as shown on Figures 2 and 5. Nine gages (P4 through P12, fig. 5) were located on the center frame, three on the blastward and leeward walls, and three on the roof. Three gages were located on the sidewall (P13 through P15, fig. 2) and five gages for measuring pressure leakage into the building were located in the interior of the building (P16 through P20). In addition, three gages (P1, P2 and P3, fig. 5) were provided for measuring the free-field

pressures in the vicinity of the building. Two of these gages were located 6.1 m (20 ft) from the side of the building containing the access door, the one gage placed in line with the blastward wall and the other one placed in line with the leeward wall. The third gage was placed 6.1 m (20 ft) from the west end of the building. Figure 6 shows a typical detail of the method utilized to attach a pressure gage to the building.

Photographic Documentation

Motion picture camera coverage of the the test was used to observe the test structure during each detonation and for documentary purposes. Three high-speed cameras were used to photograph the exterior of the building during detonation. Two cameras had a speed of 400 frames per second, while the third camera had a speed of 3,000 frames per second. The positioning of the cameras is illustrated in Figure 7. In addition, three interior cameras, with a speed of 300 frames per second, were utilized. Still photographs were taken to record the pre-test setup in terms of general arrangement, construction details and instrumentation.

Hand Measurements and Observations

Pre- and post-shot measurements were made to determine permanent deflections of all frames, girts, purlins, wall and roof panels. In addition, observations of damage and general structural behavior were noted.

Explosives

The explosives used in this test program were nitrocarbonitrate as the primary charge and Composition C-4 as the booster charge. The combined weight of the primary charge and booster in each test was approximately 900 kg (2,000 lb) with the booster weighing approximately 23 kg (50 lb). The nitrocarbonitrate explosive, consisting of 94.5 percent by weight of ammonium nitrate and 5.5 percent by weight of No. 2 fuel oil, was in the form of small pellets which were shipped to the site in 23-kg (50-lb) bags.

The total explosive charge was held in a cylindrical aluminum container (fig. 8). Each charge was formed by pouring 39 bags of nitrocarbonitrate pellets into a container after which a series of C-4 blocks, each weighing approximately 0.6 kg (1-1/4 lb), were placed on top of the nitrocarbonitrate pellets and arranged to form a cubical shape. The Composition C-4 booster

was primed with two electric detonators which initiated detonation of the entire charge.

Test Set-Up

A total of seven tests were performed. The explosive charge was located in three orientations (fig. 7). In the first four tests, the charge was centered on one long side of the structure. In the fifth and sixth tests, the charge was located in Orientation 2 and in the final test (Test No. 7), the charge was placed on the opposite side of the building. The distances from the charges to the building were calculated to produce progressively higher overpressures on the structure in successive tests. After each detonation, the test structure was inspected for damage. Still photographs were taken to document the damage. Preparation of the test structure for each subsequent test included repairing damaged components to insure the structural integrity of the building, and checking and calibrating the measuring instruments.

TEST RESULTS

General

All dynamic data were recorded on magnetic tape which was processed to develop a graphical representation of the data. A photographic record of the damage incurred in the tests, coupled with the graphic representation of the dynamic data, was used to present the test results.

Structural Damage

Test No. 1

The explosives were placed 283.8 m (931 ft) from the building face (Wall A). No damage to the structure was apparent although a pressure of approximately 6.2 kPa (0.9 psi) was recorded by Gage P4. Most of the measuring instruments failed to function properly during the test.

Test No. 2

The explosives were placed 127.1 m (417 ft) from the building face (Wall A). Due to failure of measuring instruments, all dynamic data were lost. However, except for a crack that appeared at the concrete base around Column A3, no other structural damage was apparent.

Test No. 3

Explosives were placed 62.8 m (206 ft) from the building face (Wall A). Structural damage was apparent after this test. The overlapping panel joints were opened approximately 9.5-mm (3/8-in) half way between Frames 2 and 3. In some places, the panel was slightly disengaged where it was fastened to the foundation and girts (see fig. 9). A panel-to-girt screw and a panel joint screw came out between Frames 2 and 3 at the center girt. Gage D13 recorded a displacement of 45 mm (1.78 in) which corresponded to a rotation of approximately 4^{o}, greater than the reusable criteria of 0.9^{o} for a cold-formed member. The effect of this damage was to relieve the loading on the panel, thereby reducing its deflection. Another structural damage observed was a slight web crippling at the center girt near one of the columns of the center frame.

Test No. 4

The charge was located 49.4 m (162 ft) from the building face (Wall A). More extensive structural damage was apparent in this test and although similar to that in Test 3, the damage was more severe. The blastward wall panels were torn loose from points where they were supported at the foundation and girts, as shown in Figure 10.

Wall-to-roof flashing was detached at the center portion, as shown in Figure 11. The roof panels also buckled under the increased blast loading at points between purlins near the blastward wall (Wall A). Most of the damage to the panels occurred at those places damaged in the previous test.

Test No. 5

The explosive charge was placed 47.2 (155 ft) from the building corner at 45° from the wall lines. Resulting damage in this test was similar to that in the previous tests but somewhat less severe. However, damage was not incurred on one of the sidewalls (Wall 5). The damage to Wall A was slight and limited to reopening of the panel seam at Column 3 (fig. 12). Some web crippling was also apparent in the wall panels in Wall 5 near the lower girt. Finally, the buckling in the roof panels between the first two purlins (observed in the previous test) increased between Frames 3 through 5.

Test No. 6

The explosive was 42.98 m (141 ft) from the corner of the building just as in the previous case. Repairs, as in other tests, were done to the structure before the test. Damage to Wall 5 was more severe than in Test 5. This included web crippling at the foundation joint, and the lower and middle girt for the full width. There was also some web crippling in the upper girt in Wall A.

The panel seam between Frames 2 and 3 was reopened and several foundation-connecting screws were pulled out (fig. 13). In addition, buckling was observed on some of the roof purlins and several roof panel seams opened between Frames 3 and 5. The major structural damage which occurred in Test No. 6 consisted of the failure of some of the foundation bolts. Examination proved that two bolts were properly installed; however, two bolts on the easterly side were improperly installed (cut off essentially at the floor level) and one of these failed (fig. 14).

Test No. 7

The explosive charge was located 42.98 m (141 ft) from the building face (Wall B). The foundation bolts that failed during the previous test were repaired before Test No. 7.

Almost all of the panels in Wall B between Frames 2 and 5 were ripped loose from the lower girt and foundation, and some of the panel seams opened (fig. 15). Web crippling was apparent in all of the girts. Slight damage was observed in the panels between Frames 1 and 2 in Wall B.

Minimum damage was observed in Walls 1, 5 and A. This included missing foundation screws at the panel joints. However, almost all the roof panels were torn loose from the purlins at Wall Edge B (closest to explosion) showing some buckling between the first two purlins from Wall B.

Pressure Measurement

Table 2 summarizes the peak pressures recorded by the various pressure gages. Figures 16 through 18 present several typical free-field pressures versus time measurements. In general, good agreement was obtained between predicted and measured incident overpressures. Figures 19 through 22 contain the pressure-versus-time plots recorded on the blastward wall in several of the tests. In all of the tests, the peak-reflected pressures varied over the height of the blastward walls. The measurements in Table 2 indicate that the peak pressures recorded near the base of the wall (Gage P4) varied from 1.2 to 1.6 times the incident pressure; whereas the peak pressure at the mid-height of the wall (Gage P5) was approximately twice the incident pressure and the peak pressure measured near the top of the wall (Gage P6) ranged from 0.9 to 1.2 times the incident pressure. However, the average of the peak pressures recorded by the three gages (P4, P5 and P6) was approximately 1.7 times the incident pressure in Tests Nos. 3 through 6.

Of the three pressure gages located on the roof of the building (Gages P7, P8 and P9), only two yielded acceptable results. The measurements recorded by Gages P8 and P9 in Tests No. 3 through 7 indicated that the peak pressures on the roof varied from 35 to 98 percent of the peak incident pressures. Typical pressure-versus-time measurements for the leeward wall are provided in Figures 19 through 22. The figures and the measurements tabulated in Table 2 indicate that the peak pressures on the leeward wall were significantly less than the incident pressure, varying from 50 to 75 percent. The pressure

gages on the sidewall yielded peak measurements that varied from 45 to 95 percent of the peak incident pressure in Tests No. 3, 4 and 7. For Tests No. 5 and 6, peak pressures on the sidewall were from 1.4 to 1.6 times the incident pressure.

Pressures within the structure attained peaks of approximately 16 percent of the peak side on overpressure at all pressure levels. The leakage of pressure into the building was believed to be caused by the repeated opening and closing of the panel seams during the tests.

Deflection Measurements

Table 3 summarizes the peak displacements of some of the structural components (center frame, blastward wall girts and panels) of the building. A summary of the maximum deflections recorded by Gages D1 through D20 is provided in Table 4. Typical sidesway deflection-time histories are provided in Figures 19 through 22 for the center frame of the building and in Figures 23 and 24 for the rigid end frame (Column Line 5). In addition, typical deflection-time histories are provided in Figures 25 through 27 for the relative horizontal displacement at the midspan of the blastward wall girts. Figure 28 shows the displacement-time history of a typical wall panel.

The test data provided by the deflection gages was quite extensive and was more than adequate to analyze the results. In general, the horizontal deflection gages gave higher quality deflection records than the vertical deflection gages. Among the horizontal deflection gages, those measuring frame displacements (Gages D1, D2, D4, D5, D6, D8 and D9) gave excellent displacement-versus-time histories for almost one second of response time. The excellent quality of these displacement records is attributed to the low frequency character of the responses measured by these gages and to the fact that these gages recorded absolute displacements.

The remaining horizontal deflection gages (namely, Gages D11 and D12) measured the absolute midspan displacement-time histories of an upper and lower girt. The relative girt displacement at any given time was determined by subtracting the displacement at the end of the girt (where it is attached to a main frame) from the absolute displacement at the midspan of the girt. Each girt monitored was located in an interior bay (between Column Lines 3 and 4) and, therefore, it was assumed that the frames at each end of the member had identical displacement-time histories. Based on this assumption, the horizontal deflections on the blastward column of the center

frame were taken as the girt end displacements and the relative girt displacement-time histories were determined using the measurements recorded by Gages D1, D2, D11 and D12 as follows:

1. Lower girt: Gage D11 displacements minus corresponding displacements from Gage D1.

2. Upper girt: Gage D12 displacements minus corresponding displacements from Gage D2.

In this manner, good quality displacement records such as the ones shown in Figures 25 through 27, were determined. The gages for measuring wall and roof panel deflections (D13 and D15) were mounted to frames which were attached to the members (girts and purlins) supporting the panels. In this manner, a direct measurement of the relative displacements of the panels was achieved.

The vertical deflection gages (D3, D7 and D10) were attached to the underside of the frame girders. The test data provided by Gages D7 and D10 was generally good compared to that provided by the horizontal gages. Gage D3 did not record any meaningful data. This might be attributed to deficiencies in the gage.

EVALUATION OF TEST RESULTS

General

An attempt is made in this section to understand the behavior of the structure as demonstrated by the test results. Special attention will be paid to the behavior of the center frame, rigid end frame, longitudinal frame, blastward wall girts, panels and the roof deck.

Center Frame

The behavior of the main frame subjected to blast loading did not vary significantly from one test to another. It was observed that a significant positive sidesway displacement occurred during the negative phase of the loading on the blastward wall. This also corresponded to the positive phase of the loading on the backwall. The positive displacement was then followed by a significant (almost the same value as the positive sidesway displacement) negative displacement as the loading left the structure. However, the peak sidesway displacement occurred after almost all of the loading was off the structure.

This seemingly unusual behavior can be explained by the phasing of the blast loading as follows: the first positive displacement is a result of the net positive loading on the blastward walls and backwalls. During rebounding of the frame, the negative pressure on the blastward wall and the positive pressure on the backwall are both acting in the same direction and in phase with each other, thus producing another significant negative sidesway displacement. Finally, as the structure rebounds from the positive loading on the rear walls and negative loading on the blastward wall, a peak positive displacement of the structure is obtained. The sequence of events is best demonstrated in Figures 19 through 22.

Rigid End Frame

The behavior of the rigid frame is somewhat similar to that of the center frame. The displacement curves in Figures 23 and 24 show that the first peak positive sidesway displacement occurs during the positive and negative phases of the blast loading on the leeward and blastward walls, respectively. However, unlike the center frame, the peak positive displacement is followed by a significant negative displacement occurring while some loading is still on the structure. Unlike the center frame, the displacements of the rigid frame damp out faster.

Longitudinal Frame

The longitudinal frame subdivided into four bays, had three deflection gages (D8, D9 and D10) positioned to monitor its behavior during the tests. Out of seven trials, only Trials Nos. 5 and 6 produced acceptable results. However, during these tests, Gage D9 was overwhelmed by electronic noise and, as a result, the displacement of the frame could only be measured at the center of the column (6 feet above the top of the foundation elevation). Figures 29 and 30 illustrate the high-frequency nature of vibration of the longitudinal frame which has lower displacements than the center and end frames (because it is more rigid).

Blastward Wall Girts

The girts were wide flange members (W12 x 45) of length 6.1 m (20 ft). The readings recorded by Gages D11 and D12 provide the absolute displacement of the centers of the upper and lower girts in the blastward wall. As indicated in the previous section, to obtain the true or relative displacements of the girts, the effect of the column movements has to be considered.

The ductility ratios and rotations associated with the displacements of the girts are compared to the design criteria listed in Reference 2 as follows: the 63.5-mm (2.5-in) displacement of the upper girt in Test 4 corresponds to a rotation of 1.19^{o} which is between the reusable criteria of 1^{o} and the non-reusable criteria of 2^{o}. The slight web crippling observed in the girt is consistent with this criteria..

The gage readings for the other tests were poor and, as such, no analysis was done for the girts except for Test 4.

Wall Panels and Roof Decking

The panel displacements recorded by Gage D13 already account for the displacements of the girts. The measurements are for a section of the panel spanning between girts [1.22m (4.0 ft)] which is assumed to behave more or less as a fixed supported beam. On the basis of the measured displacement, the panels were very inadequate for the magnitude of blast loading involved in the tests.

A peak panel displacement of approximately 0.193 m (7.6 in) during rebound recorded in Trial 6 corresponds to a rotation of 18^{o} which is much greater than the reusable criteria of 0.9^{o}. The opening of the panel seams and the pull-out of several screws

(connecting the panel to the foundation), thus relieving the load on the panel, are consistent with the criteria.

Like the wall panel, the roof decking material (20-gage Mayna-rib Galbestos) was found to be inadequate for the type of loading involved. Buckling of the panels was evident in almost all the tests performed. This is consistent with the reusable criteria of 0.9^{o} rotation, as calculations showed that a displacement of 47.5 mm (1.87 in) during Trial 7 corresponded to a rotation of 3.6^{o} for a 1.52-m (5-ft) span.

ANALYTICAL EVALUATION OF STRUCTURE

Introduction

Several dynamic analyses of the main frames (center, end and longitudinal) and secondary members (girts, purlins and panels) were performed using single- and multi-degree-of-freedom models to represent the structural systems. The purpose of these analyses was to evaluate the analytical and design procedures recommended in References 2 and 3.

The multi-degree-of-freedom models were analyzed with the DYNFA Computer Program (ref. 3) while numerical integration techniques were used in analyzing the single-degree-of-freedom models. The interactions between the main frames and the secondary members, between the girts and wall panels, and between the purlins and the roof decking were also checked analytically.

There were no analyses for Tests Nos. 1 and 2 since most of the gages failed during these tests. However, from the results obtained, it is apparent that the structure responded elastically in all of the remaining tests (Tests 3 to 7), and except for some slight web crippling in the some of the girts, there were no signs of plastic deformations in the structural members.

Evaluation of Frame Analysis

General

Certain factors that affect the response of the frames were not considered in the procedures given in Reference 3. To better understand the behavior of a rigid frame in a multi-framed building, under blast loading, a series of parametric studies were performed.

The design of blast-resistant structures is based on the minimum specified yield stress of the materials used. Therefore, one of the first factors to be considered in the parametric studies was the yield stress of the materials used in the fabrication of the structure. Tensile tests were performed by Pittsburgh Testing Laboratory of Salt Lake City, Utah.

In general, the yield stress of the materials exceeded the specified minimum of 248,211 kPa (36,000 psi); however, the sample taken for one of the columns had a yield stress of 245,454 kPa (35,600 psi) which was lower than the specified minimum. In calculating the capacities of the different members, the average

of the yield stresses determined by tensile tests of the specimens was used.

The procedures listed in Reference 3 consider only the positive phase of the blast loading on the structure. But as test results showed, significant peak negative pressures were recorded during the tests and these had a direct effect on the sidesway of the frames.

The effect of internal pressure was considered, but no analyses were performed. A spot-check of the measurements recorded by the interior gages showed that the interior pressure was, on the average, 16 percent of the incident pressure and it did not significantly affect the sidesway displacement of the frame.

The interaction between the responses of the secondary members (girts and purlins) and main frames was also considered. The procedures presented in Reference 3 provide for the design of the main frames on the basis of analyses on two basic frame models as shown in Figures 31 and 32. Analyses were performed, using the modified model shown in Figure 33, to determine if the responses of the secondary members would affect the responses of the main frames. The girts and purlins were represented by a series of single-degree-of-freedom models (spring with mass constrained to move in one direction only). These SDOF models were connected to the basic frame at the exact locations where the purlins and girts are attached to the structure. The spring constants and masses for these models were computed using the methods of Reference 5.

Effect of Actual vs. Design Pressure Waveforms

Although the procedures for the design of the blast-resistant structures listed in Reference 3 do not account for the negative phase of the loading, analyses indicated that this phase of the loading had a significant effect on the sidesway response of the frame. Figures 34 through 37 compare the computed sidesway response of the frame with the measurements recorded for Tests 3 through 6.

An excellent correlation of the first positive and negative peak displacements was made for Test 3 as shown in Figure 34. The available data was just enough to determine a 3/4 cycle of the sidesway displacement of the center frame for Test 4 and, again, a good correlation was made. There were significant

differences between the test and analytical results for Tests 5 and 6.

Similar analyses were performed for the rigid end and longitudinal frames. A good correlation of the first cycle of the sidesway displacement was made for Test 5 of the rigid end frame, as shown in Figure 38. However, dynamic analyses for Test 7 did not result in the same correlation as in the previous test (fig. 39). The poor correlation in Test 7 can be attributed to the failure of the wall panels, thus relieving the load on the frame. Again, analyses for the longitudinal frame for Tests 5 and 6 (illustrated in figs. 29 and 30), yielded peak positive displacements that greatly exceeded the test results. Inspection of the DYNFA results indicated that plastic deformations occurred at the beam-column connections of all the frames during all the tests. Such deformations were not apparent on the frames and the differences in the test and analytical results can be attributed to these "pseudo" deformations.

To further compare the actual and design waveforms and also evaluate the impact of the negative phase of the blast loadings, tabulations of the significant response parameters, as computed by DYNFA, are provided in Tables 5 and 6. The results in Table 5 were obtained using the procedures outlined in TM 5-1300 to predict the pressure-time histories, whereas the values of Table 6 were obtained with the actual pressure-time loadings obtained from Tests 3 and 4.

Effect of Interactions Between Responses of Secondary Members and Main Frames

Additional analyses were performed to determine the effect of the responses of the secondary members (girts and purlins) on the behavior of the main frames. Analyses were performed on the center frame for Test 4 and the model used for these analyses is shown in Figure 33. The curves in Figure 35 show that the responses of the secondary members did not significantly alter the first half cycle of the sidesway displacement of the center frame. However, the rebound displacement was altered considerably because less energy was absorbed by the girts and the remaining energy was transferred to the frame, thereby creating a greater elastic response in the rebound phase.

Evaluation of Analyses of Blastward Wall Girts

Analyses were performed to evaluate the responses of the blastward wall girts. A variety of analytical models were

utilized to compute the responses of these members. These included:

1. Single-degree-of-freedom (SDOF) models of the individual members.

2. Combined secondary member/frame interaction model (fig. 33).

3. Combined wall panel/girt interaction model (fig. 40).

These analyses were performed for Test 4 only, using the pressure waveforms recorded during that test. The actual yield strength of the material used to fabricate the girt and panels was also used in the analyses. The spring constant for the single-degree-of-freedom model of the wall panel was computed using the equations provided in Reference 2.

Plots of the results of these analyses are shown in Figure 41 for Test 4. The curves indicate that the SDOF and the combined wall panel/girt models yield responses that compare more favorably with the test results than the combined secondary model/frame model.

Evaluation of Analyses of Roof Purlins

Analyses were performed to evaluate the responses of the roof purlin computed by both single-degree-of-freedom analysis and the secondary member/frame interaction analysis. The yield strength of the material used to fabricate the purlins was taken to be 325,433 kPa (47,200 psi). This value was obtained from the tensile tests performed by the Pittsburgh Testing Laboratory of Salt Lake City, Utah. The full moment of inertia was used in the analyses which were performed for Test 4 only, since one of the two gages measuring the purlin deflection (D3) failed during the other tests.

A comparison of the results of these analyses and test results are shown in Figure 42. The SDOF model predicts a response very similar to the test results. However, the analysis which included the interaction of the secondary member and the frame produced positive and negative displacements that were 22 percent of the actual displacements recorded by Gages D3 and D14. A close inspection of the DYNFA output showed plastic deformations occurring after the first displacement cycle. No plastic deformations were apparent in the purlin after Test 4.

Evaluation of Analyses of Blastward Wall Panel

The blastward wall panel response was evaluated analytically using a single-degree-of-freedom model and a combined panel/girt interaction model. Figure 28 shows that the test results for Test 5 differ significantly with the analytical results. These discrepancies can be attributed to the failure of the panel seam connections; however, further investigation is warranted.

COMPARISON OF THE PRE-ENGINEERED AND THE STRENGTHENED STEEL BUILDINGS

The preceding sections dealt with the tests performed on the strengthened steel building, their description and evaluation, and the results were compared to the design procedures and criteria listed in References 2 and 3. Similar tests were performed on a pre-engineered building and the evaluation of those test results are presented in Reference 1.

To further understand the behavior of the pre-engineered and strengthened steel buildings, and to pinpoint the similarities and differences in their responses to dynamic (blast) loads, the two structures are compared in this section.

The overall dimensions of the structures were identical; namely, 24.4 m (80 ft) long by 6.1 m (20 ft) wide by 3.7 m (12 ft) high. Both structures were subjected to several tests involving the detonation of 900 kg (2,000 lb) of nitrocarbonitrate of different locations around the buildings. The measuring gages were located at the same positions on the structures (except for the interior pressure gages and those gages monitoring the behavior of the longitudinal frames), thus allowing for a comparison of the responses of the two structures to blast loads.

Main Frames

A typical interior rigid frame of the pre-engineered building comprised of two columns and a girder which were fabricated of place stock having a minimum static yield stress of 345,000 kPa (50,000 psi). The center (typical) frame of the strengthened steel building consisted of hot-rolled W-shaped members with a minimum static yield stress of 245,200 kPa (36,000 psi).

The responses of both structures to normal blast waves were very similar; namely, a positive peak displacement followed by a negative displacement, as the wave front travelled from one end of the frame to the other. Both structures showed a significant (maximum) sidesway displacement after all the loading was off the structures. However, at higher pressure levels (peak side-on overpressures of approximately 8.9 kPa or 1.3 psi), some plastic deformations were observed in the columns, girts and panels of the pre-engineered building. No plastic deformations were

observed in the strengthened steel building, although buckling of the wall panels occurred in the latter tests.

The longitudinal frames could not be compared because no pressure gages were positioned to monitor the behavior of the longitudinal frame of the pre-engineered building.

Secondary Members

The blastward girts of the pre-engineered building consisted of Z-shaped members, 6.1 m (20 ft) long and an ultimate flexural resistance of 73,840.0 N (16.6 kips). The outer flanges of these girts were securely fastened to the wall panels, whereas the inner flanges were unbalanced. This resulted in greater deflections of the girts during rebound and, consequently, for peak side-on overpressures as low as 5.1 kPa (0.74 psi), the clip angles connecting the girts to the columns were twisted. As the peak side-on overpressure increased, the girt connection bolts failed, and in those members whose connections survived the blast loads, plastic deformation was apparent. The only damage to the girts of the strengthened steel building was slight web crippling observed after all the tests.

Test results showed that the panels in both structures failed at higher pressure levels. Due to the inadequate connection details at the panel seams, the interior pressure levels were relatively higher in the pre-engineered building than in the steel building. Thus, the effects of these pressures (interior) were more significant in the analyses of the pre-engineered building.

In the evaluation of the effects of the secondary member displacements on the responses of the frames, it was observed that an excellent correlation of the first half cycle of the sidesway responses of both structures was obtained between analysis using the basic frame model and that using the refined model. However, during the rebound phase, analyses showed that the center frame sidesway displacement (in the pre-engineered building) was lower than shown in the test results. The opposite occurred in the case of the strengthened steel building. This is believed to have occurred because a larger amount of energy was absorbed during the plastic deformations of the girts in the pre-engineered building, thus reducing the effect on the rebound of the frame.

Since no gages were furnished to measure the responses of the purlins in the pre-engineered building, no comparison could be made for these secondary elements.

The ductility ratio for the columns and girders of the pre-engineered building approached the non-reusable design criteria of 6 for an incident pressure of 6.89 kPa (1.0 psi) and exceeded it as the pressure increased to 8.62 kPa (1.25 psi). The girders of the strengthened steel building also approached the criteria at 24.13 kPa (3.5-psi) side on overpressure and exceeded the limit as the pressure increased to 28.61 kPa (4.15 psi).

CONCLUSIONS AND RECOMMENDATIONS

Conclusions

On the basis of the test results and analytical evaluations, it was seen that the strengthened steel building survived blast overpressures as high as 48.3 kPa (7.0 psi). However, the wall and roof panels failed at a pressure range of 22.1 kPa (3.2 psi) to 29.0 kPa (4.21 psi). Furthermore, it is concluded that the methods and procedures of References 2 and 3 when used in the design of a strengthened steel building yield fairly accurate estimates of the response of the structure and the sizes of the members.

Recommendations

It is recommended that the methods and procedures of References 2 and 3 be extended for the design of strengthened steel buildings to include the following:

1. The negative phase of blast loading.

2. Increase in the yield strength of the cold-formed panels due to the effects of cold-working.

3. The interaction between the secondary member (girts and purlins) responses and the frame responses.

4. The interactions between the panel responses and the secondary member responses.

It is also recommended that other revisions be made so as to fully develop the full capacity of the structure. These include:

1. Providing bigger washers or other means to prevent the heads of panel screws from pulling through the metal.

2. Strengthening the connection of wall panels at the foundation.

3. Using high-strength bolts and increasing the capacity of anchor bolts to be consistent with the blast capacities of the structure.

REFERENCES

1. STEA, W., et al., "Blast Capacity Evaluation of Pre-Engineered Building", Technical Report prepared by Ammann & Whitney, Consulting Engineers, New York, N.Y., for Picatinny Arsenal, Dover, N.J., 1979.

2. HEALEY, J.J., et al., "Design of Steel Structures to Resist the Effects of HE Explosions", Technical Report 4837, prepared by Ammann & Whitney, Consulting Engineers, New York, N.Y., for Picatinny Arsenal, Dover, N.J., 1975.

3. STEA, W., et al., "Non-Linear Analysis of Frame Structures Subjected to Blast Overpressures", Report ARLCD-CR-77008, U.S. Army Armament Research and Development Command, Dover, N.J., May 1977.

4. Department of the Army, "Structures to Resist the Effects of Accidental Explosions (with Addenda)", Technical Manual TM 5-1300, Washington, D.C., June 1969.

5. BIGGS, J.M., Introduction to Structural Dynamics, McGraw-Hill Book Company, New York, N.Y., 1964.

6. GRANSTROM, S.A., "Loading Characteristics of Air Blasts from Detonating Charges", Report No. 100, Transactions of the Royal Institute of Technology, Stockholm, Sweden, 1956.

Table 1. Deflection gage schedule

Gage No.	Measurement description: Member	Direction	Measurement location: Column line	Height above foundation: m	ft
D1	Column	Horizontal	3-A	1.83	6'-0"
D2	Column	Horizontal	3-A	3.28	10'-9"
D3	Girder	Vertical	3-℄	3.45	11'-4"
D4	Column	Horizontal	3-B	1.83	6'-0"
D5	Column	Horizontal	5-A	1.83	6'-0"
D6	Column	Horizontal	5-A	2.97	9'-9"
D7	Girder	Vertical	5-℄	3.45	11'-4"
D8	Column	Horizontal	A-5	1.83	6'-0"
D9	Column	Horizontal	A-5	3.35	11'-0"
D10	Girder	Vertical	A-4/5	3.84	12'-7"
D11	Girt	Horizontal	A-3/4	2.44	8'-0"
D12	Girt	Horizontal	A-3/4	1.22	4'-0"
D13	Siding	Horizontal	A-3/4	1.83	6'-0"
D14	Purlin	Vertical	3/4-℄	3.84	12'-7"
D15	Roof deck	Vertical	A-4/5	4.23	13'-10.5"

Table 2. Summary of pressure measurements

Gage No.	Location	Test No. 3 (kPa)	Test No. 4 (kPa)	Test No. 5 (kPa)	Test No. 6 (kPa)	Test No. 7 (kPa)
P1	Free-field	22.06	24.13	36.61	46.82	-
P2	Free-field	17.17	17.17	20.06	31.85	28.61
P3	Free-field	16.27	22.89	18.06	20.06	29.03
P4	South wall	46.54	60.32	53.84	43.64	5.72
P5	South wall	59.98	76.11	69.36	82.87	24.47
P6	South wall	-	-	40.75	33.03	5.79
P7	Roof	18.20	13.93	25.02	37.09	27.79
P8	Roof	-	-	14.82	28.13	-
P9	Roof	16.06	23.03	19.44	23.37	37.85
P10	North wall	6.41	8.00	15.72	21.58	85.70
P11	North wall	6.89	31.03	20.20	19.10	108.51
P12	North wall	7.24	9.38	11.51	10.20	79.15
P13	East wall	22.96	24.13	60.74	64.94	23.86
P14	East wall	18.13	25.23	59.02	70.33	24.75
P15	East wall	19.44	25.44	65.02	78.81	31.72
P16	Interior	1.93	2.21	1.52	6.55	5.03
P17	Interior	2.21	2.96	2.83	5.17	2.96
P18	Interior	1.86	1.38	2.48	4.34	5.10
P19	Interior	2.69	4.00	5.58	6.83	2.55
P20	Interior	1.45	1.59	2.76	3.65	2.48

Table 3. Summary of strenghened steel building test results

Test No.	Free field pressure (kPa)	Peak horizontal displacement: Ctr frame (mm)	End frame (mm)	Long. frame (mm)	Girt (mm)*	Panel (mm)	Description of damage
3	22.06	32.77	-	-	51.05 41.91	45.21	Wall A a. Corrugation fillers were dislodged from the floor connections between Frames 2 and 3, and 3 and 4. b. The overlapping panel joints were opened approximately 0.95 cm (3/8 in) half-way between Frames 2 and 3. c. Three foundation mounting screws at the panel joints at Frames 3 and 4, and half-way between Frames 2 and 3 pulled out and the overstrip bent out. d. Slight web crippling was apparent at the center girt near Frame 3. e. A panel-to-girt screw and panel joint screw had come out between Frames 2 and 3 at the center girt.
4	24.13	33.53	-	20.07	75.18 64.77	-	In Wall A, three panels (one at A3, one at A4, and one between Frames 2 and 3) were torn loose from the foundation, and lower and middle girts. Web crippling increased in the wall panels at the lower and center girts. The wall-to-roof flashing was detached at the center section. The roof panels buckled between the two purlins on the A wall side from Frames 1 through 4. The concrete at the 4-inch angle iron foundation connection showed movement at the angle between Columns A3 and A4. Shock effects during Trial 3 caused the blast door to fly open. Therefore, prior to Trials 4 and 5, the blast door was propped shut with a 4 x 4.

* Absolute displacements of girts are listed here. Relative displacements are obtained by subtracting displacement of girt at column from displacement.

Table 3. Summary of strengthened steel building test results (continued)

Test No.	Free field pressure (kPa)	Peak horizontal displacement					Description of damage
		Ctr frame (mm)	End frame (mm)	Long. frame (mm)	Girt (mm)*	Panel (mm)	
5	36.61	37.34	13.21	-	59.44 58.93	167.64	Wall 5 showed web crippling in the wall panels only at the lower girt. Wall A damage was slight and limited to reopening of the panel seam at Column 3, reloosening of the roof flashing at Column 3, and the center of the instrument replacement panel was bulged outward at the base connection. The office sheetrock wall studs separated from the upper plate and the upper portion of the wall shifted toward the open bay area. The office door was open and jammed against the floor. Sheetrock panels were loosened. The buckling in the roof panels between the first two purlins increased between Frames 3, 4 and 5. The grout cracking increased.

* See Note on previous page.

Table 3. Summary of strengthened steel building test results
(continued)

Test No.	Free field pressure (kPa)	Peak horizontal displacement					Description of damage
		Ctr frame (mm)	End frame (mm)	Long. frame (mm)	Girt (mm)*	Panel (mm)	
6	46.82	35.31	18.29	-	64.77 61.21	192.53	Damage to Wall 5 included web crippling at the foundation joint and the lower and middle girts for the full wall width. Web crippling occurred at the upper girt from Wall A to above the door, but not to the right of the door. The panic hardware on the blast door was broken and the door could not be opened. Flashing on the right side of the door was loosened. Wall A showed very little damage. The panel seam between Frames 2 and 3 next to Gage D13 was reopened and several foundation connecting screws pulled out. Wall 1 showed minor web crippling at the girt connecting hat sections. In the roof, buckling was increased between the two northernmost purlins, between Frames 2 and 3. Four roof panel seams opened between Frames 4 and 5. Three panel seams opened between Frames 3 and 4. Column 24A showed three broken foundation bolts. Examination proved that two were properly installed. Of these, the inside bolt ruptured and the other two stretched approximately 0.635 cm (1/4 in). The two bolts on the easterly side were improperly installed (cut off essentially at the floor level) and extended only through the grout.

* See Note on previous page.

Table 3. Summary of strengthened steel building test results
(concluded)

Test No.	Free field pressure (kPa)	Peak horizontal displacement: Ctr frame (mm)	End frame (mm)	Long. frame (mm)	Girt (mm)*	Panel (mm)	Description of damage
7	29.03	53.1	20.32	-	52.07 93.73	45.97	Wall B was ripped loose from the foundation from Frame 2 through 5. All these panels, except the two closest to Frame 5, were ripped loose from the lower girt. Most of the panel seams were intact. The seam two panels east of Column 4 opened and the seam two panels east of Column 3 opened from the foundation to the middle girt. Web crippling was apparent at all girts. The wall panels in Wall B between Frames 1 and 2 showed web crippling but little other damage. Roof flashing was removed between Frames 2 and 4, and loosened between Frames 1 and 2 (Wall B). The only apparent damage to Wall 1 were missing foundation screws at Panel Joints 1, 2 and 7 from Wall B. Wall 5 showed only one mounting screw missing from the blast door flashing. On Wall A, the roof flashing was loosened from Frames 2 through 4. The 13 central panels in the roof were torn loose from the purlins at the Wall B edge and the second purlin. Five of these were loosened from the third purlin and bent back to the center purlin. The six panels west of Column B3 were lifted 30.5 cm (12 in) and the next five panels were raised 50.9 cm (20 in). The panel over B3 was broken loose on the west side, but still attached on the east side. The next five panels east were torn loose and folded back to the center purlin. The first was up 43.25 cm (17 in); the second 71 cm (28 in); the third 81 cm (32 in); the fourth 66 cm (26 in); and the fifth, bowed in center but touching the wall purlin. The next panel was loose from the wall purlin, but not peeled back. The next two panels were still attached. The next panel was over Frame 2 and was broken loose, but not peeled back. The remaining panels over the office were still attached, but showed buckling downward between the first two purlins and upward over the second purlin from Wall B.

* See Note on previous page.

Table 4. Summary of deflection measurements

Gage No.	Test #3 (mm)	Test #4 (mm)	Test #5 (mm)	Test #6 (mm)	Test #7 (mm)
D1	33.27	43.94	37.34	35.31	30.99
D2	28.96	33.53	26.67	29.97	27.69
D3	-	32.26	-	-	-
D4	32.77	22.61	21.59	28.70	32.77
D5	10.41	13.72	8.38	19.81	12.45
D6	-	-	13.21	18.29	20.80
D7	21.86	30.73	33.53	34.80	36.32
D8	4.32	5.84	6.60	10.16	5.33
D9	23.62	20.07	-	-	-
D10	8.38	20.57	20.83	31.75	20.32
D11	51.05	75.18	59.44	64.77	52.07
D12	41.91	64.77	58.39	61.21	93.73
D13	45.21	-	166.12	192.53	45.97
D14	45.47	50.55	52.83	58.93	56.90
D15	22.10	24.38	25.40	44.95	47.50

Table 5. Summary of results of DYNFA analysis utilizing design blast

Test No.	P_{so} kPa (psi)	δ mm (in)	Plastic behavior μ	Member	Location	Comments
3	18.61 (2.7)	43.18 (1.7)	1.25	Girder	Blastward	Girder has gone plastic but remains usable
			1.16	Girder	Leeward	
			1.00	Blastward column	Lower end	
			1.03	Girder	Mid-span	
4	26.89 (3.9)	63.5 (2.5)	1.48	Girder	Blastward	Girder and blastward column have gone plastic but are still reusable
			1.10	Girder	Leeward	$\delta/H \sim 25$ limit of non-reusable criteria
			1.44	Blastward column	Lower end	
			1.50	Girder	Mid-span	

Table 6. Summary of results of DYNFA analysis utilizing actual blast loads

Test No.	P_{so} (kPa)	δ (mm)	Plastic behavior			Comments
			μ	Member	Location	
3	22.06	28.96	1.842	Girder	Blastward end	μ on girder approach reusable design criteria
			2.581	Girder	Leeward end	
						$\delta/H \sim 50$, limit of reusable criteria
4	24.13	33.53	2.796	Girder	Blastward end	μ on girder approach non-reusable design criteria
			1.900	Girder	Center span	
			4.048	Girder	Leeward end	

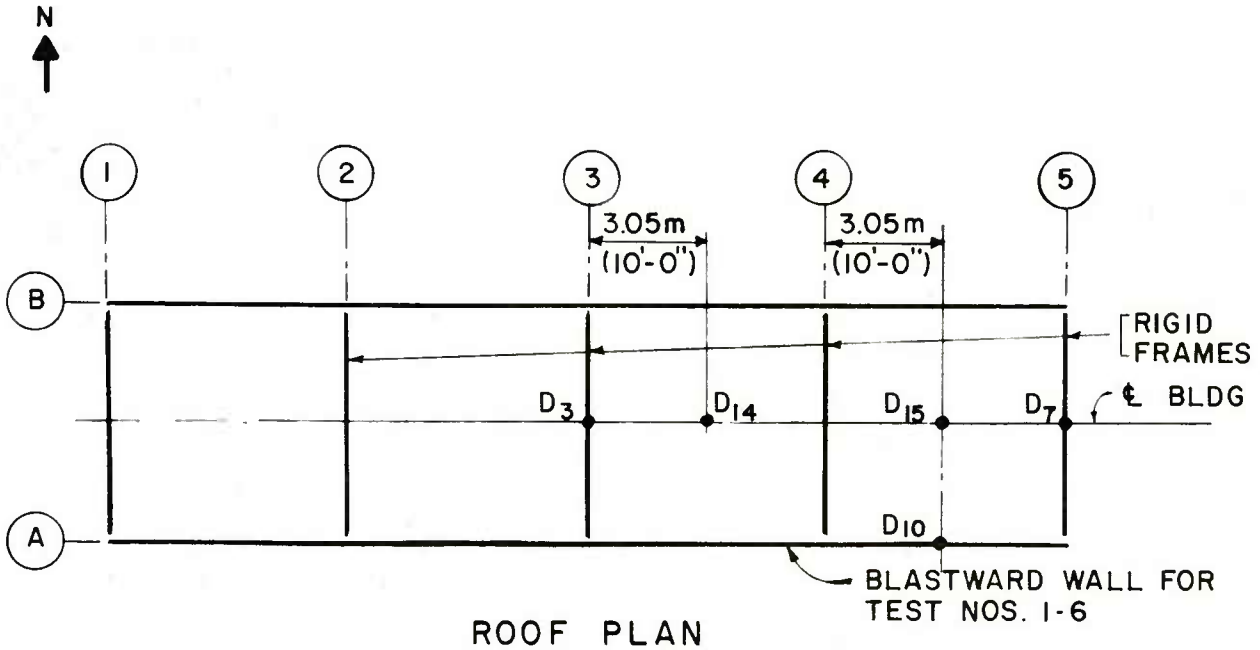

ROOF PLAN

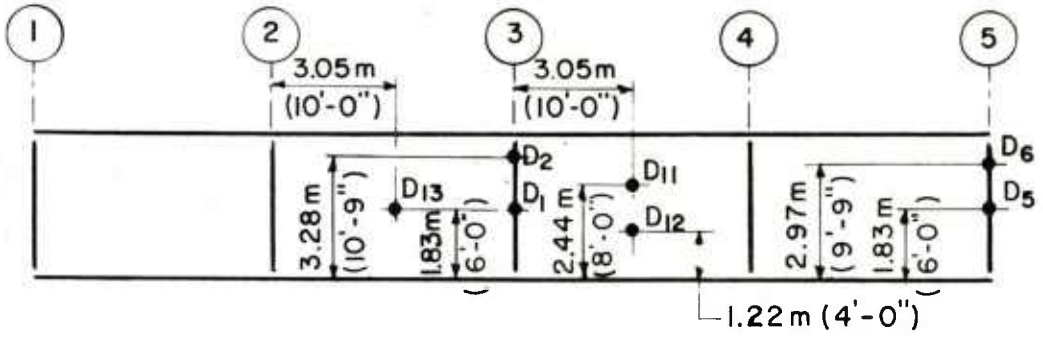

ELEVATION - BLASTWARD WALL

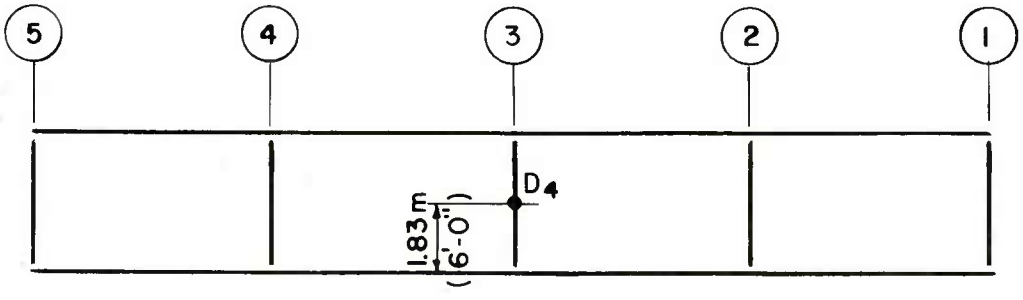

ELEVATION - LEEWARD WALL

Figure 1. Location of deflection gages on test structure

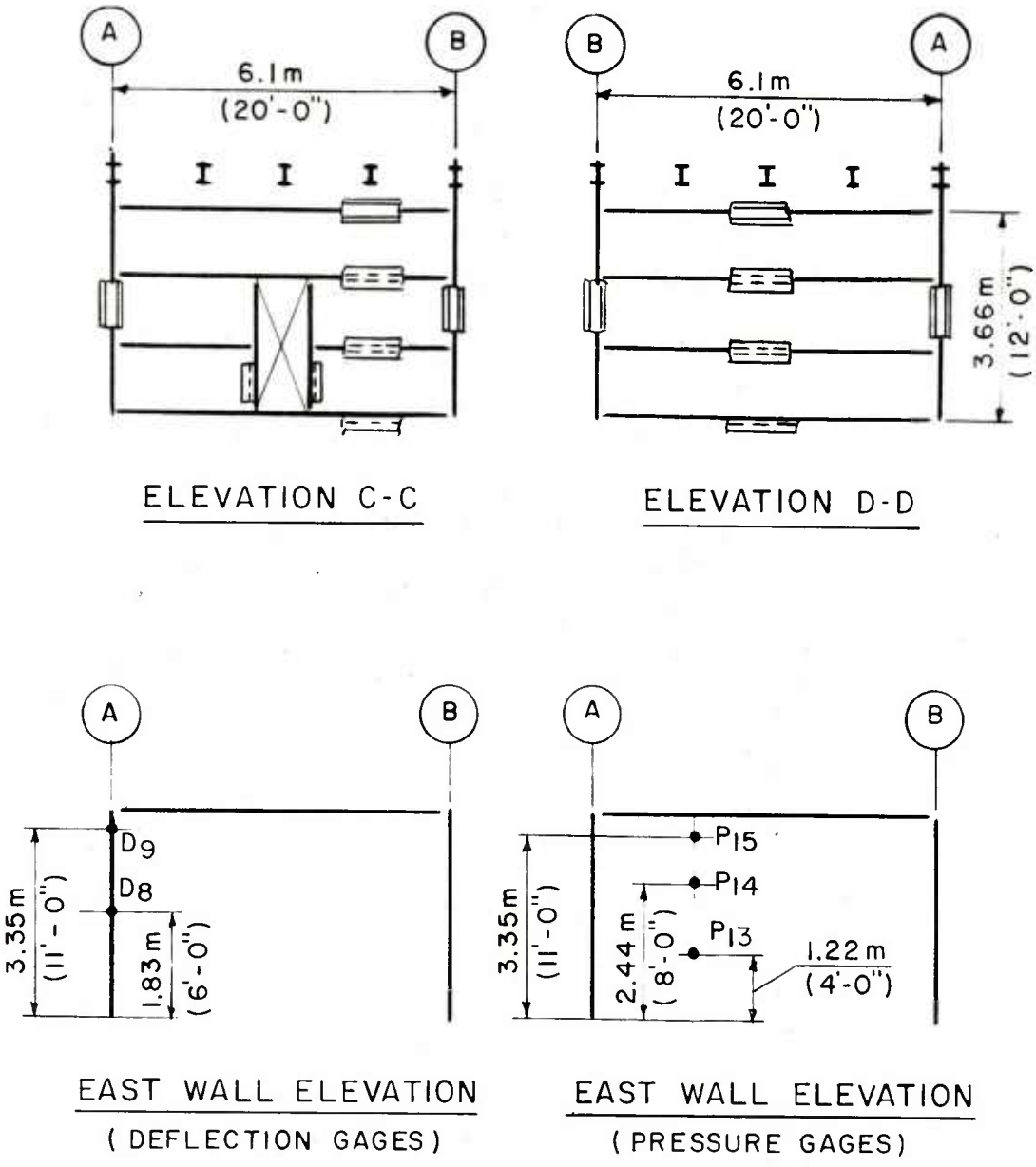

Figure 2. Location of deflection and pressure gages on side wall

Figure 3. Typical deflection gage mount

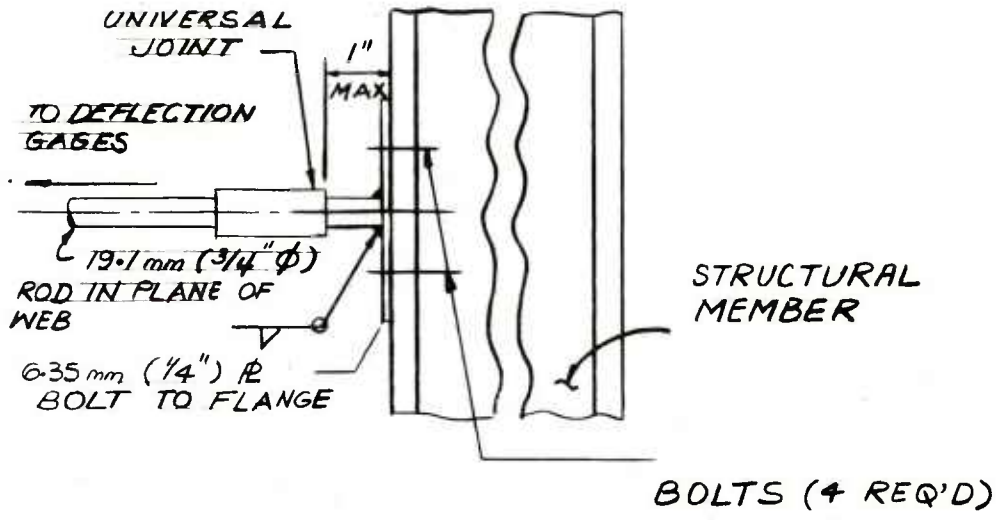

(A)

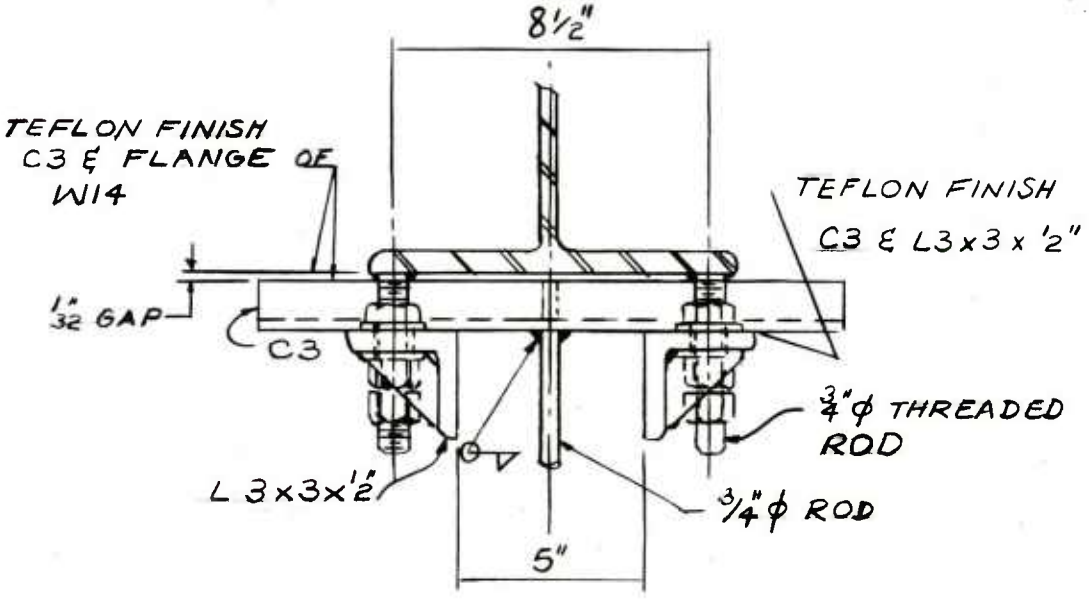

(B)

Figure 4. Deflection gage attachment details

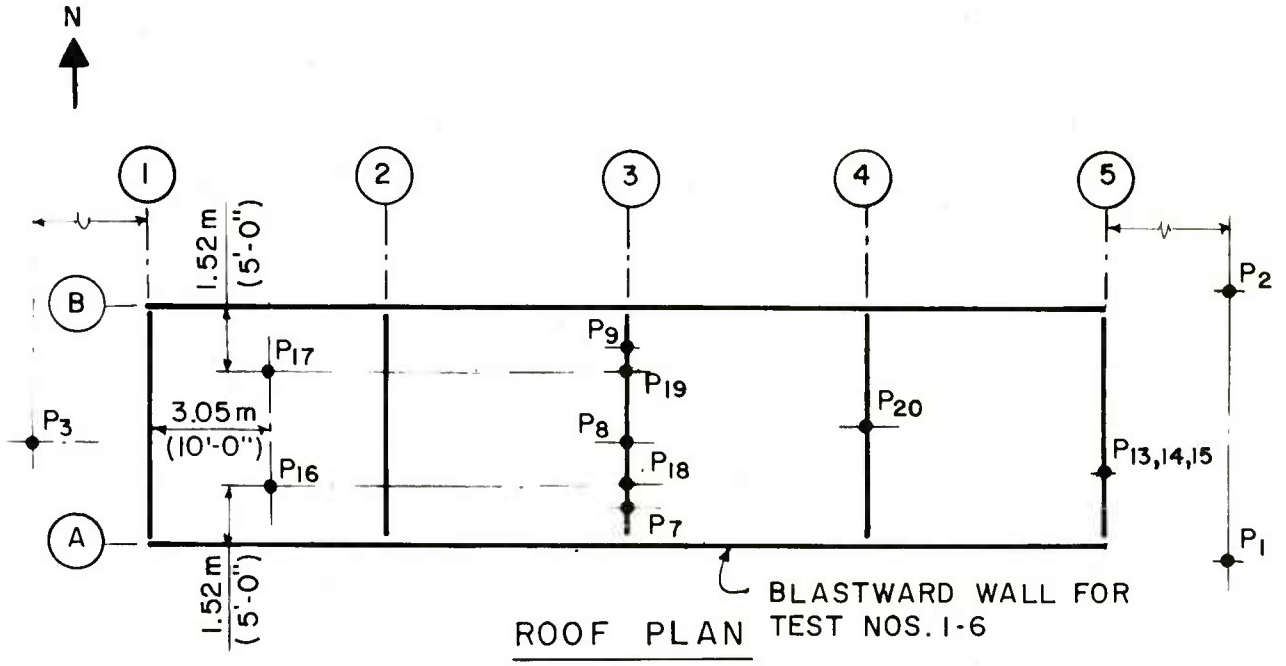

ROOF PLAN

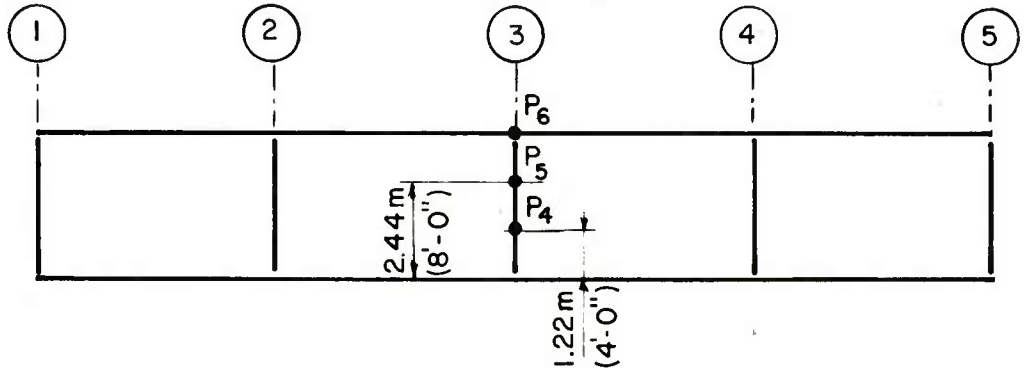

ELEVATION - BLASTWARD WALL

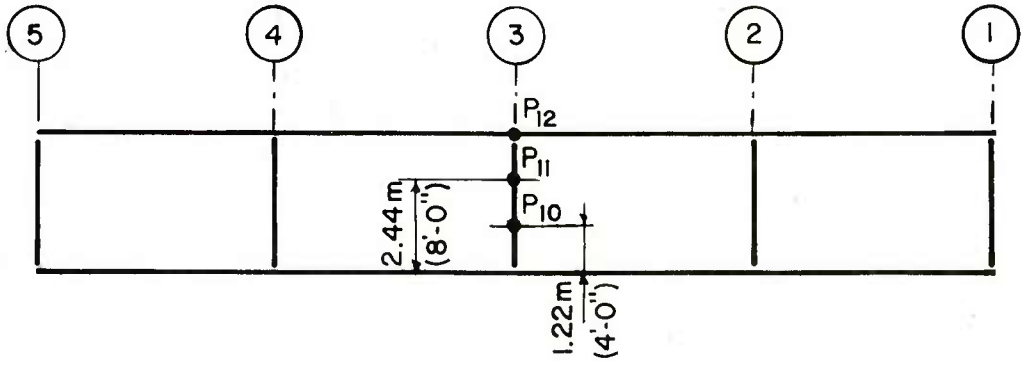

ELEVATION - LEEWARD WALL

Figure 5. Location of pressure gages on test structure

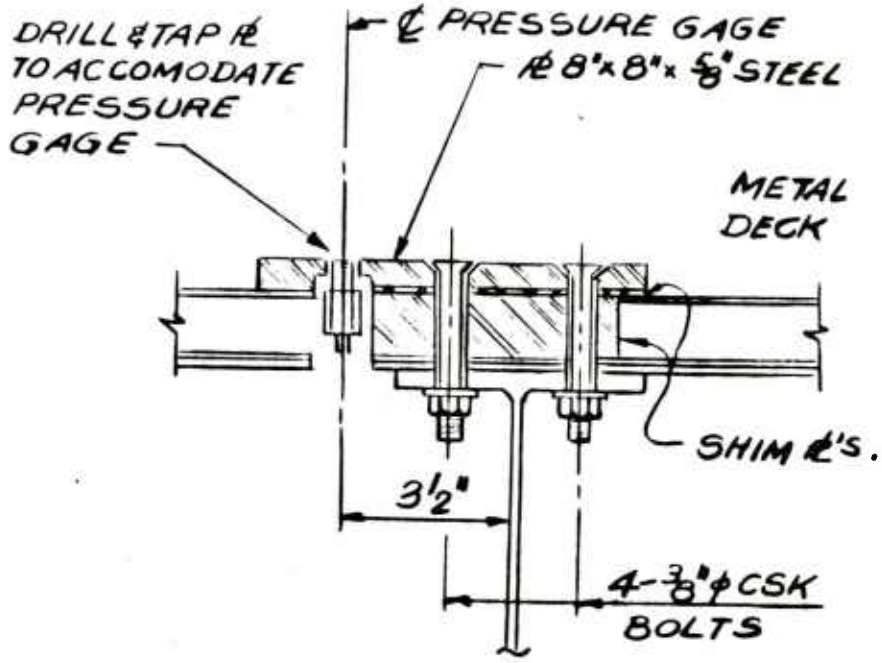

Figure 6. Typical pressure gage attachment detail

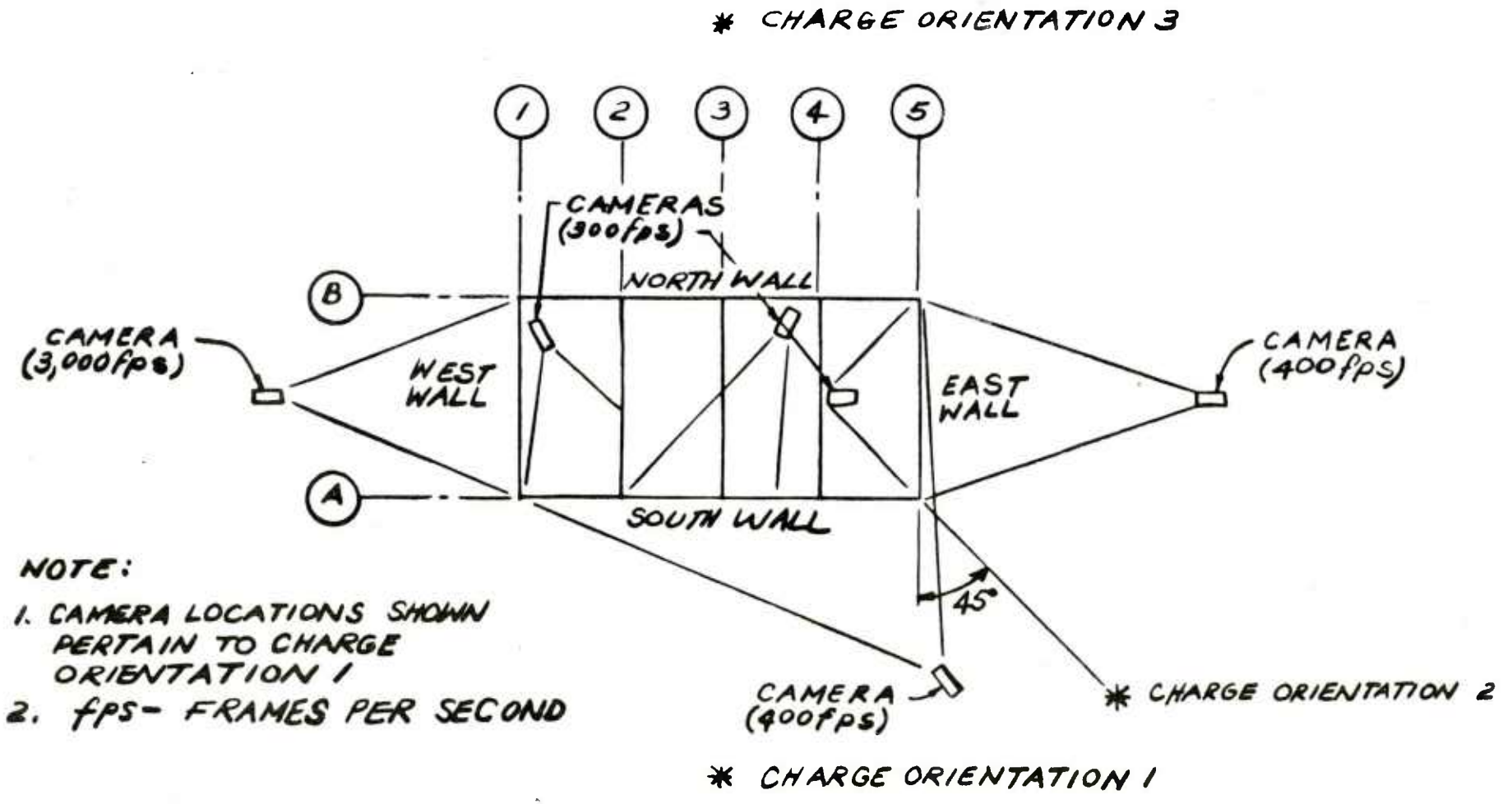

Figure 7. Orientation of explosive charge and camera coverage

Figure 8. Preparation of explosive charge

Figure 9. Pull-out of panel seam by foundation

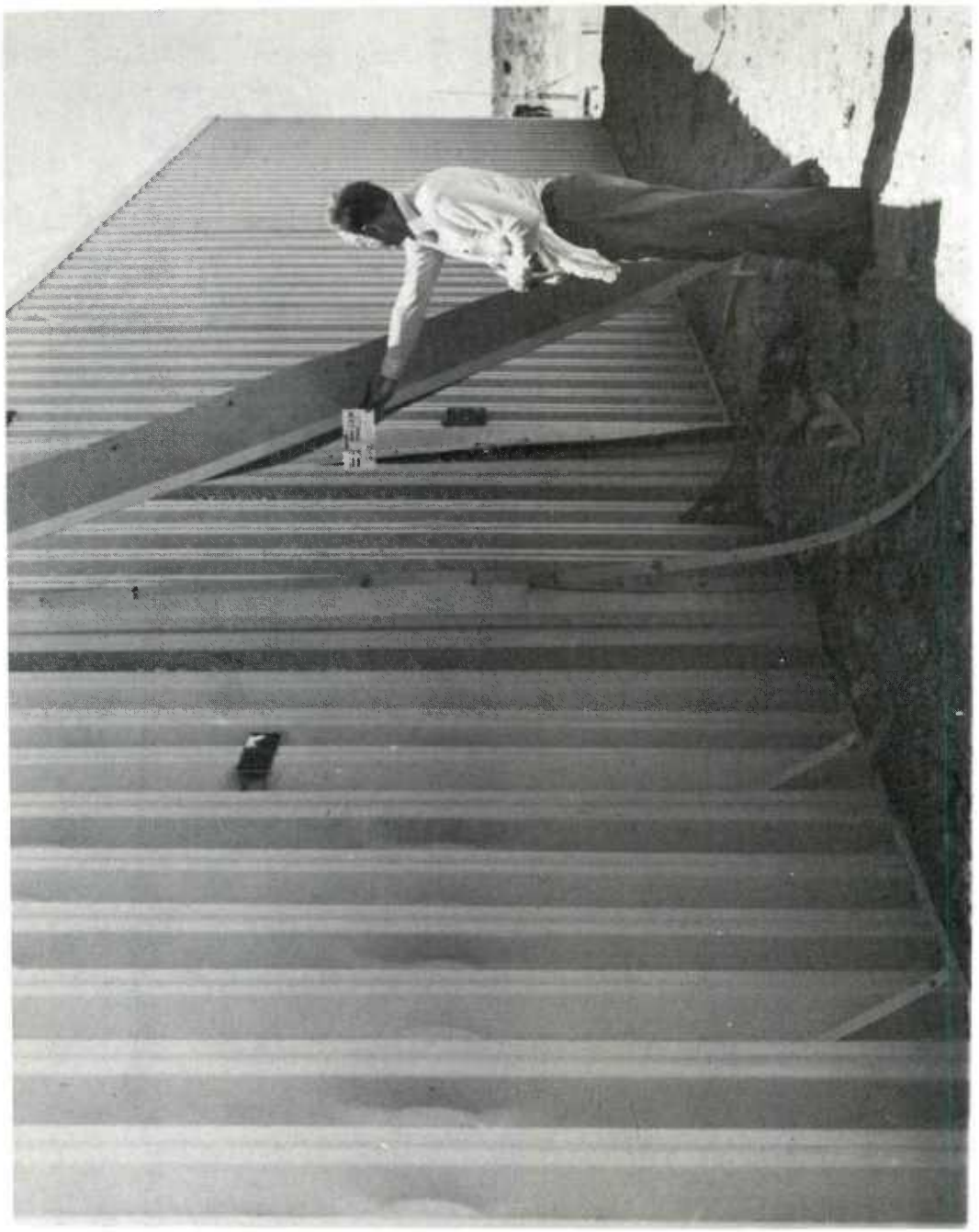

Figure 10. Blastward wall panel torn loose

Figure 11. Damage to roof flashing

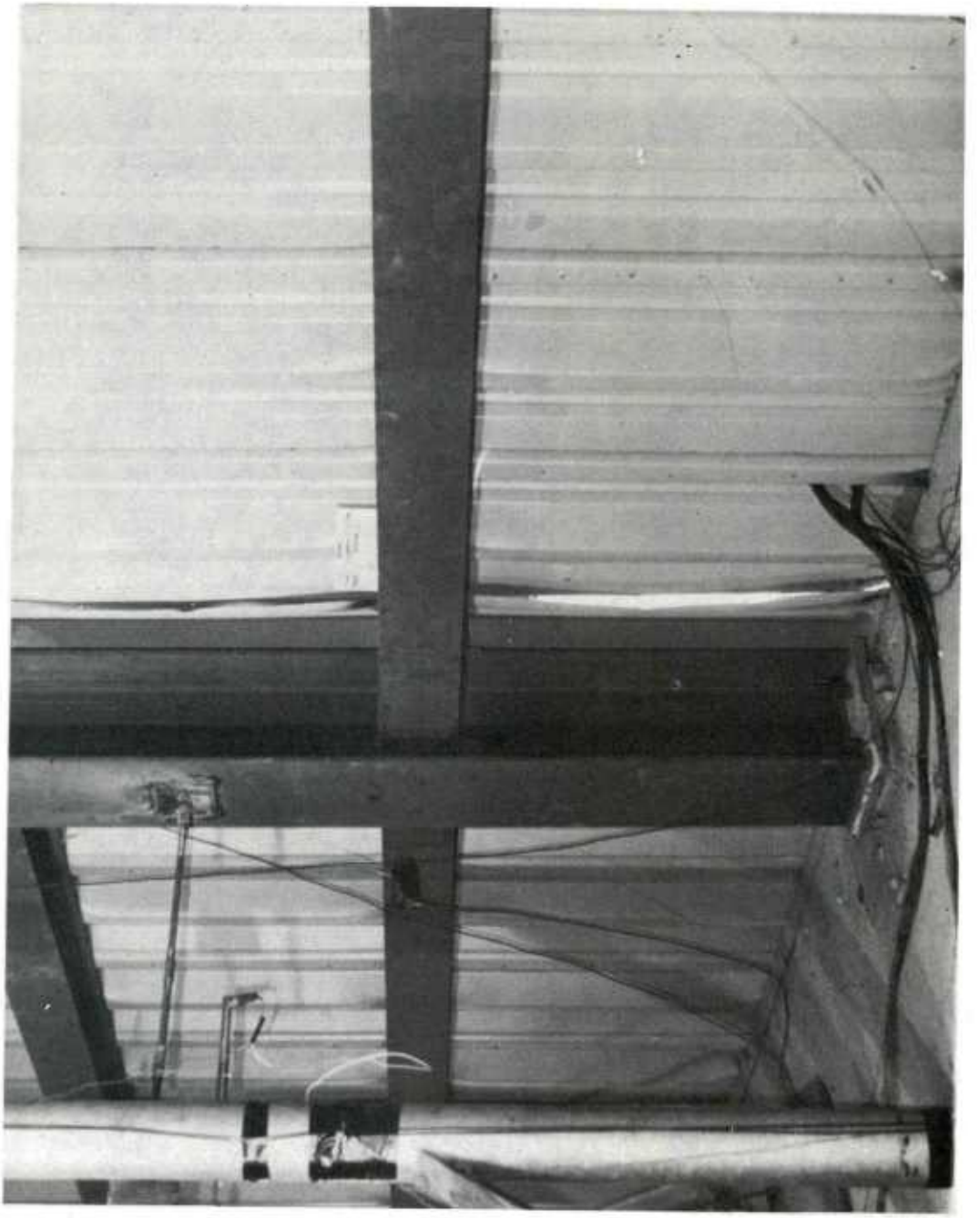

Figure 12. Permanent gaps in wall panel seams

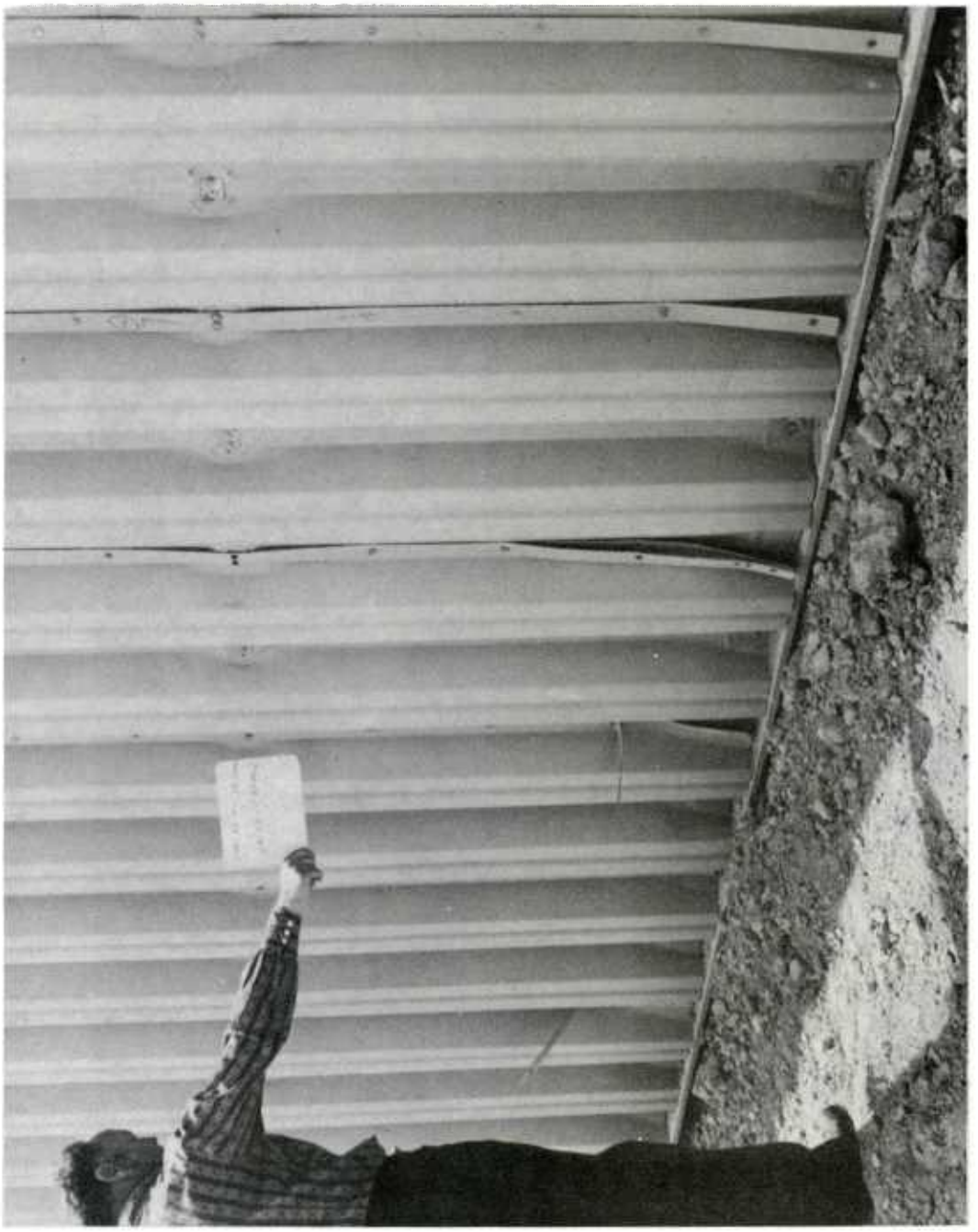

Figure 13. Pull out of panel screws

Figure 14. Failure of bolted connection at column base

Figure 15. Damaged blastward wall

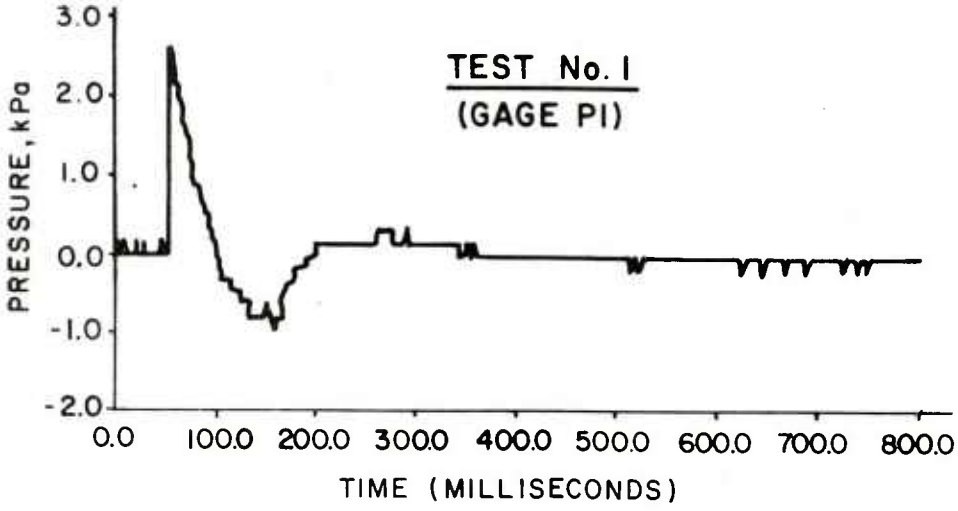

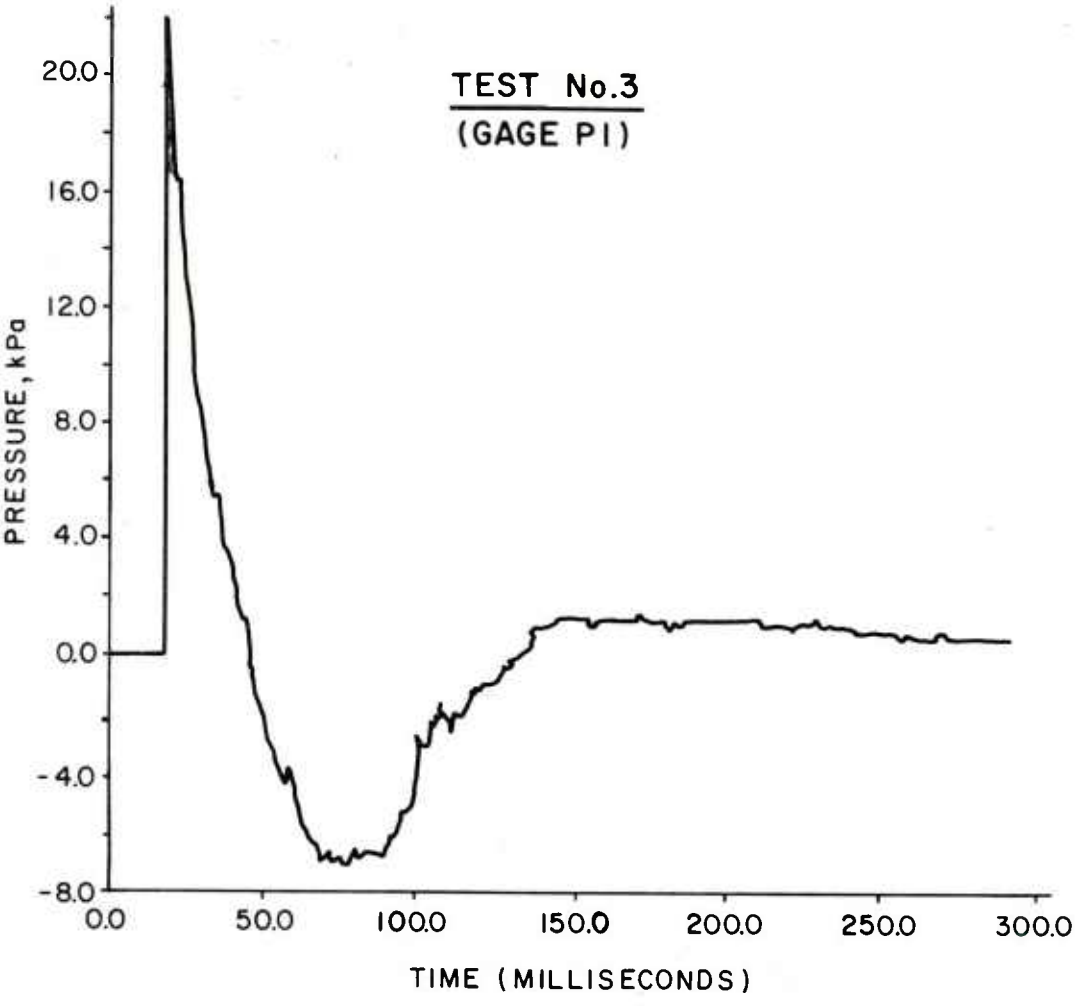

Figure 16. Measured free-field pressures for Tests 1 and 3

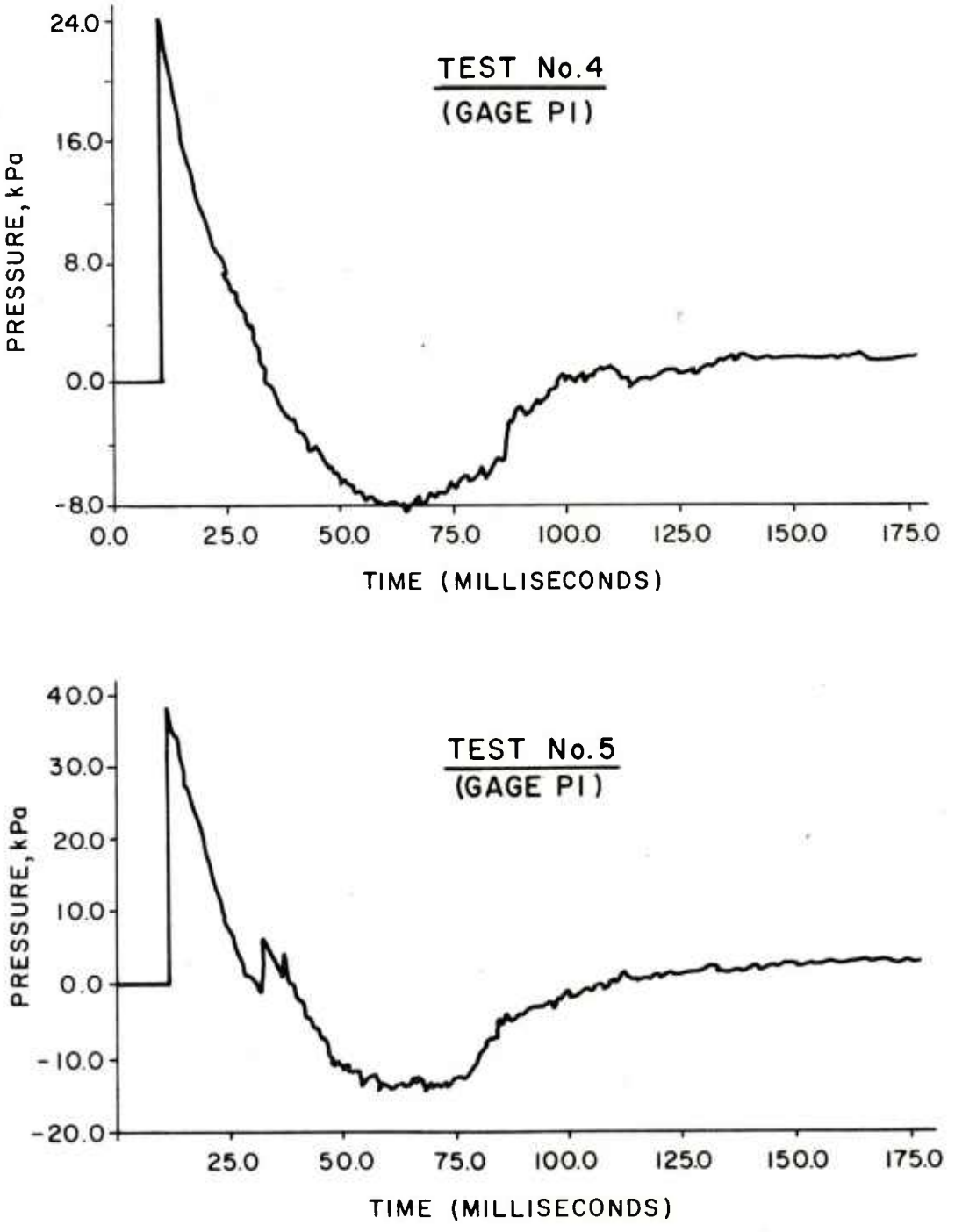

Figure 17. Measured free-field pressures for Tests 4 and 5

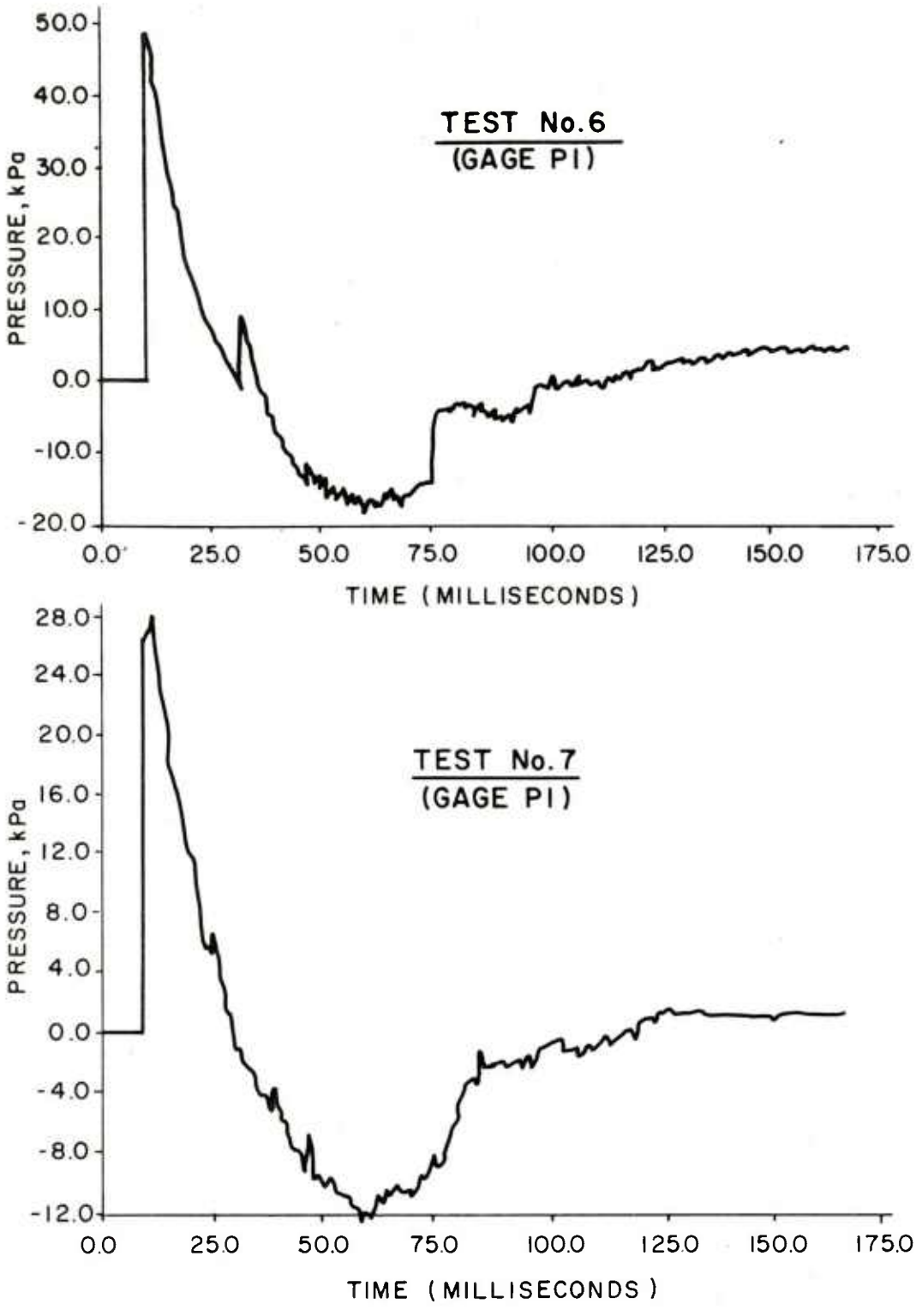

Figure 18. Measured free-field pressures for Tests 6 and 7

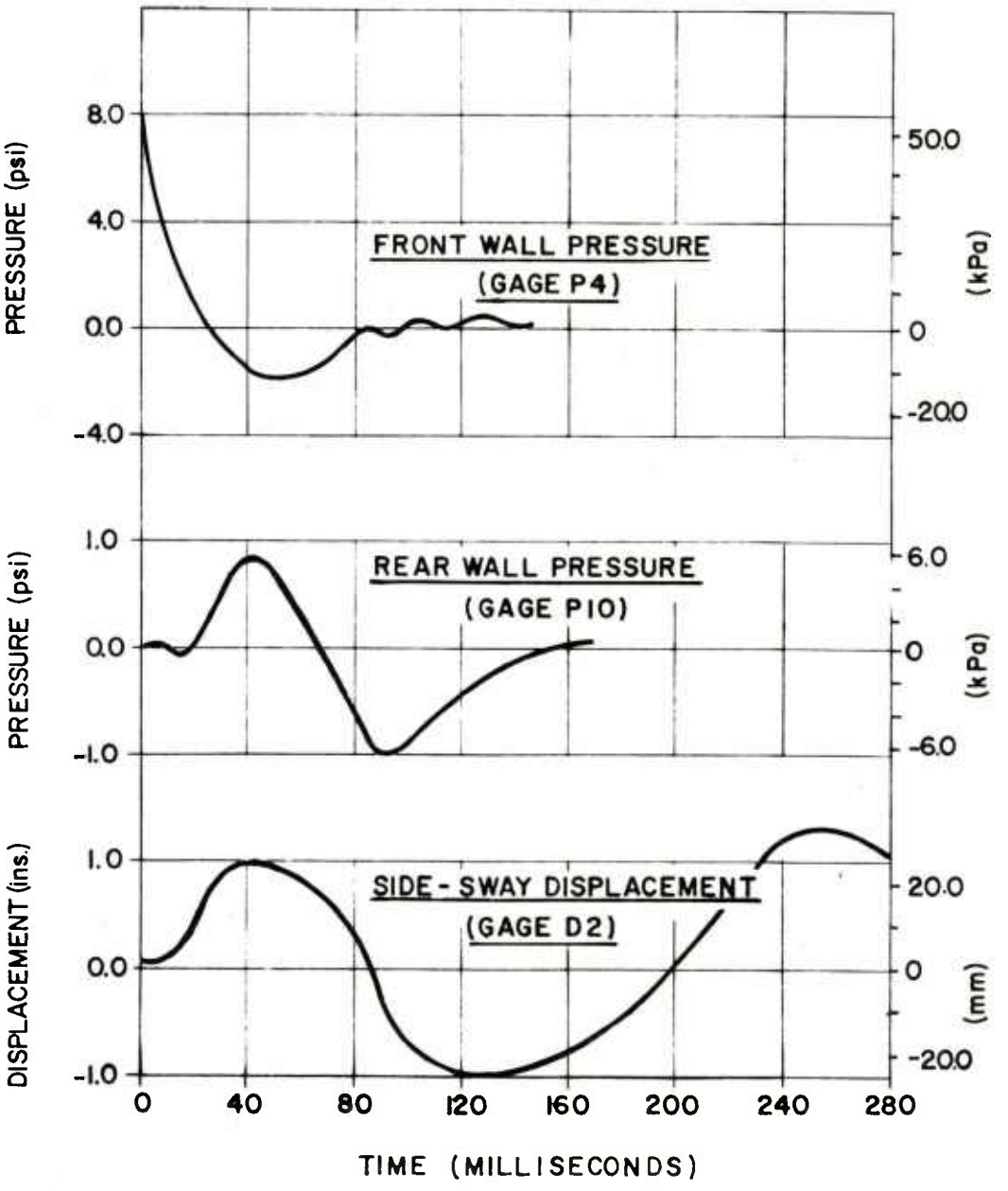

Figure 19. Measured building pressures and side-sway displacement for Test 3, Center frame

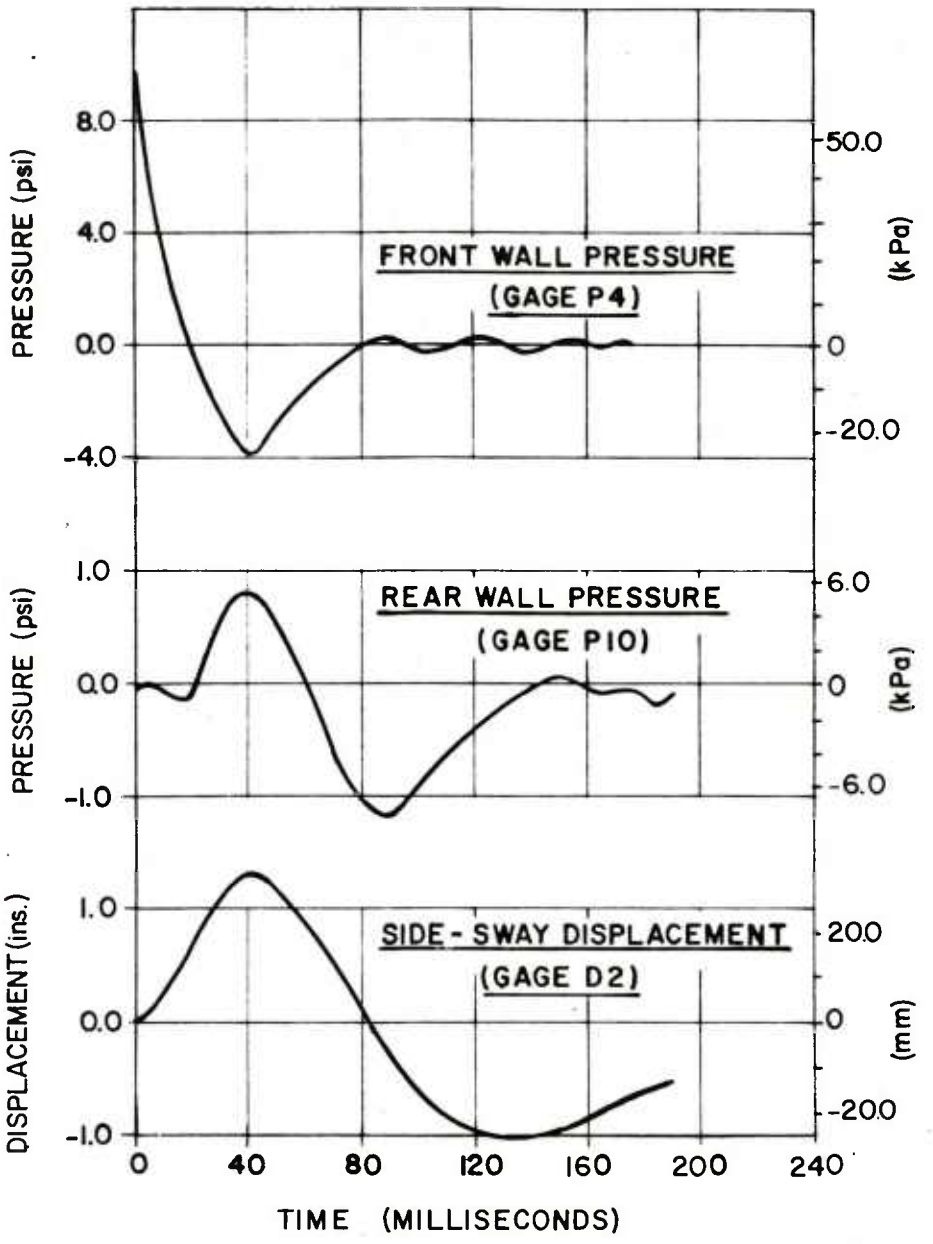

Figure 20. Measured building pressures and side-sway displacement for Test 4, Center frame

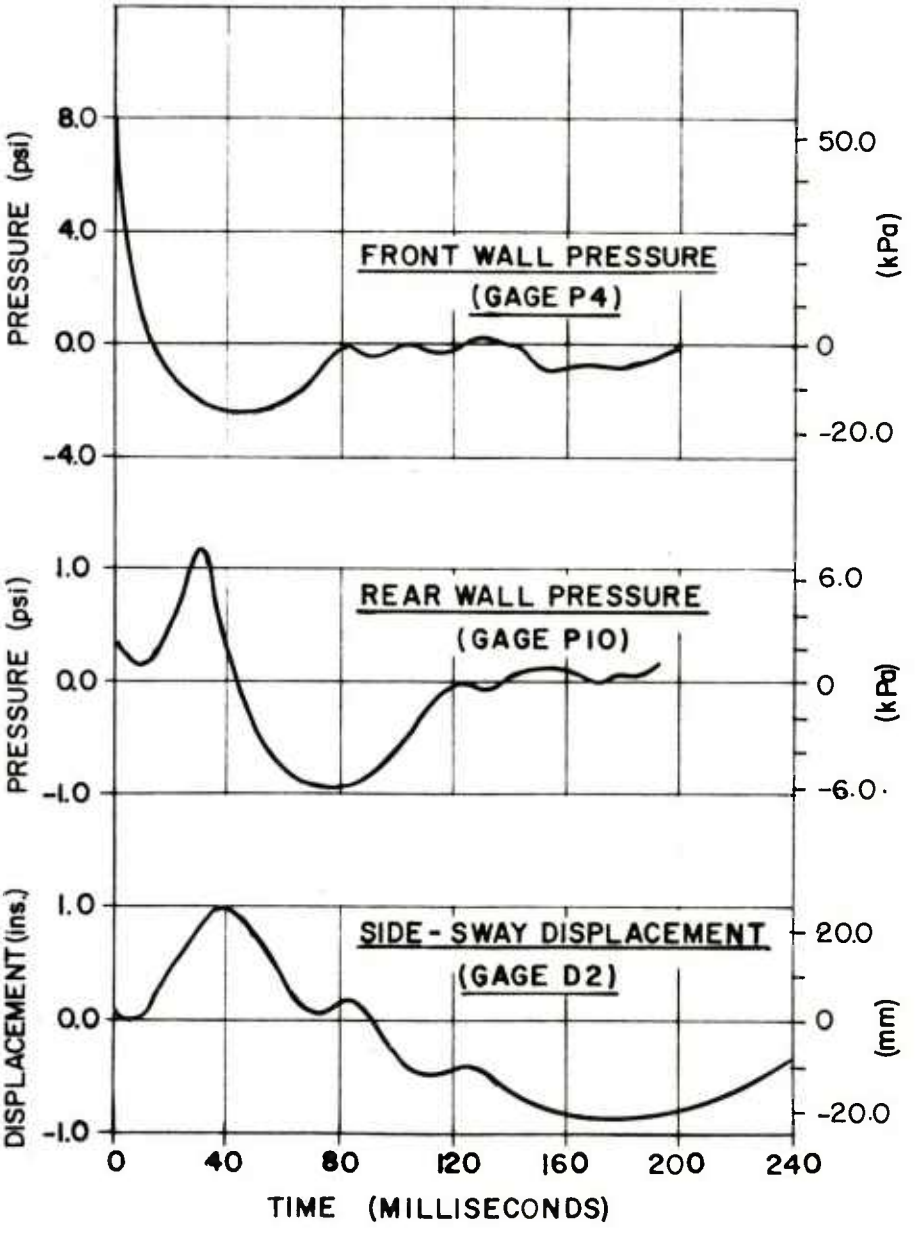

Figure 21. Measured building pressures and side-sway displacement for Test 5, Center frame

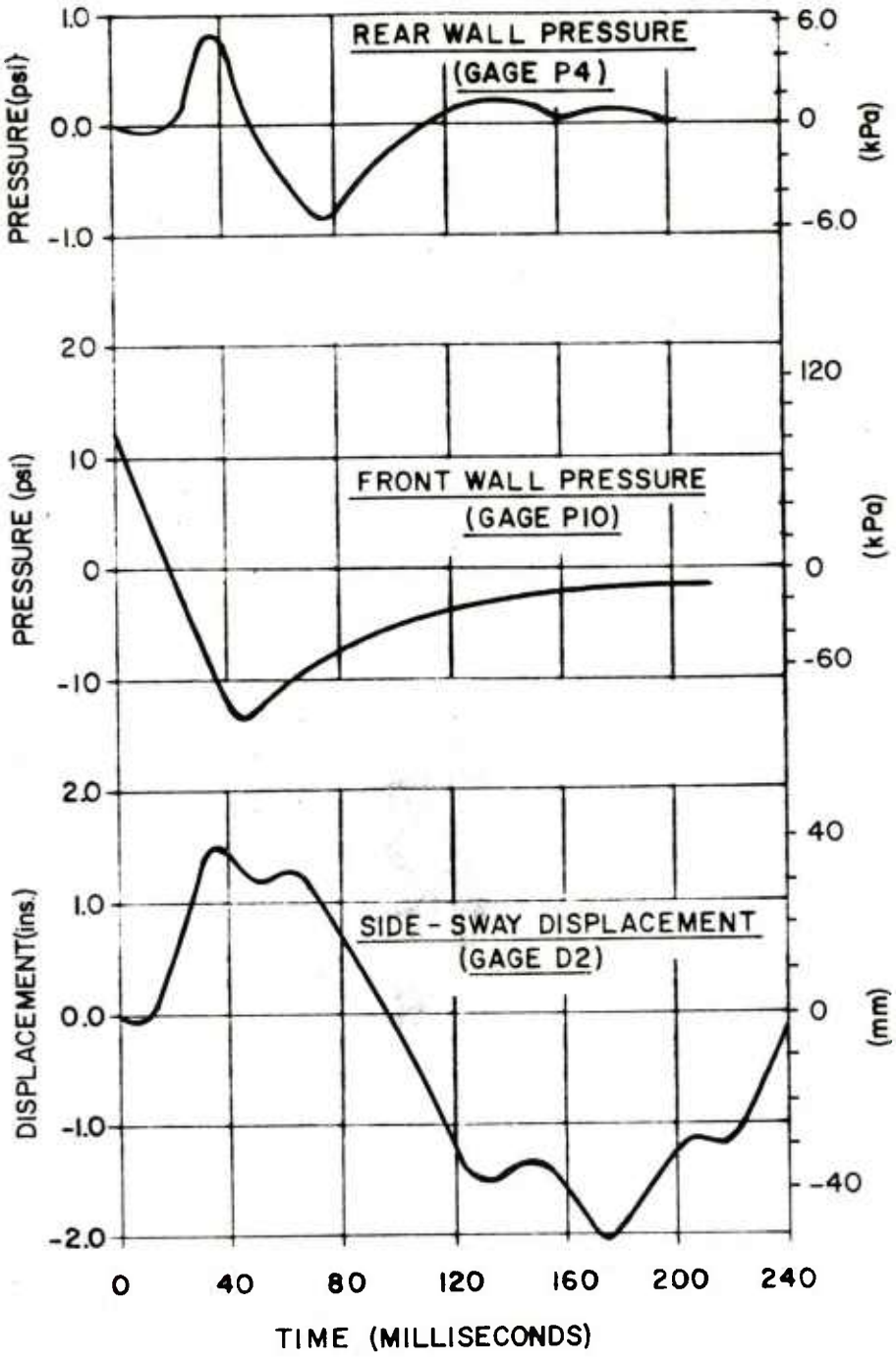

Figure 22. Measured building pressures and side-sway displacement for Test 7, Center frame

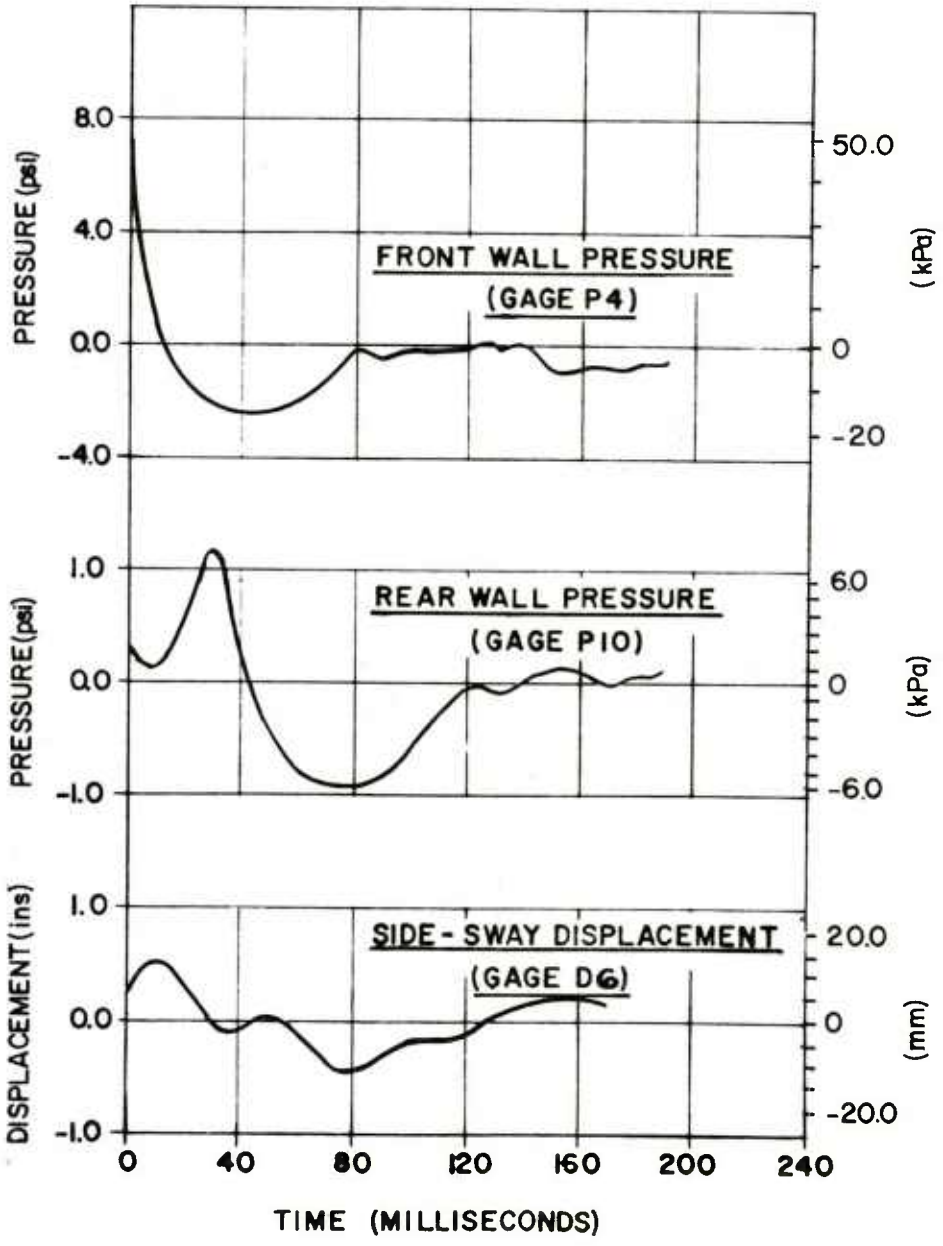

Figure 23. Measured building pressures and side-sway displacement of rigid end frame for Test 5

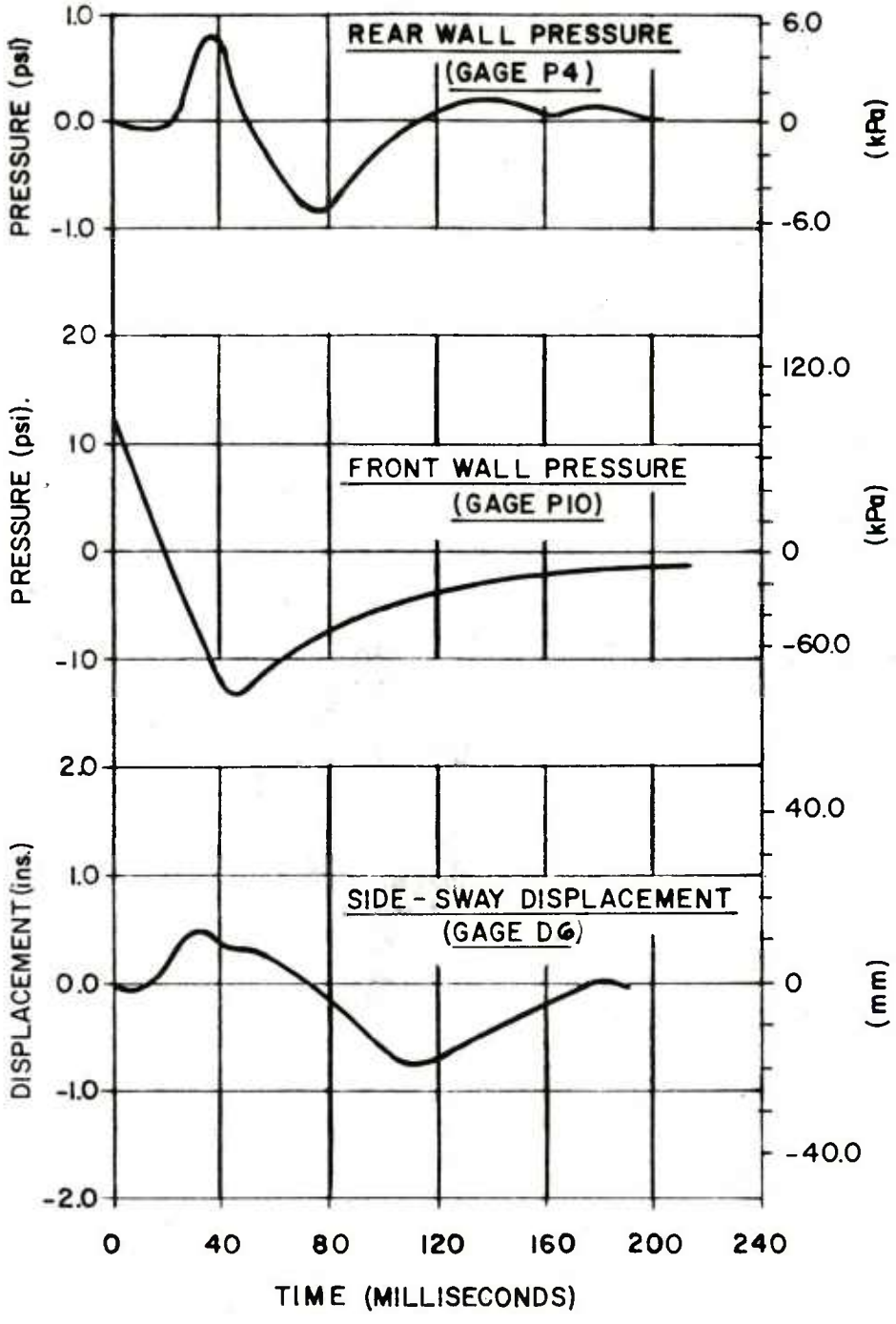

Figure 24. Measured building pressures and side-sway displacement of rigid end frame for Test 7

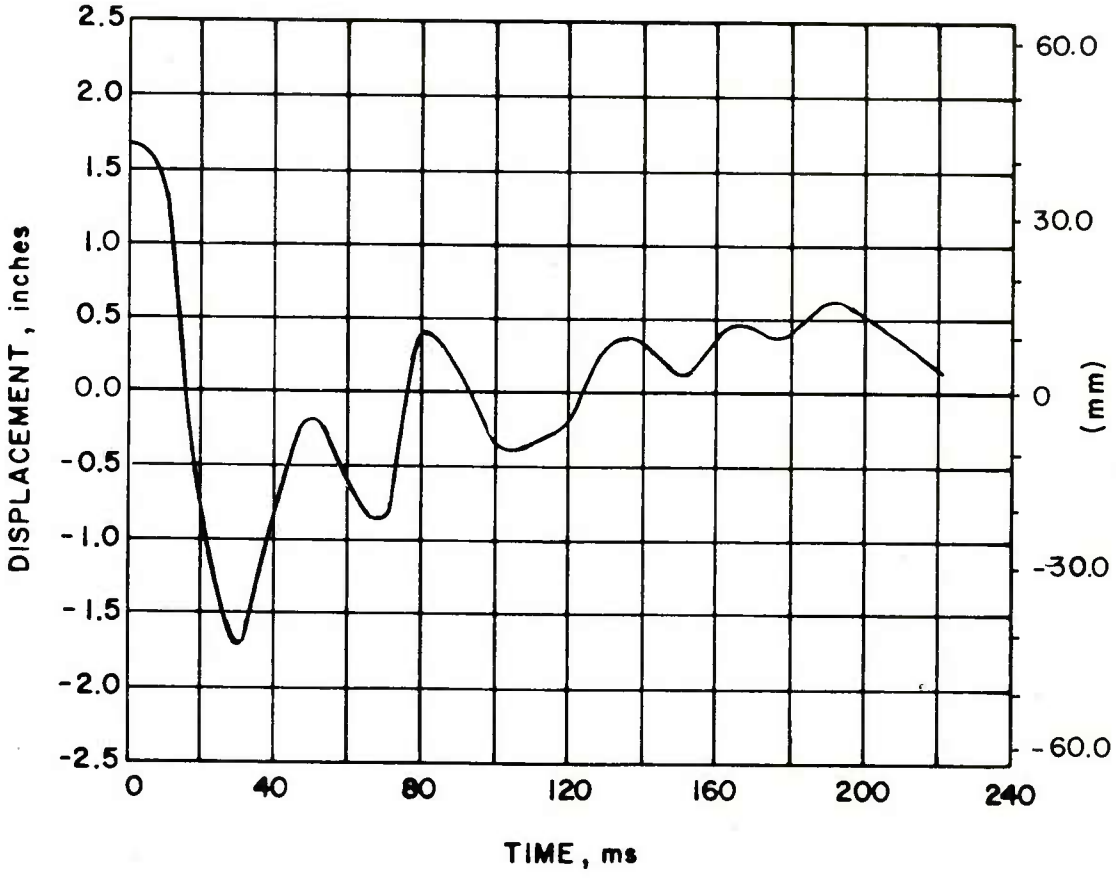

Figure 25. Measured upper girt displacement for Test 5

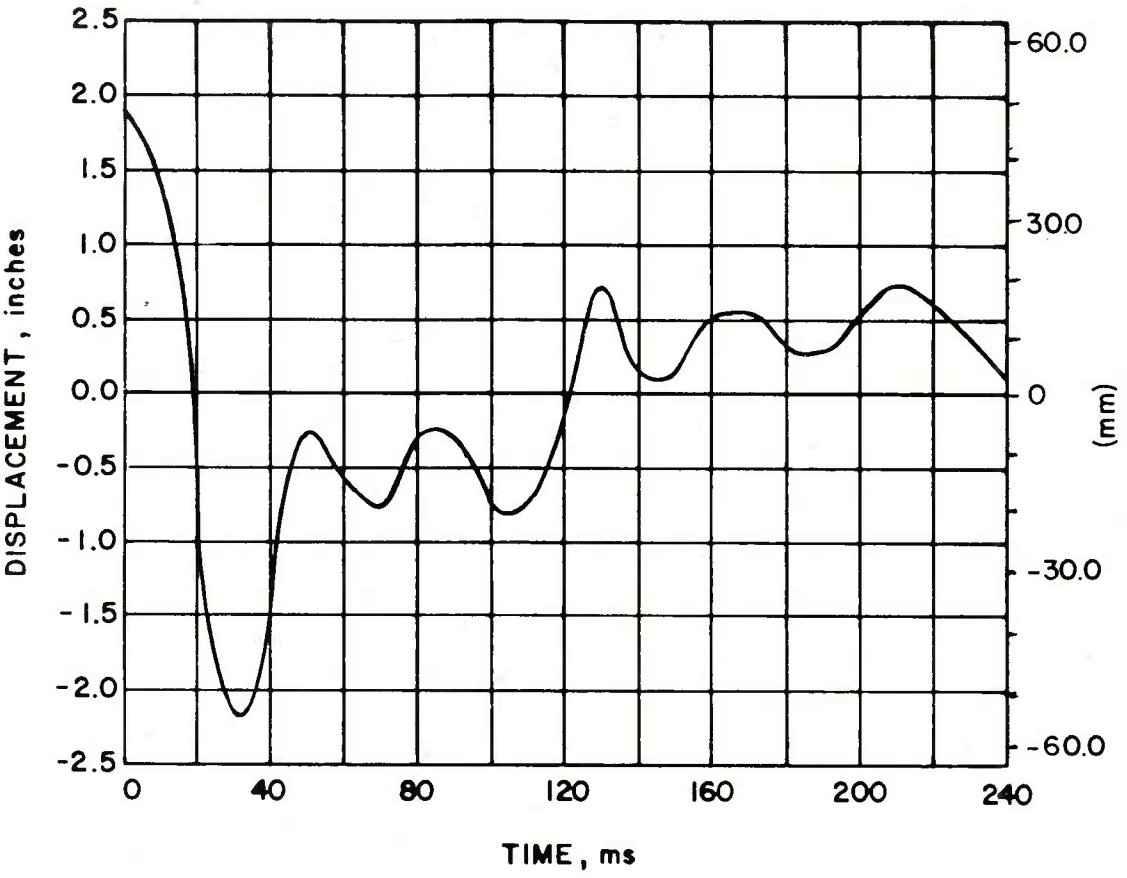

Figure 26. Measured upper girt displacement for Test 6

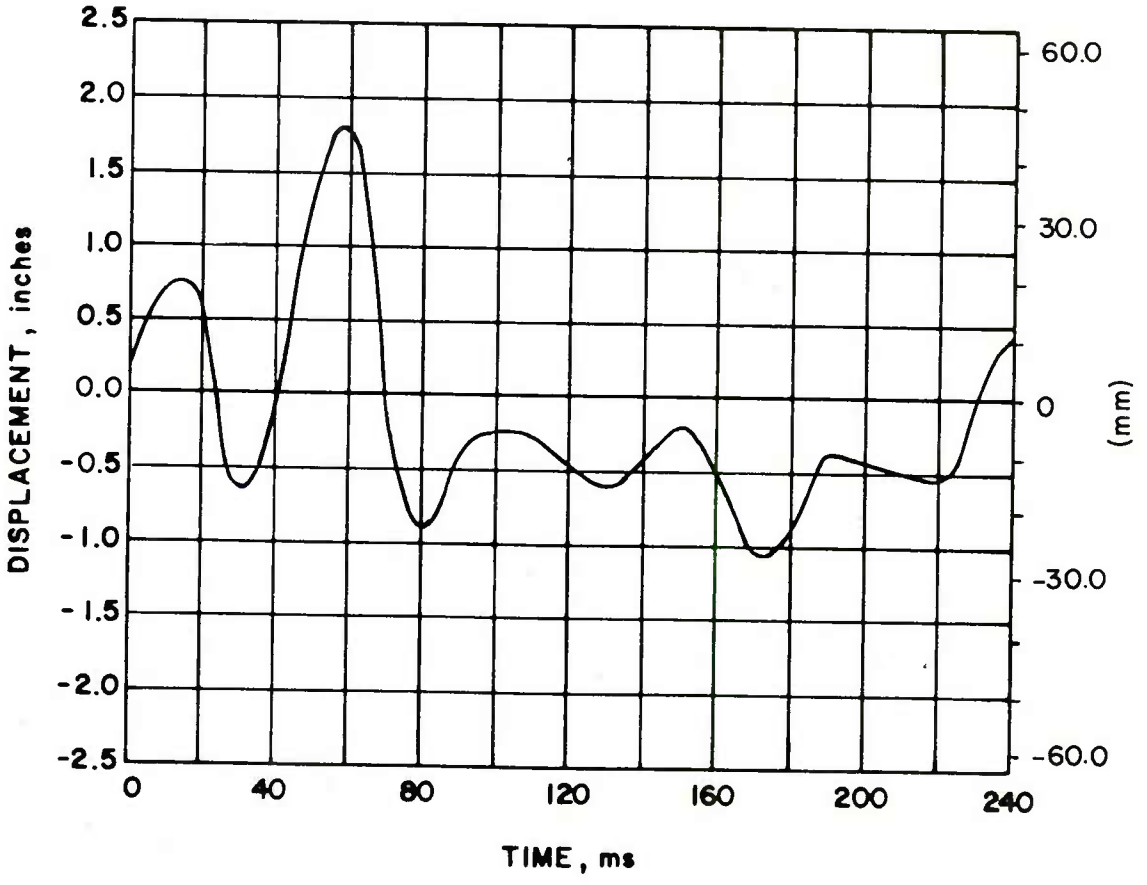

Figure 27. Measured upper girt displacement for Test 7

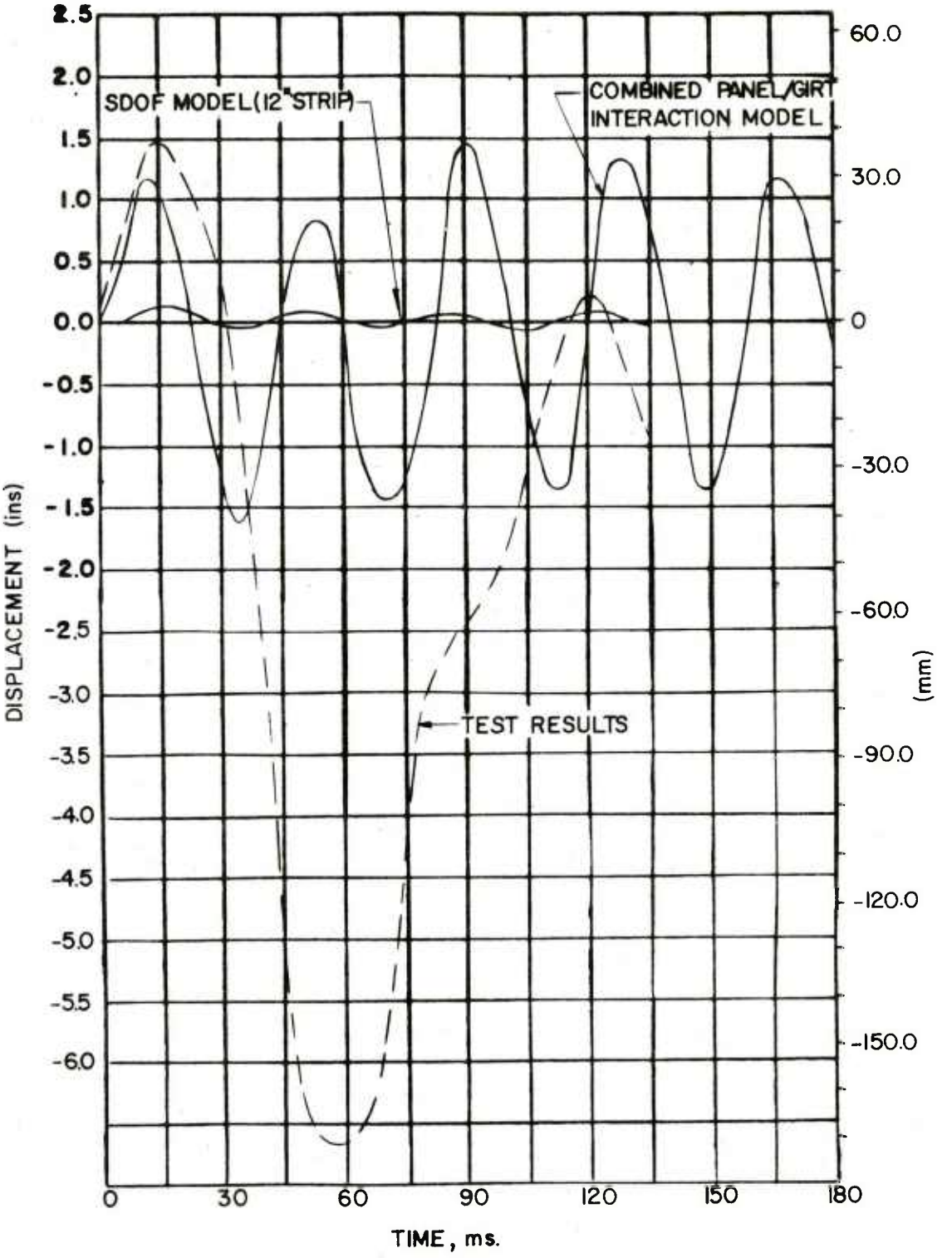

Figure 28. Typical wall panel displacement, test and analytical results

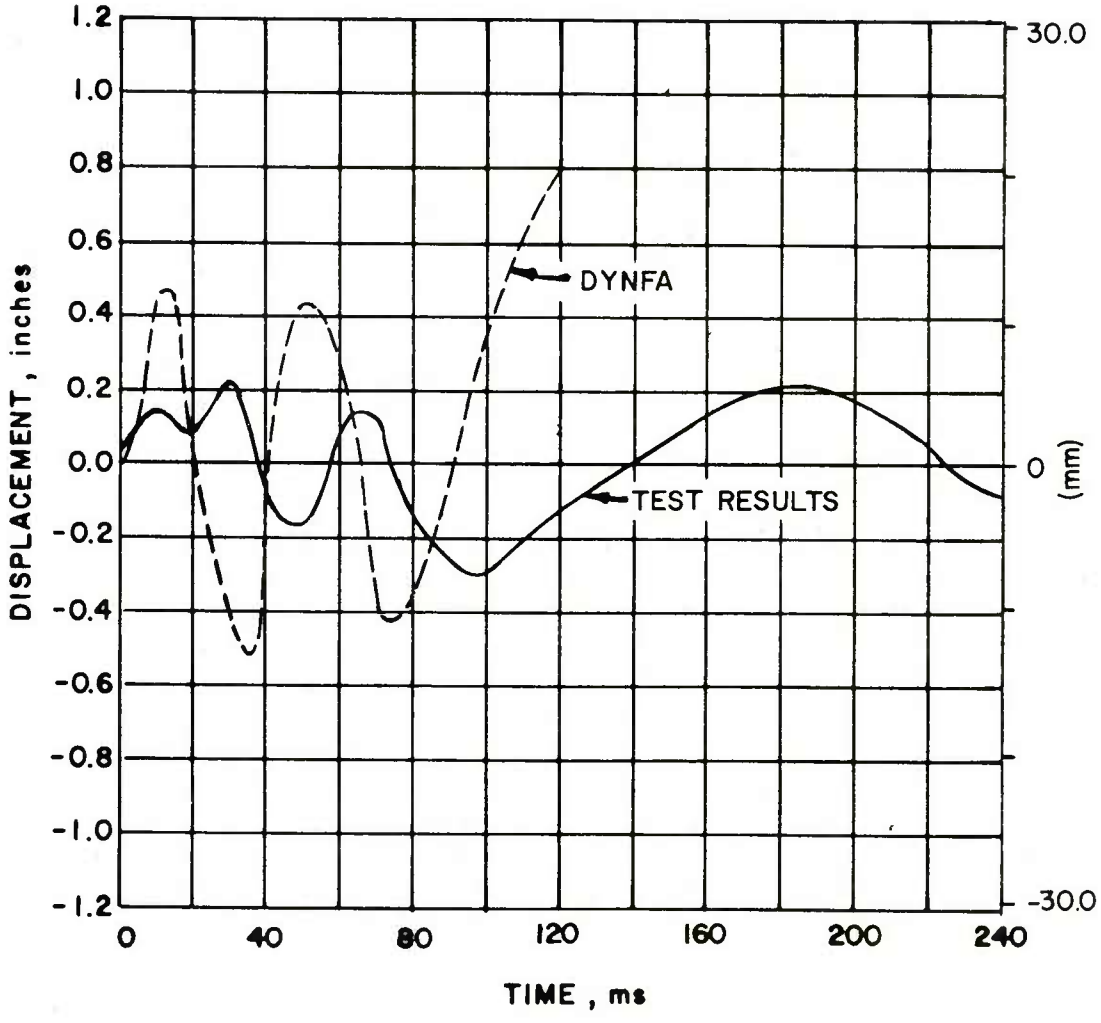

Figure 29. Longitudinal frame side-sway displacement, test and analytical results for Test 5

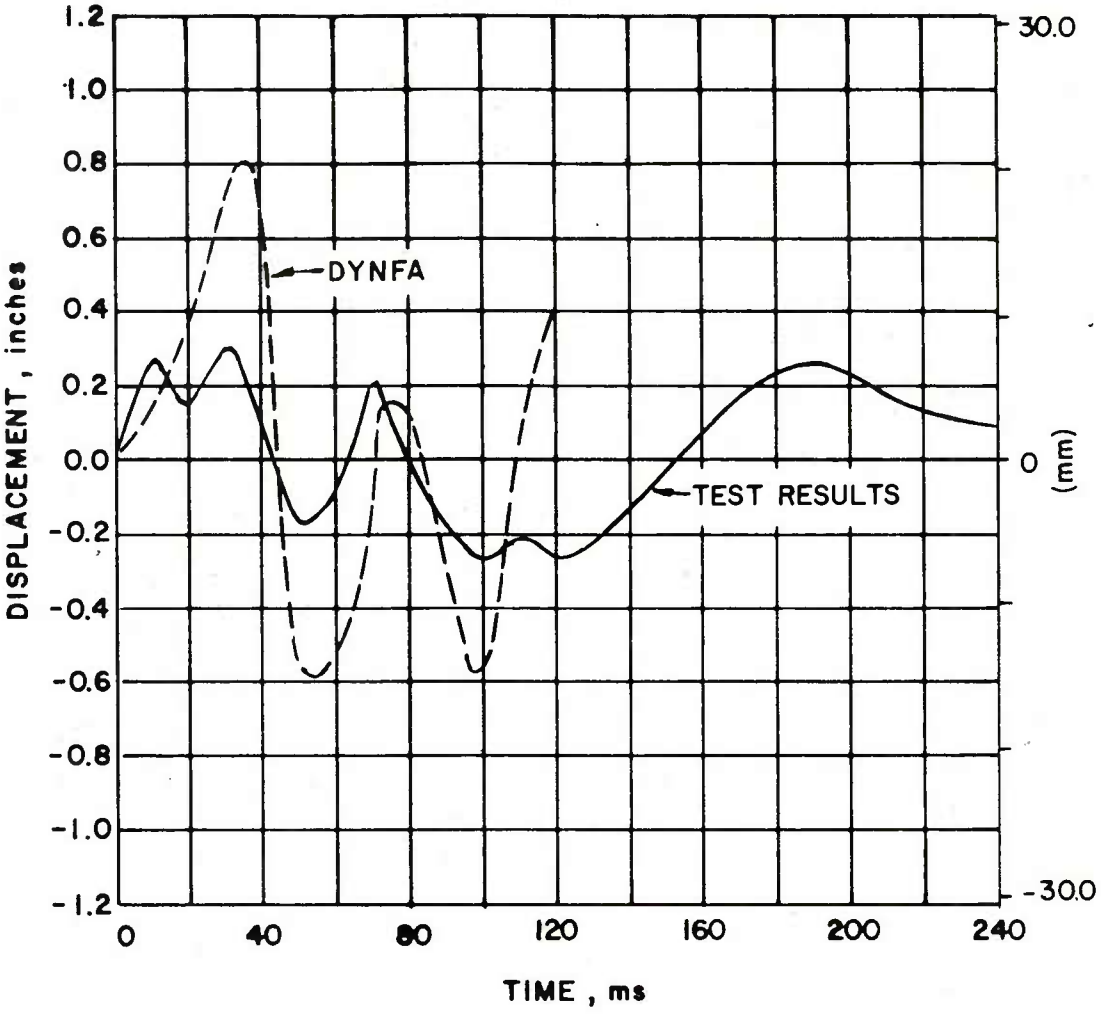

Figure 30. Longitudinal frame side-sway displacement, test and analytical results for Test 6

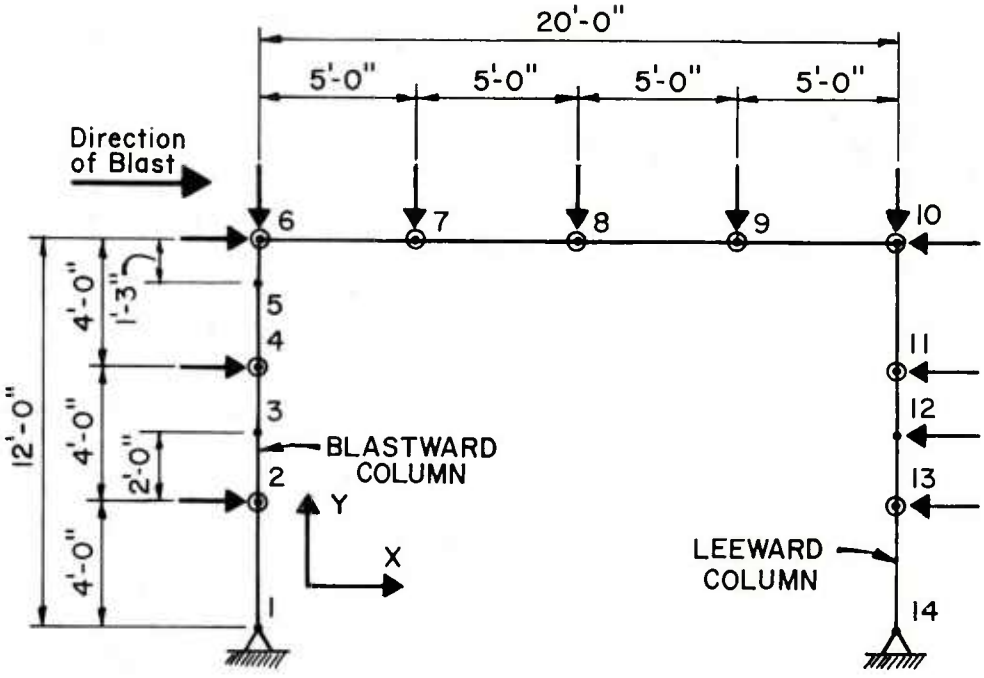

Figure 31. Basic transverse frame model

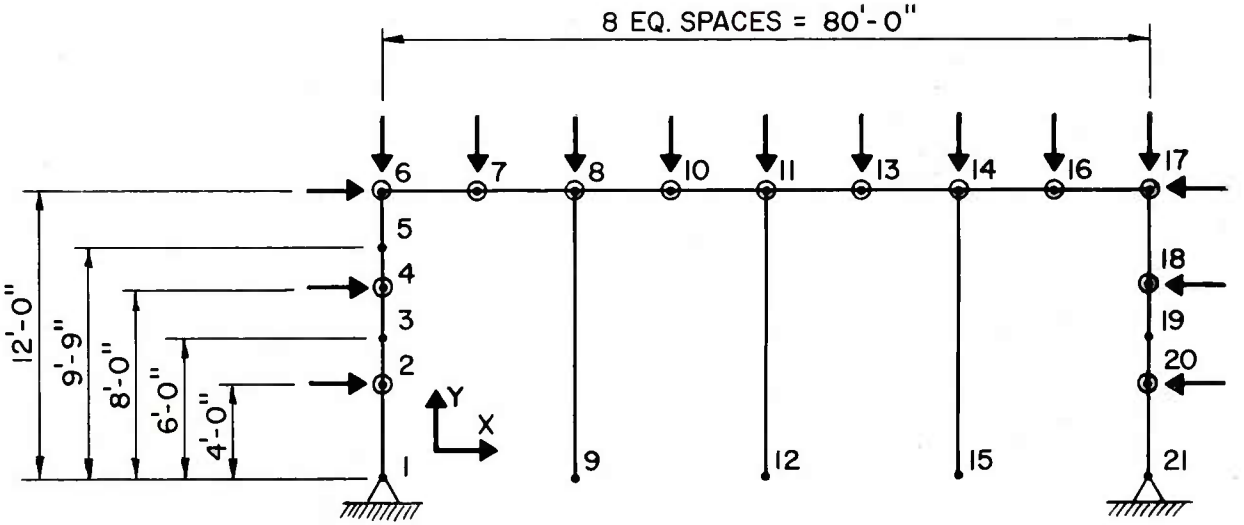

LEGEND:

- NODE
- MASS POINT
- APPLIED LOAD

Figure 32. Longitudinal frame model

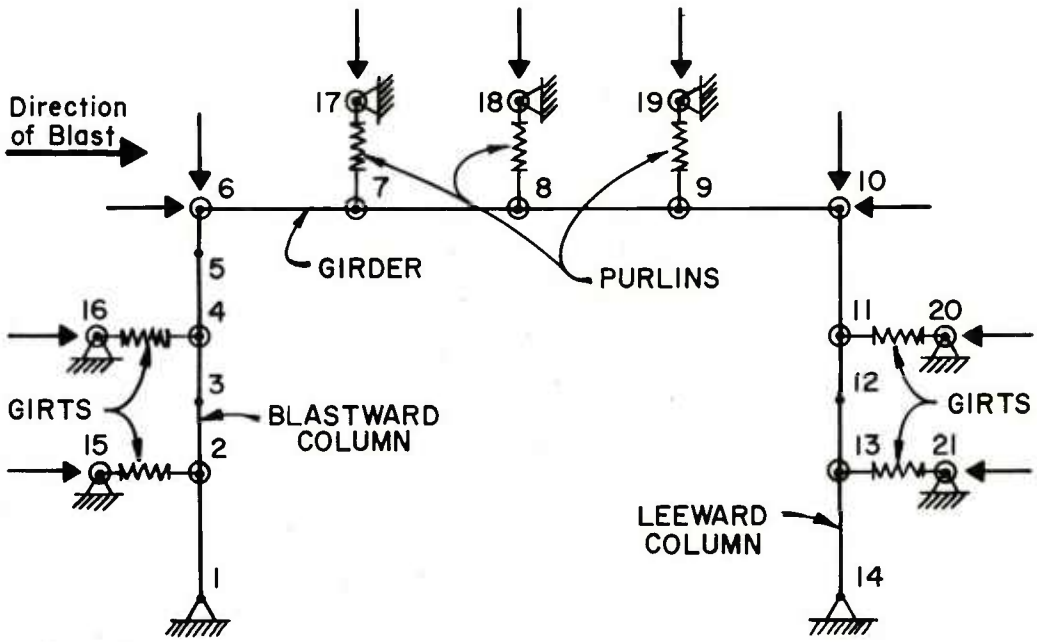

NOTE:

FOR NODE DIMENSIONS & LEGEND, SEE FIGURE 19.

Figure 33. Basic transverse frame model including purlins and girts

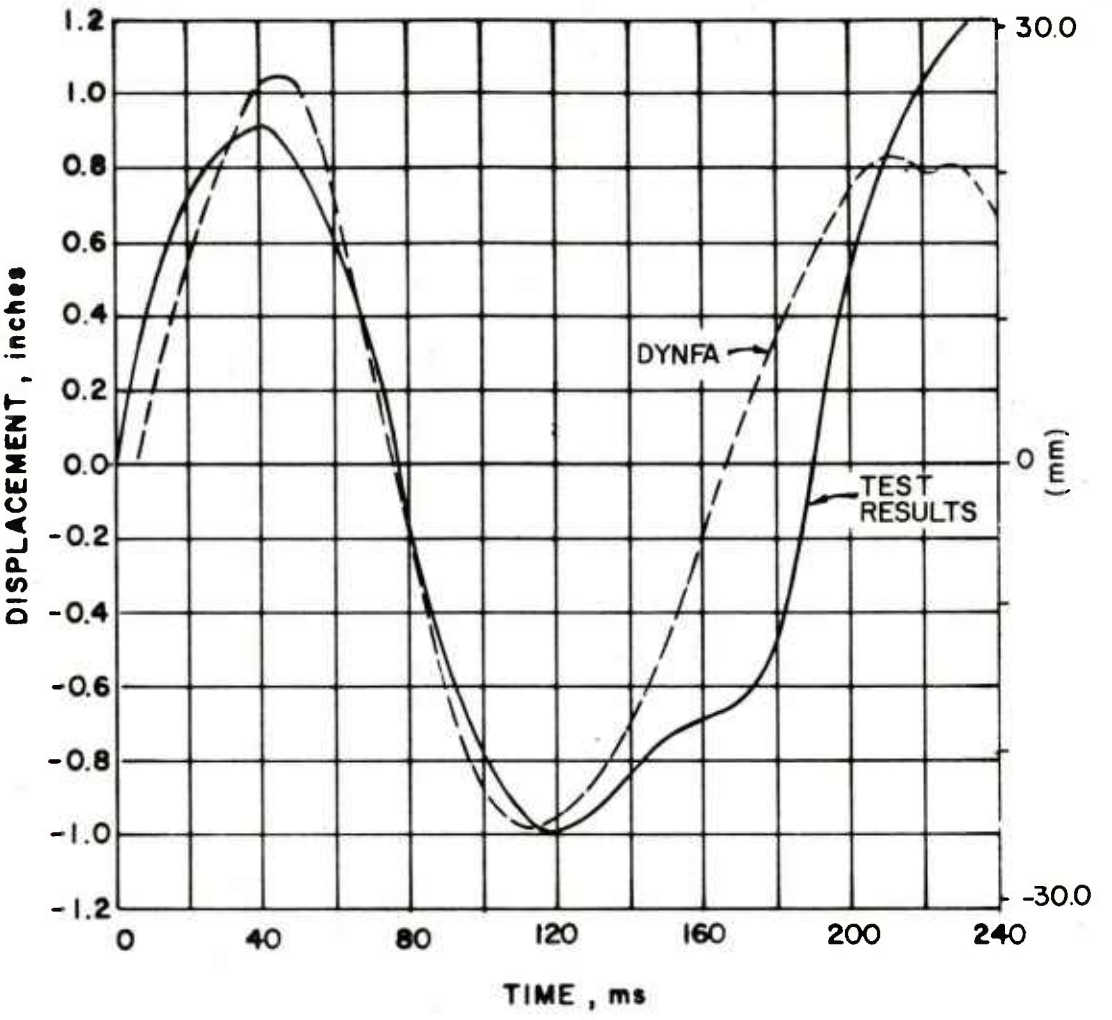

Figure 34. Center frame side-sway displacement, test and analytical results for Test 3

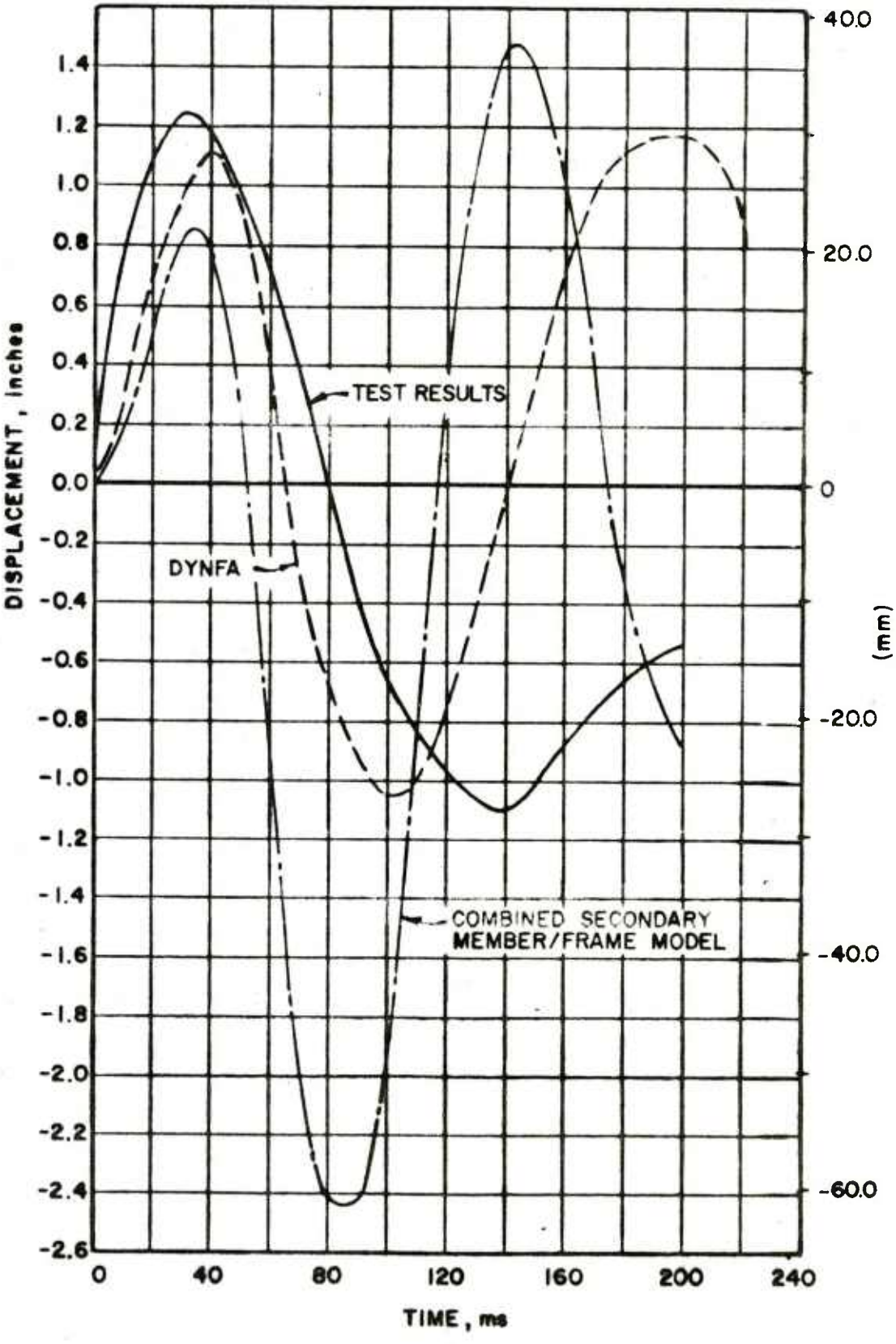

Figure 35. Center frame side-sway displacement, test and analytical results for Test 4

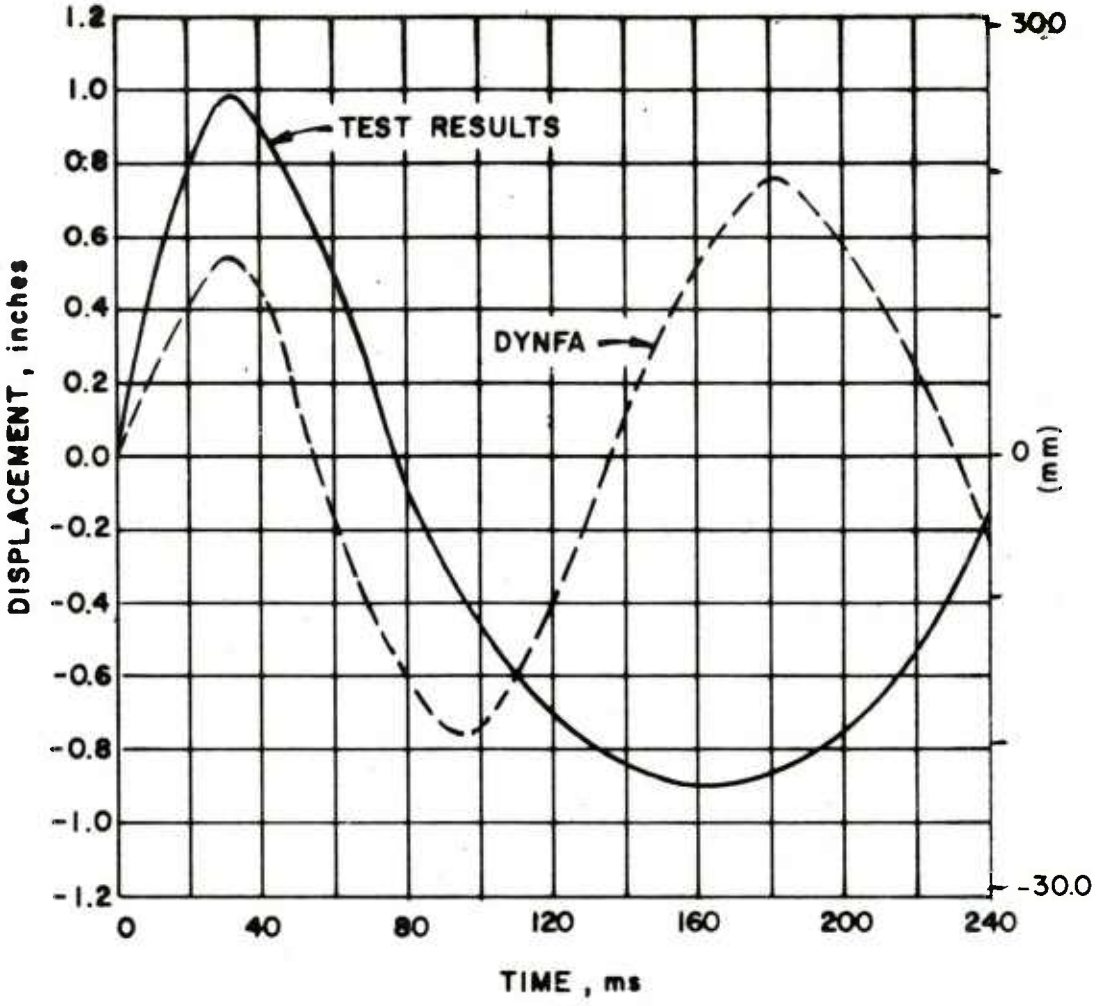

Figure 36. Center frame side-sway displacement, test and analytical results for Test 5

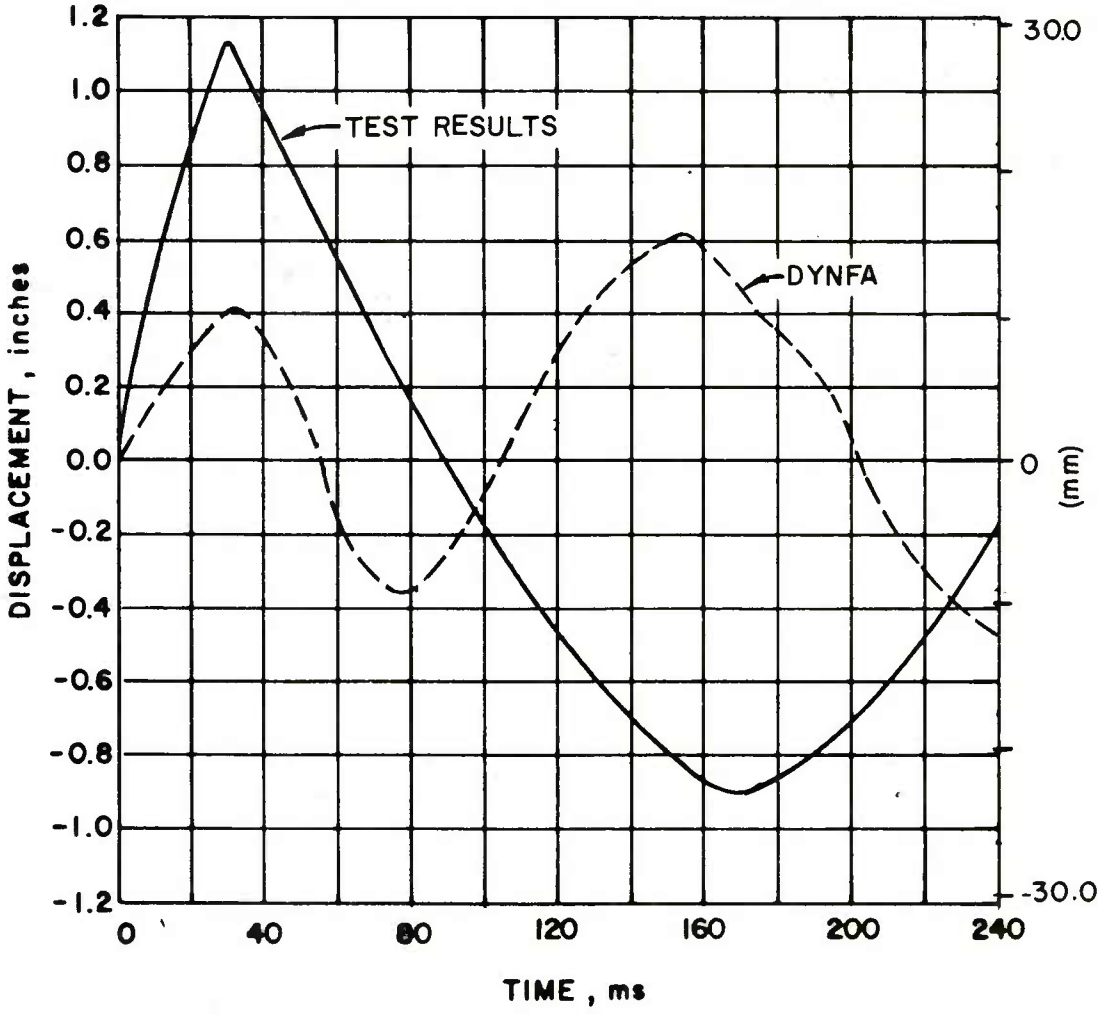

Figure 37. Center frame side-sway displacement, test and analytical results for Test 6

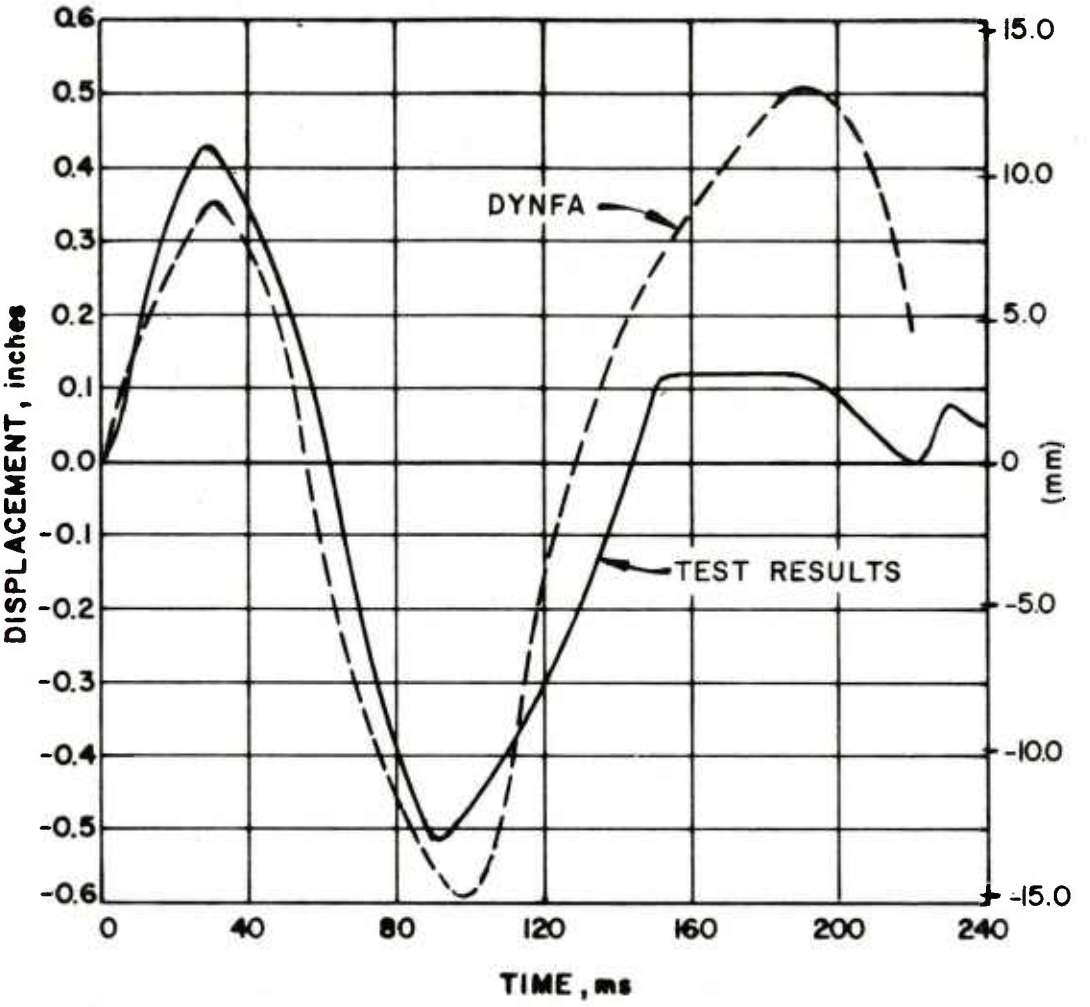

Figure 38. Rigid end frame side-sway displacement, test and analytical results for Test 5

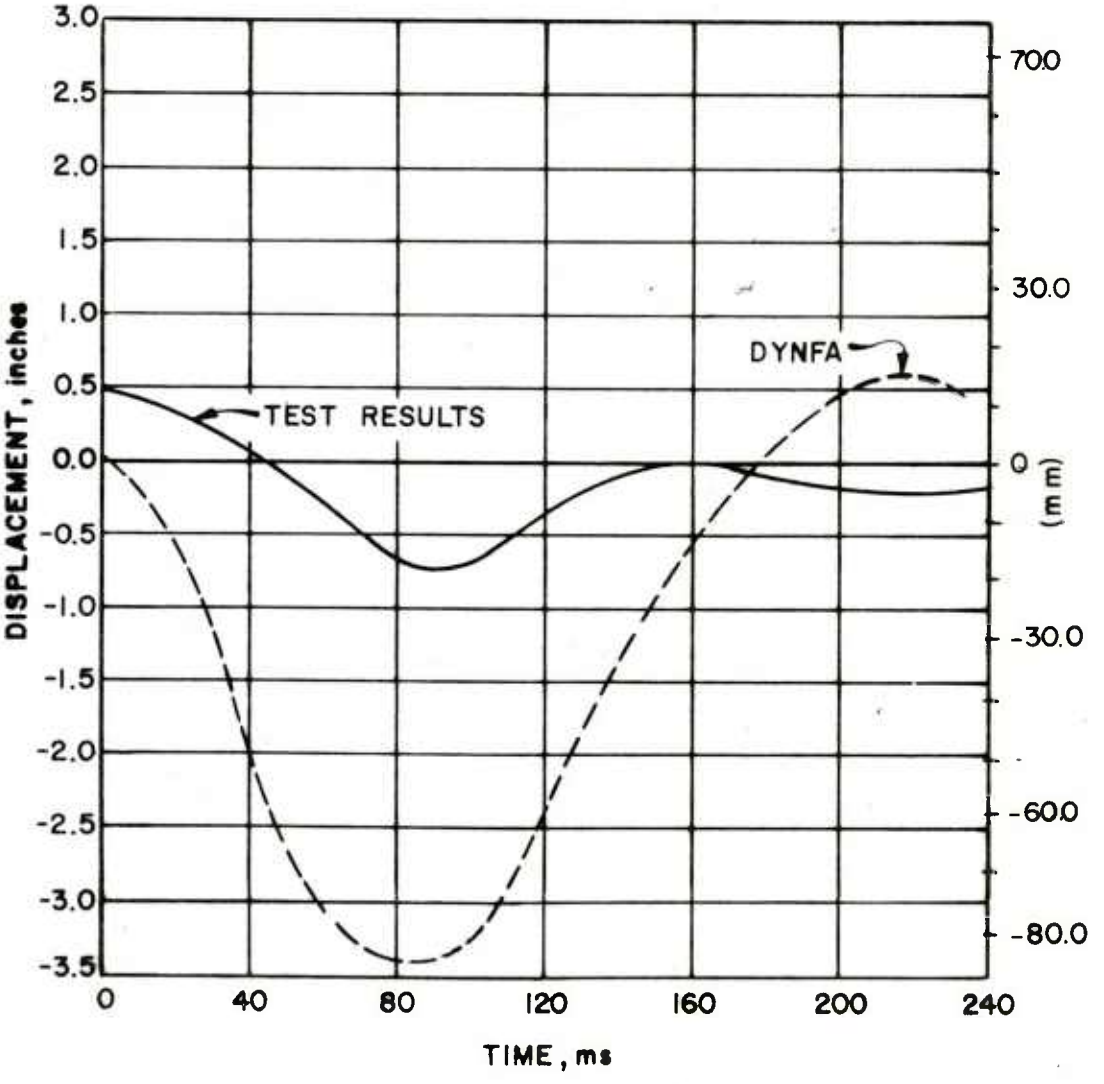

Figure 39. Rigid end frame side-sway displacement, test and analytical results for Test 7

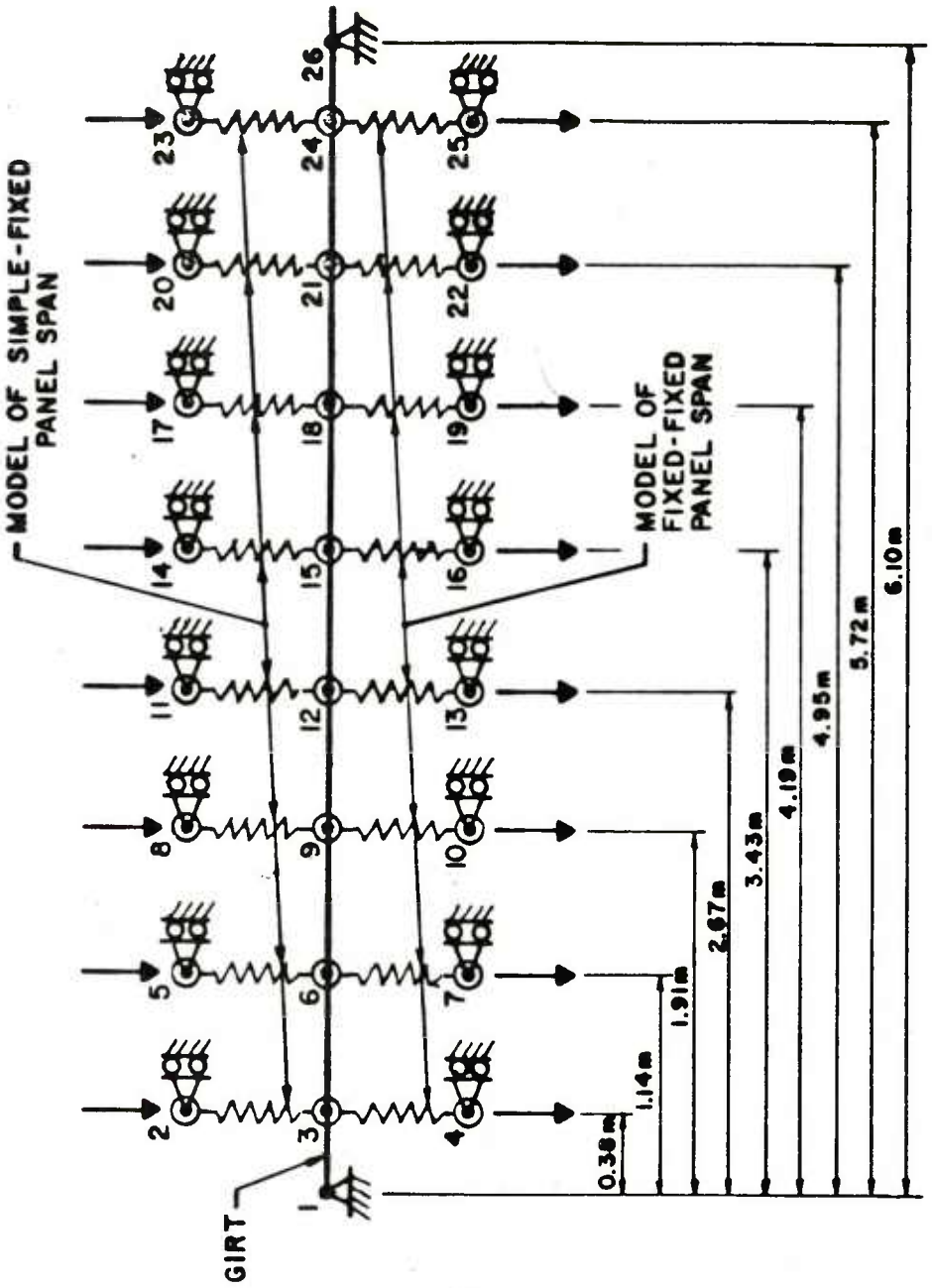

Figure 40. Combined wall panel/girt interaction model

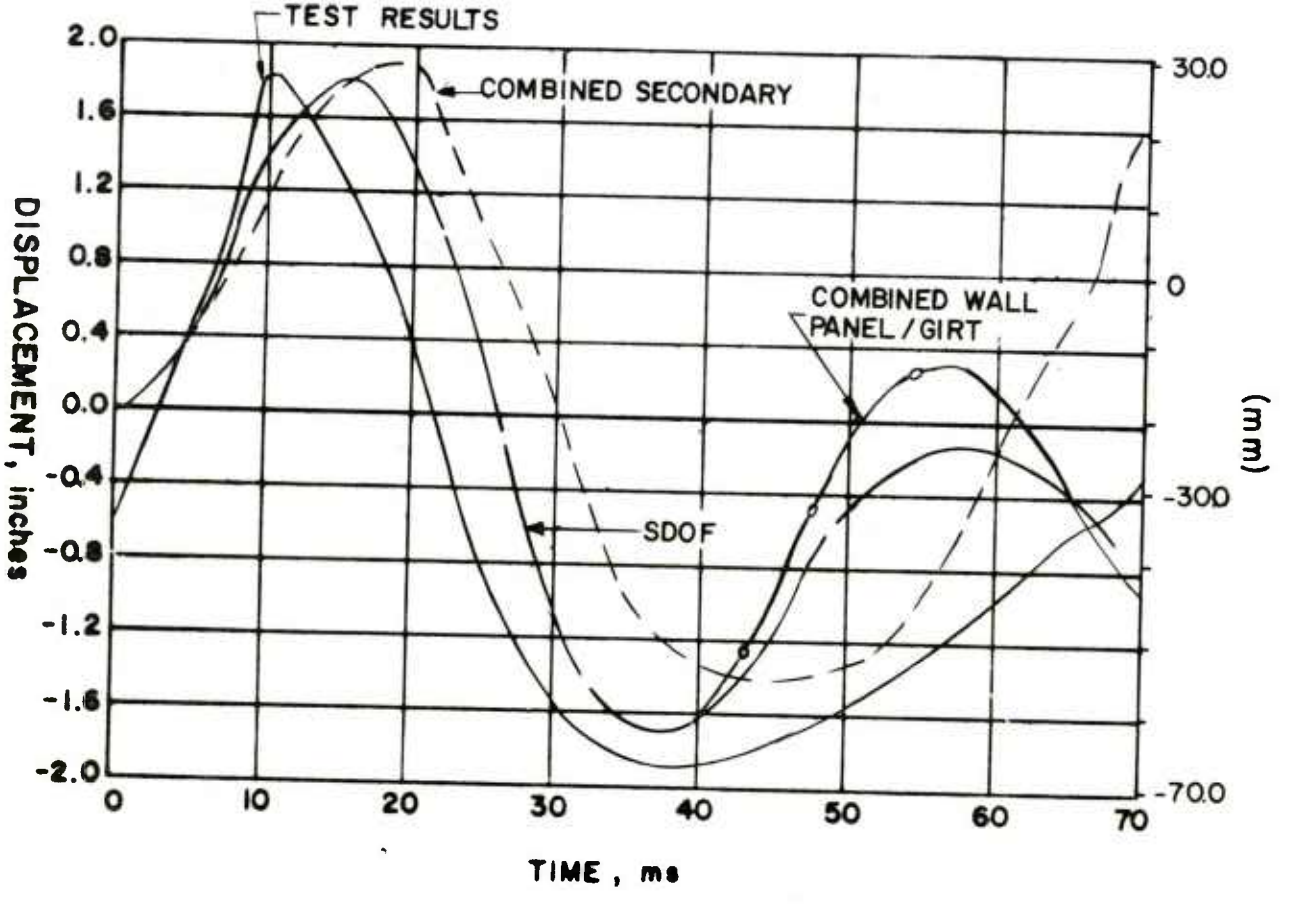

Figure 41. Lower girt response, test and analytical results for Test 4

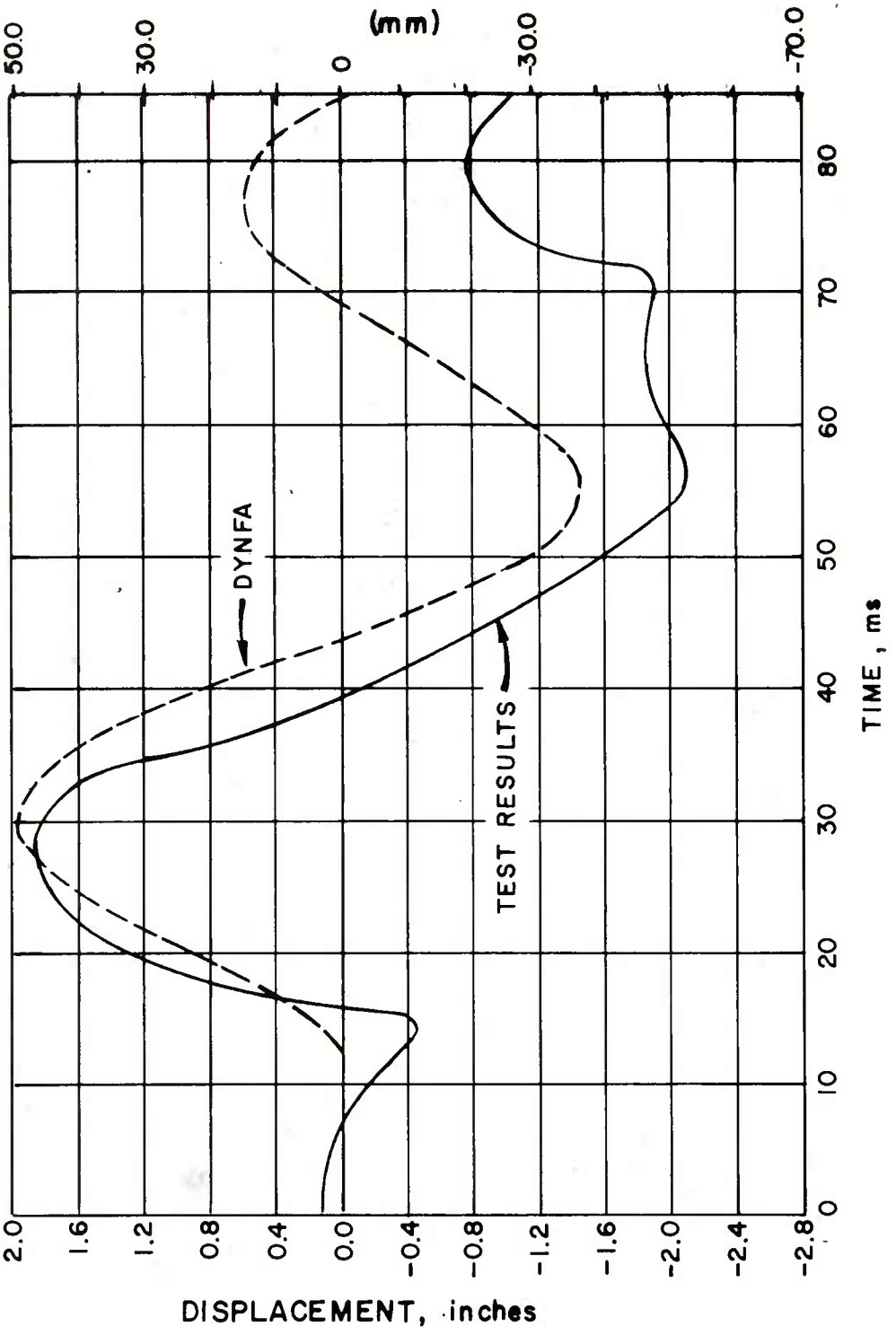

Figure 42. Purlin response, test and analytical results for Test 4

APPENDIX A

SPECIAL PROVISIONS FOR FRAME STRUCTURES

INTRODUCTION

The basic objective of the tests performed on the pre-engineered and strengthened steel buildings was to determine if the dynamic analysis, based on the methods and procedures given in Reference 3, provided a reasonable estimate of the response of a rigid frame when subjected to blast loadings.

A series of parametric studies (as indicated earlier in this report) were performed to assess the impact of the following factors on the response of the frame:

(i) The actual yield stresses of the materials used in the fabrication of the frame.

(ii) The negative phase of the blast loading.

(iii) The interaction between the response of the secondary members and the main frames.

Again, as stated earlier in this report, it was discovered that these factors greatly affected the responses of the main frames and should therefore be incorporated in the analysis procedures provided in Reference 3.

EFFECT OF ACTUAL STRENGTH OF MEMBERS

As stated in References 2 and 3, the design and analysis of blast-resistant structures is based on the minimum specified yield stress of the materials [usually 207 .x 10^6 kPa (36,000 psi)]. However, it has been discovered that in most cases, the actual materials used for the fabrication of the primary and secondary members of the rigid frame have yield stresses in excess of the specified minimum. Whenever possible, tensile tests should be performed to determine the actual strengths of the members of the frame and these yield stresses should be used in the analysis.

COMPUTATION OF BLAST LOADS

The development of loading functions for the frame analysis consists of subdividing the exposed area into a series of

tributary loading areas (each associated with a given mass point on one of the exterior members of the frame) and preparing the pressure-time histories.

The procedures for developing the loading functions for the frame analysis are described in detail in Chapter 5 of Reference 3. However, these procedures consider only the positive phase of the blast loading; the negative phase is not considered. As stated in Reference 6, the negative phase of a blast wave can roughly be compared with the cubical parabola:

$$p = p^- \times 27/4 \times (T/T^-)[1 - (T/T^-)]^2 \qquad \text{Equation A.1}$$

where p = negative pressure at time T

p^- = maximum negative pressure

T = negative phase time of interest

T^- = duration of negative phase.

By differentiating Equation A.1 with respect to T and setting it equal to zero, it is found that the rise time of the negative peak pressure (or the maximum peak pressure) occurs at one-third the duration of the negative phase, compared to one-eighth of the duration recommended in Section 4-13 of Reference 4.

In the tests performed on the pre-engineered building, it was realized that the pressures acting on the rear wall were for less than that which would be predicted by the procedures outlined in TM 5-1300. It is therefore recommended that for frame analysis, the positive phase blast loads acting on the rear wall of a structure be taken equal to 60 percent of the incident overpressure. However, for the local design of the rear wall itself, the procedures of TM 5-1300 should be adhered to. On the other hand, the magnitude of the negative pressures acting on the rear wall should not be reduced.

Figures A.1, A.2 and A.3 show typical waveforms on the blastward wall, blastward and leeward ends of the roof of a rigid frame. As stated in Section 5.3 of Reference 3, the waveforms have to be phased on a time scale to simulate the effect of the blast wave traversing the structure. The phased waveforms have to be modified again to account for the time lag effects and non-uniformity in the loading at each mass point. This latter modification is not required for the negative peak pressure because the ratio of the length of tributary area, a, (for an individual mass point) to twice the product of the duration of

the negative phase and the shock front velocity ($2Ut_{dr}$) is usually very small, and can, for most cases, be considered to be zero.

DEVELOPMENT OF MODEL

The initial task in the analysis is the formulation of the analytical model of the frame under consideration. The model should accurately reflect the configuration, stiffness characteristics, and the mass distribution of the structure. A detailed description of the modeling techniques is provided in Chapter 4 of Reference 3.

However, the methods of Reference 3 provide for the analysis of the main building frames based on the model shown in Figure 31 of this report. To incorporate the interaction of the secondary members (girts and purlins) with the main frames, an analytical model similar to the one shown in Figure 33 can be used. In this model, the girts and purlins are represented by a series of Single-Degree-Of-Freedom (SDOF) systems with equivalent masses and stiffnesses. These SDOF models are attached at the exact locations where the girts and purlins are attached to the frame. The blast loadings are applied directly to these SDOF models; hence, the direct loading on the frame members consists of the reactions of the girts and purlins.

PLACEMENT OF NODAL POINTS IN THE MODEL

Nodal points in the model are usually positioned at the following locations:

1. The intersection of two or more frame members or the connection of frame members to a supporting structure (such as foundation).

2. Intermediate points on the exterior members to accommodate mass points.

3. Intermediate points on exterior members, other than mass points, where additional response information (deflections, bending moments) are required.

4. Intermediate points on members with gradual or abrupt variations in shape, or at the locations of structural discontinuities.

A detailed description of the above four items is presented in Reference 3.

DESIGNATION OF DYNAMIC DEGREES OF FREEDOM

With the model completely defined in terms of beam elements and nodal points, each discrete mass of the model must be assigned a degree of freedom (either horizontal or vertical) as well as magnitude. The purpose of this is to reproduce the forces developed by the accelerating mass of the structure when the frame responds to the blast loads.

Intermediate mass points on exterior members are allotted one dynamic degree of freedom. The direction of these degrees of freedom is always normal to the longitudinal axis of the member. To develop the primary sidesway response of the frame, each nodal point corresponding to a girder/column intersection is assigned a horizontal and a vertical dynamic degree of freedom.

COMPUTATION OF NODAL MASSES

A detailed description of the computation of the nodal masses is provided in Section 4.3 of Reference 3. However, when the interaction of the secondary members with the main frame's responses is taken into account, slight adjustments have to be made in the procedure in Section 4.3.

The ends of the SDOF members (girts and purlins) are modeled as support points. These nodes are also considered as mass points and an equivalent panel mass is assigned to them. In the example that follows in this appendix, a method of assigning equivalent masses to these nodal points is given. The distribution of the panel mass among the other nodal points follows the procedure given in Reference 3.

In the following sections, an attempt is made to illustrate how procedures in References 2 and especially 3 can be extended to incorporate those factors that affect the responses of the main frames. The example presented here illustrates how the strengthened steel building, described in the first part of this report, was analyzed.

Example: Modeling of Frame Structures for Analysis with the DYNFA Program

Problem: Construct the analytical model of the unbraced, rigid center frame of a single-story strengthened steel building (Appendix B) subjected to a normal shock wave. Prepare the related input data for DYNFA (Reference 3).

Procedure:

Step 1. Establish the design parameters:

a. Geometry of frame

b. Sizes of primary frame members, secondary members, decking and siding

c. Support conditions of frame

d. Post-explosion condition of structure

e. Static tensile stress, F_y

f. Dynamic increase factor, c

g. Modulus of Elasticity, E.

These data are available from the Engineering Drawings and tensile test results.

Step 2. Establish the scope of the model on the basis of the guidelines given in Section 4.2 of Reference 3. Sketch a line diagram of the frame to be analyzed; designate nodal points at the appropriate locations on the model. Assign identification numbers to the nodal points and elements as shown in Figure A.4 and specify which nodal points are designated as mass points (see Sections 4.2 and 8.3 of Reference 3).

Step 3. Assign dynamic degrees of freedom to the mass points of the model as shown in Figure A.5, using the guidelines given in the previous section of this appendix and in Section 4.3 of Reference 3.

Step 4. Compute the masses of the individual panels of the walls and roof with the tributary strip supported by the frame.

Step 5. Compute the concentrated masses assigned to the dynamic degrees of freedom on each panel. Tabulate these masses as shown in Table A.1. Include the mass of the transverse girders in this tabulation.

Step 6. Determine cross-sectional properties and capacities of the frame members. The cross-sectional properties required for the analysis are:

a. Area of cross-section, A

b. Moment of inertia about an axis normal to the plane of the frame, I_x or I_y, as the case may be.

The cross-sectional properties required to compute the member capacities are:

a. Area of cross-section, A

b. Radii of gyration, r_x and r_y

c. Plastic section modulus, Z_x or Z_y, as required.

The capacities required for the analysis are:

a. Ultimate dynamic load capacity in axial tension, P_p (Equation 13, Ref. 3).

b. Ultimate dynamic load capacity in axial compression, P_u (Equation 14, Ref. 3).

c. Ultimate bending capacity in the absence of axial load, M_{mx} or M_{my}, depending upon the axis of bending (Equation 5a or 5b, Ref. 3).

Tabulate, as shown in Table 4.2, the nodal connectivities, cross-sectional properties and the axial load and bending capacities for all elements. Indicate location of local pins in this tabulation, if any, utilized in the analysis.

Step 7. Using the guidelines provided in Figures 23 and/or 24 of Reference 3, establish the dimensions of the tributary loading areas that are assigned to the mass points on the frame. Compute the tributary areas and tabulate both the dimensions and the areas as shown in Table A.3. Note that the tributary areas for the girts and purlins, modeled as SDOF systems, are equivalent to the nodes of the main frame to which they are connected. Combine adjacent coplanar areas assigned to the mass point (Figure A.6).

Step 8. Establish the following blast load parameters:

a. Location of the charge

b. Charge weight, W

c. TNT Equivalency. Note that the safety factor is not included in an analysis problem.

d. Normal distance, R_A, from the center of the charge to the blastward and leeward walls of the building.

Calculate equivalent charge weight, W_E = W x TNT Equivalency.

If frame gages are located on the structure, to accurately determine the blast loading at or near each nodal mass point, then this and the next four steps (Steps 8 - 12) can be ignored. However, it shall be assumed that no gages are present on the structure being analyzed.

Step 9. a. Compute the scaled distances from the center of the charge to the blastward and leeward ends of the building:

$$Z = R_A/W_E^{1/3}$$

b. Enter Figure 4-5, 4-11 or 4-12 of Reference 4 with each of the scaled distances determined above, and read from the appropriate curves:

Peak positive and negative incident pressures, P_{so} and P_{so}^-

Scaled unit positive and negative impulses, $i_s/w^{1/3}$ and $i_s^-/w^{1/3}$

Shock front velocity, U.

c. Enter Figure 4-5 or 4-12 of Reference 4 with the scaled distance for the blastward wall and read from the appropriate curves:

Peak positive and negative normal reflected pressures, P_r and P_r^-

Scaled unit positive and negative normal reflected impulses, $i_r/w^{1/3}$ and $i_r^-/w^{1/3}$

d. Tabulate all values as shown in Table A.4.

Step 10. Using the blast wave parameters determined in Steps 9b and 9c, construct the reflected pressure-time history on the blastward wall:

a. Calculate clearing time, t_c:

$$t_c = 3S/U$$

where S = height of blastward wall or one-half its width.

b. Calculate fictitious positive and negative phase durations, t_{of} and $\bar{t}_{of}$:

$$t_{of} = 2i_s/P_{so}$$

c. Determine peak dynamic pressure, q, from Figure 4-66 of Reference 4 for P_{so}.

d. Calculate $P_{so} + C_D q_o$. Obtain C_D from paragraph 4-146 of Reference 4.

e. Calculate fictitious reflected positive and negative pressure durations, t_r and $\bar{t}_r$:

$$t_r = 2i_r/p_r \text{ and } \bar{t}_r = 2\bar{i}_r/\bar{p}_r$$

f. Calculate the rise time of the negative pressure-time curve, $\bar{t}_{pk}$:

$$\bar{t}_{pk} = 0.333\bar{t}_r$$

g. Construct the reflected pressure-time curve as shown in Figure A.7.

h. Tabulate all values as shown in Table A.4.

Step 11. Using the blast wave parameters determined in Step 9b, determine the combined incident/drag pressure-time histories at the blastward and leeward ends of the roof as follows:

a. Calculate fictitious positive and negative phase durations, t_{of} and $\bar{t}_{of}$:

$$t_{of} = 2i_s/P_{so} \text{ and } \bar{t}_{of} = 2\bar{i}_s/\bar{P}_{so}$$

b. Determine peak dynamic pressure q from Figure 4-66 of Reference 4 for P_{so}.

c. Calculate $P_{so} + C_D q_o$ for the blastward end of roof. Obtain C_D from paragraph 4-14c of Reference 4. For the combined incident/drag pressure at the leeward end of the roof, use 60 percent of incident overpressure.

d. Tabulate all values as shown in Table A.4.

Note that one negative pressure-time history is assumed for all points on the roof and another for all points on the leeward wall.

Step 12. a. Determine the pressure history at the location of each mass point on the roof by linear interpretation for both the peak pressure and the duration, using the data computed in Step 11 and Equations 15 and 16 of Reference 3.

b. Determine the pressure history for each mass point on the leeward wall using Equation 18 of Reference 3 and the data computed in Step 11.

c. In a similar manner, interpolate for the shock front velocities at the mass points on the roof, and extrapolate for these quantities at the mass points on the leeward wall.

Tabulate the peak pressures, durations and shock front velocities as shown in Table A.5.

If large pressure differentials occur between the blastward and leeward ends of the roof, a more refined interpolation for the pressure-time histories may be required. Refer to Section 5.3 of Reference 3 for guidance, if this is necessary.

Step 13. Determine the values of parameters a and D for each tributary area. Refer to Figures 30, 32, 33 and 34 for guidance when computing these quantities. Tabulate all values as shown in Table A.5.

Step 14. a. Using the pressure histories and shock front velocities determined in Steps 10 and 12, the values for a and D determined in Step 13, and the equations given in Section 5.3 of Reference 3, compute the following blast-loading parameters for each tributary area:

(1) Travel time, t_a, computed using Equation 19 (Ref. 3).

(2) Rise time, t_{rt}, computed using Equation 20 (Ref. 3).

(3) Average peak positive pressure, $(P_{pk})_{AVG}$, computed using Equation 21 (Ref. 3).

(4) Time, t_{pk}, at which $(P_{pk})_{AVG}$ occurs, computed using Equation 23 (Ref. 3).

(5) Duration of the pressure loading on the tributary area, t_{DI}, computed using Equation 25 (Ref. 3).

(6) Time at which the positive pressure on the tributary area decays to zero, t_T, computed using Equation 26 (Ref. 3).

(7) Time at which negative pressure is maximum, t^*_{pk}, computed as indicated in Table A.5.

(8) Time at which the negative pressure decays to zero, t^*_T, computed as indicated in Table A.5.

Tabulate these data as shown in Table A.5.

b. Using the parameters determine above, generate the digitized data defining the pressure-time history input for DYNFA as described in Section 8.9 of Reference 3 and illustrated in Figure A.8. Assign an identification number for each pressure waveform entered in the DYNFA input.

Step 15. Compute the dead and, where appropriate, live loads acting on the frame. Distribute these quantities as uniform and concentrated loads as described in Section 8.10 of Reference 3. Tabulate all values as shown in Tables A.6 and A.7.

Step 16. Compute the integration time interval on the basis of either Equation 34 or 35 of Reference 3 (whichever governs). In addition, specify the desired duration of the response on the basis of the sidesway natural period of the frame as computed using the data in Table A.8 of this appendix and either Equation 36 or 37 (as the case may require).

Step 17. Locate the origin of the global system for the model, establish the direction of the global axes, (Section 8.4 of Reference 3), and specify the nodal coordinates (Fig. A.4).

Step 18. Transfer the nodal coordinates, together with the tabulated data (as contained in Tables A.1 through A.7) to punched cards using the input formats for DYNFA, which are specified in Section 8.13 of Reference 3.

Example: Construct the analytical model of the unbraced, rigid center frame of the single-story strengthened steel building (Appendix B) subjected to a normal shock wave, and prepare the related input data for DYNFA.

Required: The analytical model and all related input data for DYNFA.

Step 1. a. Geometry of center frame on Column Line 3 (see Appendix B) with the girts and purlins included as springs (Figure A.4).

b. Sizes of the primary frame members:

(1) Roof girder W14 x 68

(2) Columns W14 x 84

Sizes of secondary members, decking and siding are shown in Appendix B.

c. Pin-ended column supports

d. Reusable structure

e. From the tensile test results:

(1) Columns: F_{yAVG} = 251 x 10^3 kPa (36,410 psi)

(2) Girder: F_{yAVG} = 280.7 x 10^3 kPa (40,713 psi)

(3) Girts: F_{yAVG} = 273.6 x 10^3 kPa (39,680 psi)

(4) Purlins: F_{yAVG} = 327.1 x 10^3 kPa (47,433 psi)

f. c = 1.1

g. E = 207 x 10^6 kPa (30 x 10^6 psi).

Step 2. The center frame is modeled for analysis as shown in Figure A.4. The model includes the steel frame, purlins and girts. The foundation response is assumed to have a negligible impact on the frame's response.

Step 3. Assign dynamic degrees of freedom to the mass points of the model.

Consistent with the guidelines given in Section 4.3 of Reference 3, the dynamic degrees of freedom for the model are designated as shown in Figure A.5. Note that Mass Points 6 and 10 are assigned two dynamic degrees of freedom.

Step 4. Compute the masses of the individual wall and roof panels within the tributary strip supported by the frame (Fig. A.6).

a. Wall Panel:

(1) Siding: Type 2 - 4 x 12

Weight = 14.6 kg/m^2 (3 psf)

Mass = 14.6 x 6.1 x 4.2 = 374 kg
(832.5 lb)

(2) Columns: 125 kg/m (W14 x 84)

Length = 4.2 m (13.875 ft)

Mass = 4.2 x 125 = 525 kg
(1,165.5 lb)

(3) The mass of a wall panel, M_W, is:

M_W = 374 + 525 = 899 kg (1,998 lb)

b. Roof Panel:

(1) Decking, Weight = 18.6 kg/m^2 (3.8 psf)

Mass = 18.6 x 6.1 x 6.1 = 692.1 kg
(1,520 lb)

(2) Girder: 101 kg/m (W14 x 68)

Length = 6.1 m (20 ft)

Mass = 101 x 6.1 = 616.1 kg
(1,360 lb)

(3) Mass of Roof Panel, M_R, is:

M_R = 692.1 + 616.1 = 1,308.2 kg (2,880 lb)

c. Girts: 67 kg/m (W12 x 45)

Length = 6.1 m (20 ft)

Mass, m_g = 67 x 6.1 = 408.7 kg (900 lb)

d. Purlins: 32.7 kg/m (W14 x 22)

Length = 6.1 m (20 ft)

Mass, m_p = 32.7 x 6.1 = 199.5 kg (440 lb)

e. Transverse Girders: 59.5 kg/m (W14 x 40)

Length = 6.1 m (20 ft)

Mass, m_{tg} = 6.1 x 59.5

= 363 kg (800 lb)

Girt at Top: 67 kg/m (W12 x 45)

Length = 61 m (20 ft)

Mass = 6.1 x 67 = 408.7 kg (900 lb)

Channels: 14.6 kg/m (C7 x 9.8)

Length = 6.1 m (20 ft)

Mass = 6.1 x 14.6 = 89.1 kg (196 lb)

Two 4 x 12 Sections: 10.3 kg/m (6.9 lb/ft)

Length = 6.1 m (20 ft)

Mass = 6.1 x 10.3 = 62.8 kg
(138 lb)

Total Mass = 363 + 408.7 + 89.1 + 62.8

= 923.6 kg (2,034 lb)

Step 5. Compute the concentrated masses assigned to the dynamic degrees of freedom in each panel.

a. Intermediate mass points on blastward wall (Nodes 2, 4, 11, 13, 15, 16, 20 and 21)

For each node:

M_{panel} = 14.6 x 1.22 x 6.1 = 109 kg (240 lb)

M_{girt} = 67 x 6.1 = 408.7 kg (900 lb)

$M_{panel} + M_{girt}$ = 109 + 408.7

= 517.7 kg (1,140 lb)

$M_e = K_{LM} (M_{panel} + M_{girt})$

From Reference 5:

K_{LM} = (0.78 + 0.66)/2 = 0.72

M_e = 0.72 x 517.7 = 372.7 kg (820.8 lb)

$(M_{IH})_W = [M_W/(N_{DOFH} + 1)] + M_{girt}$

= [899/(2 + 1)] + 408.7

= 708.4 kg (1,566 lb)

$(M_{IH})^*_W = (M_{IH})_W - M_e$

= 708.4 - 372.7 = 335.7 kg (745.2 lb)

b. End Mass Points (Nodes 6 and 10)

(1) Horizontal

(a) Wall panel contribution:

$(M_{EH})_W = M_W/[2(N_{DOFH} + 1)]$

= 899/2(2 + 1) = 149.8 kg (333 lb)

(b) Girder contribution:

$$M_{girder} = M_g/2 = 616.1/2$$

$$= 308.1 \text{ kg } (680 \text{ lb})$$

(c) Transverse girder contribution:

$$M_{TGH} = 923.6 \text{ kg } (2{,}034 \text{ lb})$$

(d) Roof panel contribution:

$$(\bar{M}_{EH})_R = (M_{decking} + \sum_{1}^{hp} M_{purlin})/2$$

$$= [692.1 = 3(199.5)]/2$$

$$= 645.3 \text{ kg } (1{,}420 \text{ lb})$$

$$(M_{EH})_R^* = K_{LM}(\bar{M}_{EH})_R$$

$$= 0.72(645.3)$$

$$= 464.6 \text{ kg } (1{,}022.4 \text{ lb})$$

(2) Vertical direction:

(a) Roof panel contribution:

$$(M_{EV})_R = M_R/[2(N_{DOFV} + 1)]$$

$$= 1{,}308/[2(3 + 1)]$$

$$= 163.5 \text{ kg } (360 \text{ lb})$$

(b) Column contribution:

$$M_{col}/2 = 525/2 = 262.5 \text{ kg } (582.8 \text{ lb})$$

(c) Wall Panel contribution:

$$K_{LM}(M_{siding} + \sum_{i}^{ng} M_{girt}/2$$

$$= 0.78[374 + 2(408.7)]/2$$

$$= 464.6 \text{ kg } (1{,}026.7 \text{ lb})$$

(d) Transverse Girder contribution:

M_{TGV} = 923.6 kg (2,034 lb)

c. Intermediate Mass Points on Roof (Nodes 7, 8, 9, 17, 18 and 19)

M_{purlin} = 32.7 x 6.1 = 199.5 kg (440 lb)

M_{panel} = 1.52 x 6.1 x 18.6 = 172.5 kg

$M_e = K_{LM}(M_{panel} + M_{purlin})$

= 0.78(199.5 + 172.5) = 290.2 kg (639.6 lb)

$(M_{IV})_R = [M_R/(N_{DOFV} + 1)] = M_{purlin}$

= [1.308/(3 + 1)] + 199.5

= 526.5 kg (1,160 lb)

$(M_{IV})_R^* = 526.5 - 290.2 = 236.3$ kg (520.4 lb)

The concentrated masses for the wall and roof panels are tabulated in Table A.1. Note that these are several contributory masses assigned to the mass points at the girder/column connection.

Step 6. Determine the cross-sectional properties and capacities of the frame members:

a. Girts: W12 x 45

(1) Spring constants

$K = 384EI/5L^3$

$= [384 \times (207 \times 10^6) \times 0.00015]/5(6.3)^3$

= 10,505.9 kN/m (58,333.3 lb/in)

(2) Equivalent area of spring

$A = KL/E$

$= (10,505.91)(6.1)/(207 \times 10^6)$

$= 0.00031\ m^2$ (0.4.66 in^2)

(3) Resistance

$r_u = 8M_p/L^2$

(4) Moment capacity

$M_p = F_{dy}S = (1.1)(273.6 \times 10^3)(0.00095)$

$= 285.91$ kN-m (2,540.3 k-in)

(5) Capacity in axial direction

$r_u = 8(285.91)/(6.1)^2 = 61.5$ kN/m (0.353 k/in)

$P_p = P_u = r_uL = (61.5)(6.1)$

$= 375.12$ kN (84,720 lb)

b. Purlins W14 x 22

(1) Spring constant

$K_E = 307EI/L^3$

$= 307(207 \times 10^6)(0.00008)/(6.1)^3$

$= 22,398$ kN/m (132,580.3 lb/in)

(2) Equivalent area of spring system

$A = K_EL/E$

$= 22,398\ (6.1)/(207 \times 10^6)$

$= 0.00066\ m^2\ (1.06\ in^2)$

(3) Resistance

$r_u = 16M_u/L^2$

(4) Moment capacity

$M_u = F_{dy}S = (1.1)(327.1 \times 10^3)(0.00047)$

$= 169.1$ kN-m (1,507,895.1 lb-in)

(5) Capacity in axial direction:

$$P_p = P_u = r_u L = 16(169.1)/6.1$$

$$= 443.6 \text{ kN } (100{,}526.3 \text{ lb})$$

c. Girder W14 x 68:

$F_{dy} = 308.77 \times 10^3$ kPa

$E = 207 \times 10^6$ kPa

$l/r_y = 1.524/0.0625 = 24.4$

$M_{mx} = [1.07 - (24.4 \times \sqrt{380.77 \times 10^3})/262{,}394]M_{px}$

$\leq M_{px}$

$= 0.91\ M_{px}$

$M_{px} = F_{dy}Z_x = (380.77 \times 10^3)(0.00188)$

$= 580.5$ kN-m (5,150,194.5 lb-in)

$M_{mx} = 0.91(580.5) = 528.3$ kN-m

$P_p = F_{dy}A = (280.7 \times 10^3)(0.013) = 4{,}014$ kN

$P_u = 1.7\ F_aA$

$$F_a = \frac{[1 - (Kl/r)^2/2C_c^2]F_{dy}}{5/3 + 3/8[(Kl/r)/(C_c)] - [(Kl/r)^3/8C_c^3]}$$

$$C_c = \sqrt{2\pi^2E/F_{ay}} = \sqrt{2\pi^2(207 \times 10^6)/308.8 \times 10^3} = 115.$$

$l/r_y = 24.4$

$Kl/r_x = (0.75 \times 6.1)/0.153 = 29.9$

$$F_a = \frac{[1 - (29.9)^2/2(115)^2]308.8 \times 10^3}{5/3 + 3/8(29.9/115) - (1/8)(29.9/115)^3}$$

$= 168.9 \times 10^3$ kPa (24.5 ksi)

$P_u = (1.7)(168.9 \times 10^3)(0.013)$

$= 3{,}732$ kN (833.4 lb)

d. Column W14 x 84

$F_{dy} = cF_y = (1.1)(251 \times 10^3)$

$= 276.1 \times 10^3$ kPa (40,051 psi)

$M_{px} = F_{dy}Z_x = (276.1 \times 10^3)(0.0024)$

$= 656.1$ kN-m (5,807,395 lb-in)

l = distance between girts

$l/r_y = 1.22/0.077 = 15.9$

$kl/r_x = (1.5)(3.66)/0.156 = 35.2$

$M_{mx} = [1.07 - (15.9\sqrt{276.1 \times 10^3})/262,394]M_{px} \leq M_{px}$

$= 1,038\ M_{ps}$

Use $M_{mx} = M_{px}$ 656.1 kN-m (5,870,395 lb-in)

$P_p = F_{dy}A = (276.1 \times 10^3)(0.0159)$

$= 4,389.9$ kN (989,259.7 lb)

$P_u = 1.7\ F_aA$

$C_c = \sqrt{2\pi^2E/F_{dy}} = \sqrt{2\pi^2(207 \times 10^6)/276.1 \times 10^3}$

$= 121.7$

$$F_a = \frac{[1 - (35.2)^2/2(122)^2]276.1 \times 10^3}{5/3 + 3/8(35.2/122) - (35.2)^3/8(122)^3}$$

$= 149.3 \times 10^3$ kPa (21.4 psi)

$P_u = (1.7)(149.3 \times 10^3)(0.0159)$

$= 4,035.58$ kN (899.4 k)

Values for P_p, P_u and M_{mx} for all members are tabulated in Table A.2, together with the identification numbers and nodal connectivities for the elements representing them.

Step 7. Establish the dimensions of the tributary areas assigned to the mass points on the frame.

Dimensions of tributary areas for each nodal mass point are shown in Figure A.6. For the girts and purlins, the same tributary areas assigned to the nodes to which the girts and purlins are connected, are used also. The dimensions of each tributary area are shown in Table A.3.

Step 8. Establish blast loading parameters.

Note: In order to use figures in Reference 4, units will be kept in the normal convention. This applies through Step 14:

a. Location of charge: Surface burst

b. Charge weight: W = 2,000 lb

c. TNT Equivalency = 0.455

d. Normal distance to blastward wall: 162 ft

e. Normal distance to leeward wall: 182 ft

f. Effective charge weight: W_E = W x TNT Equivalency

= (0.455)(2,000)

= 910 lb.

Step 9. W_E = 910 lb; $W_E^{1/3}$ = 9.69 lb

Point on blastward wall:

a. R_A = 162 ft

Z = 162/9.69 = 16.72 ft/lb$^{1/3}$

b. Entering Figure 4-12, Reference 4 with:

Z = 16.72 ft/lb$^{1/3}$

P_{so} = 3.8 psi; $\bar{P}_{so}$ = 0.82

$i_s/w^{1/3}$ = 6.0 psi-ms/lb$^{1/3}$

$\bar{i}_s/W'^{3}$ = 5.4 7.8 psi-ms/lb$^{1/3}$

$i_s = (6.0)(9.69) = 58.12$ psi-ms

$\bar{i}_s = (5.4)(9.69) = 52.3$ psi-ms

$U = 1.2$ ft/ms

Steps 9a. and 9b. are repeated for the point on the leaward wall.

c. Entering Figure 4-12, Reference 4 with:

$Z = 16.72$ ft/lb$^{1/3}$

$P_r = 8.6$ psi

$\bar{P}_r = 1.7$ psi

$i_r/w^{1/3} = 13.0$ psi-ms/lb$^{1/3}$

$\bar{i}_r/w^{1/3} = 10.0$ psi-ms/lb$^{1/3}$

$i_r = (13)(9.69) = 125.98$ psi-ms

$\bar{i}_r = (10)(9.69) = 96.90$ psi-ms

d. All values are tabulated in Table A.4.

Step 10. Determine the reflected pressure-time history for the blastward wall:

a. $t_c = 35/U = 3(12.0)/1.25 = 28.8$ ms

b. $t_{of} = 2i_s/P_{so}$

$= 2(58.12)/3.8 = 30.59$ msec

c. $q_o = 0.34$ psi (Fig. 4-66, Ref. 4)

d. From paragraph 4-14b of Reference 4:

$C_D = 1.0$ for the blastward wall

$P_{so} + C_D q_o = 3.8 + 1.0(0.34) = 4.14$ psi

e. $t_r = 2i_r/P_r = 2(125.98)/8.6 = 29.3$ ms

$\bar{t}_r = 2\bar{i}_r/\bar{P}_r = 2(96.9)/1.7 = 114.0$ ms

f. $\bar{t}_{pk} = (1/3)\bar{t}_r = (1/3)(114.0) = 38.0$ ms

g. The reflected pressure-time history for the blastward wall is shown in Figure A.7.

h. All values are tabulated in Table A.4.

Step 11. Determine the combined incident/drag pressure-time history at the blastward end of the roof.

a. $t_{so} = 2i_s/P_{so}$

t_{of} = 30.59 ms (from Step 10b)

$\bar{t}_{of} = 2\bar{i}_s/\bar{P}_{so} = 2(52.33)/0.82 = 127.63$ ms

b. q_o = 0.34 psi (from Step 10c)

c. From paragraph 4-14c of Reference 4:

$C_D = -0.4$

Therefore, $P_{so} + C_D q_o = 3.8 + (-0.4)(0.34)$

$= 3.66$ psi

d. Steps 11a. and 11b. are repeated for the point at the leeward end of the roof, all values are shown in Table A.4. Note that one negative pressure-time history is assumed for all mass points on the roof and another for all points on the leeward wall.

Step 12. a. Determine the pressure-time histories at the locations of all mass points on the roof, using Equations 15 and 16 of Reference 3, and the data determined in Step 11.

At the blastward end of the frame:

$(P_{pk})_B = P_{so} + C_D q_o = 3.66$ psi

$(t_{dr})_B = t_{of} = 30.59$ ms

At the leeward end of the frame:

$(P_{pk})_L = P_{so} + C_D q_o = 3.19$ psi

$(t_{dr})_L = t_{of} = 32.4$ ms

$L_R = 20$ ft

For Node Point 8 on the roof, for example:

l_8 = 10 ft

Using Equations 15 and 16 of Reference 3:

$(P_{pk})_8$ = 3.664 - (3.664 - 3.196)10/20 = 3.43 psi

$(t_{dr})_8$ = 30.59 - (30.59 - 32.4)10/20 = 31.5 ms

b. Determine the pressure-time histories at the locations of all mass points on the leeward wall using Equation 18 of Reference 3 and the data determined in Step 11:

For Node Point 11 on the leeward wall:

l_{11} = 6.0 ft

$(P_{pk})_{11}$ = 0.60 x 3.8 = 2.28 psi

$(t_{dr})_{11}$ = 37.0 ms

The blast loading parameters defining the pressure waveforms (P_{pk}, t_{dr}) at all of the mass points are shown in Table A.5. For Nodes 15 through 21, values determined for Nodes 2, 4, 7, 8, 9, 11 and 13 are used, respectively.

c. The shock front velocity remains constant as the wave traverses the building; therefore, no interpolation or extrapolation of this quantity is required in this problem.

Step 13. Determine the values of a and D for the tributary areas.

Based on the dimensions of the tributary areas shown in Figure A.6, and using Figure 32 of Reference 3 for guidance, the values of a and D are shown in Table A.5.

Step 14. a. Compute the blast loading parameters for modifying the pressure-time histories at each mass point.

For Node Point 8:

From Step 12a. $(P_{pk})_8 = 3.42$ psi

$(t_{dr})_8 = 31.5$ ms

$U_8 = 1.2$ ft/ms

From Step 13: $a = 5.0$ ft, $D = 7.5$ ft

(From Eq. 19, Ref. 3) 1. $t_a = D/U_{AVG}$

$= 7.5/1.2 = 6.25$ ms

(From Eq. 20, Ref. 3) 2. $t_{rt} = a/U_8$

$= 5/1.2 = 4.17$ ms

(From Eq. 21, Ref. 3) 3. $(P_{pk})_{AVG} = P_{pk}[1 - (a/2Ut_{dr})]$

$(P_{pk})_{AVG8} = 3.43[1 - 5/(2 \times 1.2 \times 31.5)] = 3.2$ psi

(From Eq. 23, Ref. 3) 4. $t_{pk} = t_a + t_{rt}$

$= 6.25 + 4.17$

$= 10.42$ ms

(From Eq. 25, Ref. 5) 5. $t_{DI} = t_{rt}/2 + t_{dr}$

$= 4.17/2 + 31.5$

$= 33.59$ ms

(From Eq. 26, Ref. 3) 6. $t_T = t_a + t_{DI}$

$= 6.25 + 33.59$

$= 39.83$ ms

7. $t^*_{pk} = t_T + \bar{t}_{pk}$

$= t_T + (1/3)\bar{t}_{of}$

$$= 39.83 + (1/3)127.0$$

$$= 82.2 \text{ ms}$$

8. $t_T^* = t_T + \bar{t}_{of}$

$$= 39.83 + 127.0$$

$$= 166.8 \text{ ms}$$

The values of these parameters for other mass points are computed in a similar manner and all results are tabulated in Table A.5.

b. Generate the digitized data defining the pressure-time history input for DYNFA as described in Section 8.9 (Ref. 3).

For Node 8:

	Pressure		Time	
Point	Parameter	Value (psi)	Parameter	Value (sec)
1	-	0.00	-	0.0000
2	-	0.00	t_a	0.0056
3	$(P_{pk})_{AVG}$	3.20	t_{pk}	0.0104
4	-	0.00	t_T	0.0398
5	$\bar{P}_{pk}$	0.82	t_{pk}^*	0.0822
6	-	0.00	t_T^*	0.1668
7	-	0.00	t_f	0.2000

Step 15. Compute the dead loads acting on the frame and distribute these loads among the elements and nodal points of the model.

a. Distribution of the weight of a roof panel:

(1) The uniform load acting on the girder consists of its own weight.

w = 101.2 kg/m (5.67 lb/in)

This load is applied to Elements 6, 7, 8 and 9.

(2) The concentrated loads acting along the girder consists of the reactions of the purlins. Each purlin supports its own weight as well as one-third the weight of the decking with each roof panel.

From Step 4:

Weight of decking = 689.5 kg (1,520 lb)

Weight of purlin = 199.6 kg (440 lb)

Concentrated load acting along girder

(Nodes 7, 8 and 9)

= (1/4)(689.5) + 199.6 = 372 kg (820 lb)

The remaining one-fourth of the decking weight is supported by the transverse girders and, therefore, is applied at each girder/column connection.

Decking weight = 689.5 kg (1,520 lb)

Weight shared by Nodes 6 and 10 = 689.5/4

= 172.4 kg (380 lb)

Therefore, each node gets 172.4/2

= 86.2 kg (190 lb)

Apply this concentrated load to Nodes 6 and 10.

b. Distribution of the weight of a wall panel:

(1) The distributed load acting on the column is its own weight:

w = 125 kg/m (7 lb/in)

This load is applied to Elements 1 through 5, and 10 through 13.

(2) Weight of girt plus that of wall panel supported by girt is applied to the girt/column connection.

From Step 5:

Weight of panel = 14.6 x 6.1 x 1.22

= 108.9 kg (900 lb)

Total weight = 108.9 + 408.7

= 517.6 kg (1,140 lb)

Applied to Nodes 2, 4, 11 and 13.

(3) The portion of the wall panel supported by the transvere girder is:

1.22 x 6.1 x 14.6 = 108.9 kg (240 lb)

Applied to Nodes 6 and 10.

c. The weight of the transverse girders is applied directly to the girder/column connection (Nodes 6 and 10).

Transverse girder = 922.6 kg (2,034 lb)

(From Step 4)

The dead loads applied to the elements are tabulated in Table A.6; concentrated loads applied to the appropriate nodal points are shown in Table A.7.

Step 16. Compute the integration time interval and specify the duration of the response.

Integration time interval:

Check extensional modes for primary numbers.

$T_a = 2\pi\sqrt{LM_e/AE}$ (Eq. 34, Ref. 3)

a. Column: $L = 3.66$ m (12 ft)

M_e = Contributions from roof panel + wall panel + main girder + transverse girder

= 163.5 + 464.5 + 308.1 + 923.6

= 1,859 kg (4,100.7 lb)

= 1.860 kN-sec^2/m (10.6 lb-sec^2/in)

$A = 0.0159$ m^2 (24.7 in^2)

$E = 207 \times 10^6$ kPa (30×10^6 psi)

$T_a = 2\pi\sqrt{3.66(1.860)/(0.0159)(207 \times 10^6)}$

= 0.00902 sec

b. Roof girder: $L = 6.1$ m (20 ft)

M_e = Contributions from wall panel + roof panel + column + transverse girder

= 464.5 + 163.5 + 262.5 + 923.6

= 1,814.1 kg (4,003.5 lb)

= 1.814 kN-sec^2/m (10.4 lb-sec^2/in)

$A = 0.013$ m^2 (20 in^2)

$E = 207 \times 10^6$ kPa (30×10^6 psi)

$T_a = 2\pi\sqrt{6.1(1.814)/(0.013)(207 \times 10^6)}$

= 0.0128 sec

Check second bending modes of vibration of columns and roof girder.

$T_b = (1/C)\sqrt{M_i L^3/EI}$ (Eq. 35, Ref. 3)

(1) Column:

$C = 7.95$

$$M_i = \sum_{i=1}^{2} m_i = 2(335.7) = 671.4 \text{ kg } (1{,}490.4 \text{ lb})$$

$$= 0.671 \text{ kN-sec}^2/\text{m } (3.86 \text{ lb-sec}^2/\text{in})$$

$$L = 3.66 \text{ m } (12 \text{ ft})$$

$$I = 0.00039 \text{ M}^4 \ (928 \text{ in}^4)$$

$$E = 207 \times 10^6 \text{ kPa } (30 \times 10^6 \text{ psi})$$

$$T_b = \sqrt{(1/7.95)\ (0.671)(3.66)^3/(207 \times 10^6)(0.00039)}$$

$$= 0.00254 \text{ sec}$$

(2) Roof girder:

$$C = 19.2$$

$$L = 6.1 \text{ m } (20 \text{ ft})$$

$$M_i = \sum_{i=1}^{3} m_i = 3(236.3)$$

$$= 708.9 \text{ kg } (1{,}561.2 \text{ lb})$$

$$I = 0.00030 \text{ m}^4 \ (724 \text{ in}^4)$$

$$T_b = \sqrt{(1/19.2)\ (0.7089)(6.1)^3/(207 \times 10^6)(0.0003)}$$

$$= 0.00265 \text{ sec}$$

Inspection of these results indicates that the second bending mode of the column has the shortest period; hence, the integration time increment used is 1/20 of this period.

$$\Delta t = 0.00254/20 = 0.00013 \text{ sec}$$

Use $\Delta t = 0.00015$ sec.

Duration of response and number of integration-time increments:

Compute sidesway natural period of frame.

$T_s = 2\pi\sqrt{m_e/KK_L}$ (Eq. 36, Ref. 3)

From Step 4:

Mass of roof panel	1,308.0 kg
Mass of purlins (3 x 199.5)	598.5
Mass of transverse girder (2 x 923.6)	1,847.2
	3,753.7 kg
Mass of wall panel (2 x 899)	1,798.0 kg
Mass of girt (4 x 408.7)	1,634.8
	3,432.8 kg

$M_e = 3,753.7 + 3,432.8$

$= 7,186.5$ kg (10,800 lb)

$= 7.187 \text{kN-sec}^2/\text{m}$

From Table 8, Reference 3:

$K = (EI)_{ca}/H \times C_2[1 + (0.7 - 0.1)(n - 1)]$

$n = 1; \quad \beta = 0; \quad I_{ca} = I$

$D = I_g/L/[I_{ca}(0.75 + 0.25)/H]$

$= (0.003/6.1)/[90.00039)(0.75)/3.66] = 0.62$

Interpolating for C_2:

$D_2 = 0.62$ implies $C_2 = 4.99$

$K = (207 \times 10^6 \times 0.00039)(4.99)/(3.66)^3$

$= 6,216.6$ kN/m (46,524.56 lb/in)

$K_L = 0.55 (1 - 0.25\beta); \quad \beta = 0$

$T_s = 2\pi\sqrt{7.187/(0.55)(6,216.6)} = 0.288$ sec.

Here, the response will be computed for a duration T_f, of (1/1) T_s; therefore, the number of intergration-time increments, NDT, is:

$$NDT = 1 + T_g/\ t$$

$$T_f = (1/2)T_s = 0.104 \text{ sec}$$

$$t = 0.00015$$

$$NDT = 1 + 0.104/0.00015 = 694$$

Use 700 increments in the analysis.

Step 17. The origin of the global coordinate systems is located at Nodal Point 1, which is the lower left-hand support point of the model. The nodal coordinates are specified on the sketch of the model (Fig. A.2).

Step 18. The nodal coordinates, together with the data contained in Tables A.1 through A.7 are punched on input data cards according to the format specifications in Section 8.13, Reference 3. A listing of the input data deck for this problem is given in this appendix also. Note that the blast loads on the leeward walls and roof act in the negative directions of the global x- and y-axes, respectively. Therefore, the tributary areas on these surfaces are entered as negative quantities in the input to DYNFA. In addition, the dead loads act in the negative direction of the global y-axis. Therefore, in the DYNFA input, -y is entered as the direction of the element uniform loads and the concentrated nodal loads in Table A.6 are entered as negative quantities.

Note: The result of the analysis is shown in Figure A-9. Again, the computer results do not quite agree with the test results, but the difference between the predicted and the actual sidesway displacements is small compared to the overall height of the structure. In determining the TNT equivalency of the charged used (nitro-carbo-nitrate), it was necessary to plot the incident pressure, P_{so} versus the scaled distance, Z_A for both charges, TNT and nitro-carbo-nitrate (see Figure A-10). For some value of incident pressure P_{so}, the corresponding scaled distances for TNT and nitro-carbo-nitrate were read off Figure A-10. The TNT equivalency of the charge was determined as follows:

$$\text{TNT Equivalency} = (Z_A \text{ charge}/Z_A \text{ TNT})^3$$

This procedure is repeated for different incident pressures and a plot of scaled distance vs. TNT equivalence for the charge is made, as shown in Fig. A-11.

TABLE A.1

TABULATION OF CONCENTRATED MASSES AT MASS POINTS OF MODEL OF FRAME ON COLUMN LINE 3

Node Number of Mass Point	Horizontal Dynamic Degrees of Freedom		Vertical Dynamic Degrees of Freedom	
	Item	Mass (kg)	Item	Mass (kg)
2, 4, 11, 13	Exterior wall panel $(M_{IH})_W^*$	335.7	-	-
6, 10	Exterior wall panel $(M_{EH})_W$	149.8	Exterior wall panel	464.4
	Girder	308.1	Column	262.5
	Roof panel $(M_{EH})_R^*$	464.6	Roof panel $(M_{EV})_R$	163.5
	Transverse girder	923.6	Transverse girder	923.6
		1,846.1		1,814.0
7, 8, 9	-	-	Roof panel $(M_{IV})_R^*$	236.3
15, 16 20, 21	Exterior wall panel (M_e)	372.7	-	-
17, 18, 19	-	-	Roof panel	290.2

TABLE A.2

INPUT DATA FOR ELEMENTS OF MODEL OF FRAME

Member	Size	I.D. No.	Nodal Connectives End A	Nodal Connectives End B	Pin Codes End A	Pin Codes End B	A (cm^2)	I (cm^4)	M_m^* (kN - m)	P_p (kN)	P_u (kN)
Blastward Column	W14 x 84	1	1	2	0	0	159.4	38,626	656.1	4,390	4,036
		2	2	3	0	0	159.4	38,626	656.1	4,390	4,036
		3	3	4	0	0	159.4	38,626	656.1	4,390	4,036
		4	4	5	0	0	159.4	38,626	656.1	4,390	4,036
		5	5	6	0	0	159.4	38,626	656.1	4,390	4,036
Roof Girder	W14 x 68	6	6	7	0	0	129.0	30,094	528.3	4,014	3,732
		7	7	8	0	0	129.0	30,094	528.3	4,014	3,732
		8	8	9	0	0	129.0	30,094	528.3	4,014	3,732
		9	9	10	0	0	129.0	30,094	528.3	4,014	3 732
Leeward Column	W14 x 84	10	11	10	0	0	159.4	38,626	656.1	4,390	4,036
		11	12	11	0	0	159.4	38,626	656.1	4,390	4,036
		12	13	12	0	0	159.4	38,626	656.1	4,390	4,036
		13	14	13	0	0	159.4	38,626	656.1	4,390	4,036
Blastward Girt	W12 x 45	14	15	2	0	0	3.0	14,568	285.9	375.2	375.2
Blastward Girt	W12 x 45	15	16	4	0	0	3.0	14,568	285.9	375.2	375.2
Purlin	W14 x 22	16	7	17	0	0	6.8	8,283	169.1	443.6	443.6
Purlin	W14 x 22	17	8	18	0	0	6.8	8,283	169.1	443.6	443.6
Purlin	W14 x 22	18	9	19	0	0	6.8	8,283	169.1	443.6	443.6
Leeward Girt	W12 x 45	19	11	20	0	0	3.0	14,568	285.9	375.2	375.2
Leeward Girt	W12 x 45	20	3	21	0	0	3.0	14,568	285.9	375.2	375.2

TABLE A.3

TRIBUTARY AREAS FOR MASS POINTS OF MODEL OF FRAME

Node No. of Mass Point	Tributary Areas					
	For Horizontal Loads			For Vertical Loads		
	Loaded Surface	Dimensions of Area (m)	Area (m^2)	Loaded Surface	Dimensions of Area (m)	Area (m^2)
2, 4, 11, 13 15, 16, 20, 21	Blastward Wall	6.1 x 1.2	7.3	-	-	-
6, 10	Blastward Wall	6.1 x 1.2	7.3	Roof	6.1 x 0.8	4.9
7, 8, 9, 17, 18, 19	-	-	-	Roof	6.1 x 1.5	9.2

TABLE A.4

BLAST LOADING PARAMETERS

TABLE A.4

BLAST LOADING PARAMETERS

Location	R_A (ft)	Z (ft/lb$^{1/3}$)	P_{so} (psi)	$\bar{P}_{so}$ (psi)	$i_s/w^{1/3}$ (psi-ms/lb$^{1/3}$)	i_s (psi-ms)	$\bar{i}_s/w^{1/3}$ (psi-ms/$^{1/3}$)	$\bar{i}_s$ (psi-ms)	U (ft/ms)	P_r (psi)	P_r (kPa)
Blastward wall	162	16.72	3.8	0.82	6.0	58.12	5.4	52.33	1.2	8.6	59.30
Roof-blastward	162	16.72	3.8	0.82	6.0	58.12	5.4	52.33	1.2	-	-
Roof-leeward	192	14.3	3.3	0.78	5.4	53.46	5.0	49.50	1.2	-	-

$\bar{P}_r$ (psi)	$\bar{P}_r$ (kPa)	$i_r/w^{1/3}$ (psi-ms/ lb$^{1/3}$)	i_r (psi-ms)	$\bar{i}_r/w^{1/3}$ (psi-ms/lb$^{1/3}$)	$\bar{i}_r$ (psi-ms)	t_c (sec)	t_{of} (sec)	$\bar{t}_{of}$ (sec)	t_r (sec)	$\bar{t}_r$ (sec)	$\bar{t}_o/w^{1/3}$ (ms/lb$^{1/3}$)
1.7	15.9	13.0	125.98	10.0	96.91	0.0336	0.0306	0.128	0.0293	0.114	10.5
-	-	-	-	-	-	-	0.0306	0.128	-	-	10.5
-	-	-	-	-	-	-	0.0324	0.127	-	-	10.5

$\bar{t}_o$ (sec	q_o (psi)	C_D	$P_{so} + C_D q_o$ (psi)	$P_{so} + C_D q_o$ (kPa)	Location
0.102	0.34	1.0	4.14	28.54	Blastward wall
0.102	0.34	-0.4	3.66	25.24	Roof - Blastward end
0.102	0.26	-0.4	3.20	22.06	Roof - Leeward end

TABLE A.5

BLAST LOADING PARAMETERS FOR DYNFA

Node No. of Mass Point	Direction of Load	Blast Loading Parameters at Mass Points								Parameters a and D for Areas	
		P^a_{pk} (kPa)	t^a_{dr} (sec)	P^a_s (kPa)	t^a_c (sec)	P^-_{pk} (kPa)	t^-_{of} (sec)	t^-_{pk} (sec)	U (m/sec)	a (m)	D (m)
2, 15	Horizontal	59.3	0.0306	3.5	0.0288	5.65	0.128	0.038	-	-	-
4, 16	Horizontal	59.3	0.0306	3.5	0.0288	5.65	0.128	0.038	-	-	-
6	Horizontal	59.3	0.0306	3.5	0.0288	5.65	0.128	0.038	-	-	-
6	Vertical	25.3	0.0306	-	-	5.4	0.127	0.0423	381.0	0.76	0.00
7, 17	Vertical	24.5	0.0310	-	-	5.4	0.127	0.0423	381.0	1.52	0.76
8, 18	Vertical	23.6	0.0315	-	-	5.4	0.127	0.0423	381.0	1.52	2.29
9, 19	Vertical	22.8	0.0320	-	-	5.4	0.127	0.0423	381.0	1.52	3.81
10	Vertical	22.0	0.0324	-	-	5.4	0.127	0.0423	381.0	0.76	5.33
10	Horizontal	35.6	0.0293	-	-	5.7	0.128	0.038	381.0	1.22	6.10
11, 20	Horizontal	35.6	0.0293	-	-	5.7	0.128	0.038	381.0	1.22	7.32
13, 21	Horizontal	35.6	0.0293	-	-	5.7	0.128	0.038	381.0	1.22	8.53

[a]Parameters used to generate pressure-time input for horizontal loading applied to mass points on blastward wall.

$$t^-_{pk} = \begin{cases} (1/3)t^-_r \text{ for blastward wall} \\ (1/3)t^-_o \text{ for roof and leeward walls} \end{cases}$$

TABLE A.5 (cont'd)

BLAST LOADING PARAMETERS FOR DYNFA

Parameters Used For Modifying Pressure Wavefronts

t_a^b (sec)	t_{rt} (sec)	$(P_{pk}^b)_{avg}$ (kPa)	t_{pk}^b (sec)	t_{DI}^b (sec)	t_T^b (sec)	t_{pk}^* (sec)	t_T^* (sec)	t_f (sec)	Waveform ID
-	-	-	-	-	-	0.0673	0.1573	0.200	1
-	-	-	-	-	-	0.0673	0.1573	0.200	1
-	-	-	-	-	-	0.0673	0.1573	0.200	1
0.0	0.0021	24.4	0.0021	0.0316	0.0316	0.0739	0.1506	0.200	2
0.0021	0.0042	22.8	0.0063	0.0331	0.0352	0.0775	0.1601	0.200	3
0.0063	0.0042	22.1	0.0104	0.0336	0.0398	0.0821	0.1668	0.200	4
0.0104	0.0042	21.4	0.0146	0.0340	0.0445	0.0868	0.1715	0.200	5
0.0146	0.0021	21.3	0.0167	0.0335	0.0480	0.0903	0.1750	0.200	6
0.0167	0.0017	15.31	0.0183	0.0314	0.0481	0.0861	0.1761	0.200	7
0.0183	0.0033	14.87	0.0216	0.0323	0.0506	0.0886	0.1786	0.200	8
0.0217	0.0033	14.87	0.0250	0.0323	0.0539	0.0919	0.1819	0.200	9

[b] Parameters used to generate pressure-time input for loading applied to mass points on roof and leeward walls.

$t_{pk}^* = t_T + t_{pk}^-$

$t_T^* = t_T + t_{of}^-$

Table A.6

DEAD LOADS APPLIED TO ELEMENTS OF MODEL OF FRAME

Element No.	Uniform Load (kg/m)	Element No.	Uniform Load (kg/m)
1	125.0	11	125.0
2	125.0	12	125.0
3	125.0	13	125.0
4	125.0	14	0.0
5	125.0	15	0.0
6	101.2	16	0.0
7	101.2	17	0.0
8	101.2	18	0.0
9	101.2	19	0.0
10	125.0	20	0.0

TABLE A.7

DEAD LOADS APPLIED AT NODAL POINTS OF MODEL OF FRAME

Nodal Point	Item	Load (kg)
2, 4, 1	Wall panel	108.9
11, 13	Girt	408.2
		517.1
6,10	Roof panel	86.2
	Wall panel	108.9
	Transverse girder	922.6
		1,117.7
7, 8, 9	Roof panel	689.5
	Purlin	199.6
		889.1

TABLE A.8

STIFFNESS FACTORS FOR SINGLE-STORY MULTI-BAY RIGID FRAMES SUBJECT TO UNIFORM HORIZONTAL LOADING

Stiffness factor: $K = EI_{ca}/H^3 \times C_2[1 + (0.7 - 0.1)(n - 1)]$

n = number of bays

= base fixity factor[a]

$$\frac{I_g/L}{I_{ca}(0.75 + 0.25)/H}$$

I_{ca} = average column moment of inertia

$= I_c/(n + 1)$

	C_2		
	= 1.0	= 0.5[b]	= 0
0.25	26.7	14.9	3.06
0.50	32.0	17.8	4.65
1.00	37.3	20.6	6.04

[a]Values of C_2 are approximate for this

[b] = 1.0 for fixed base
= 0.0 for hinged base

[Source: Stea, W., et al., "Non-Linear Analysis of Frame Structures Subjected to Blast Overpressures", Report ARLCD-CR-77008, U.S. Army Armament Research and Development Command, Dover, N.J., May 1977.]

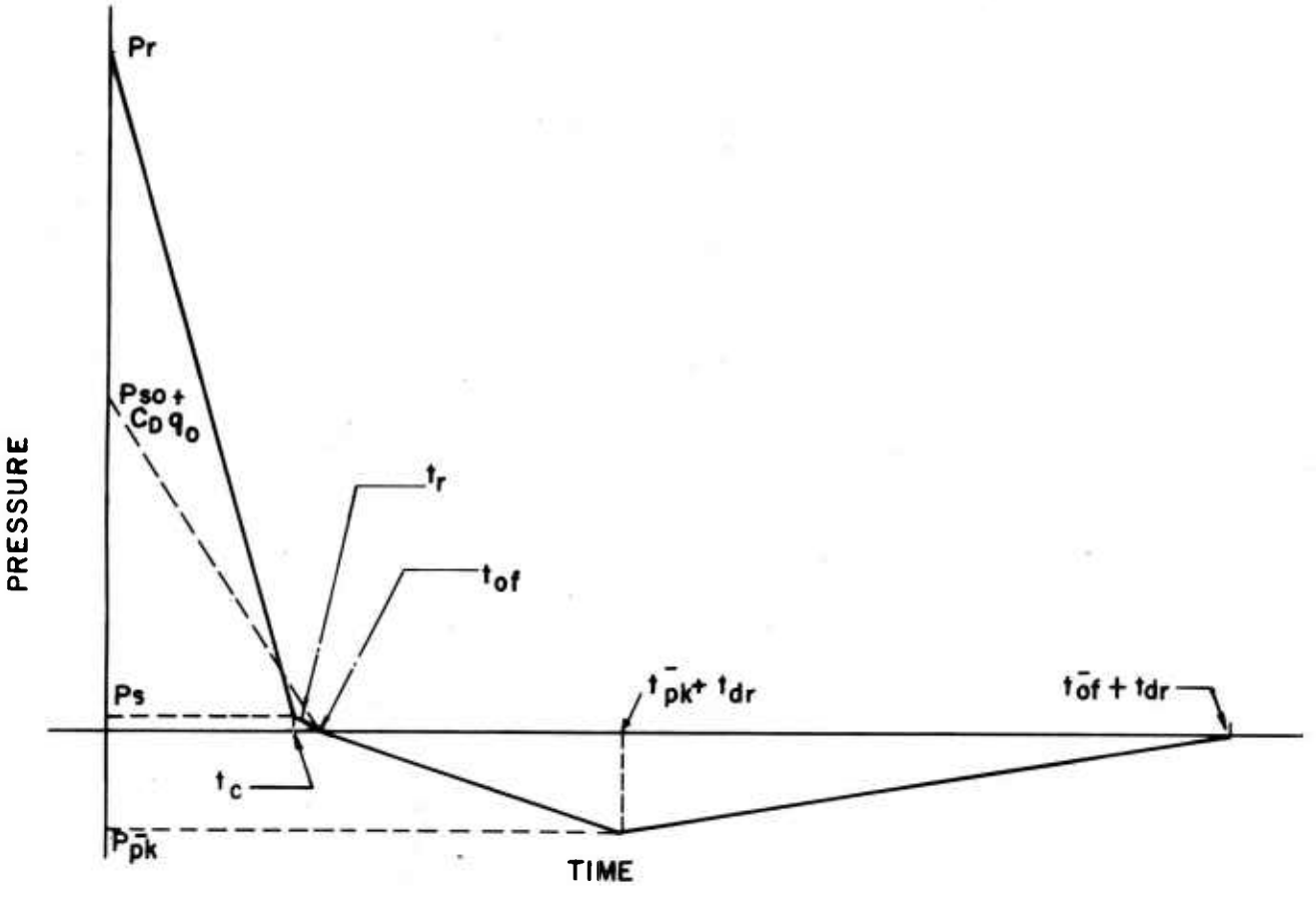

Figure A-1. LOADING ON BLASTWARD WALL

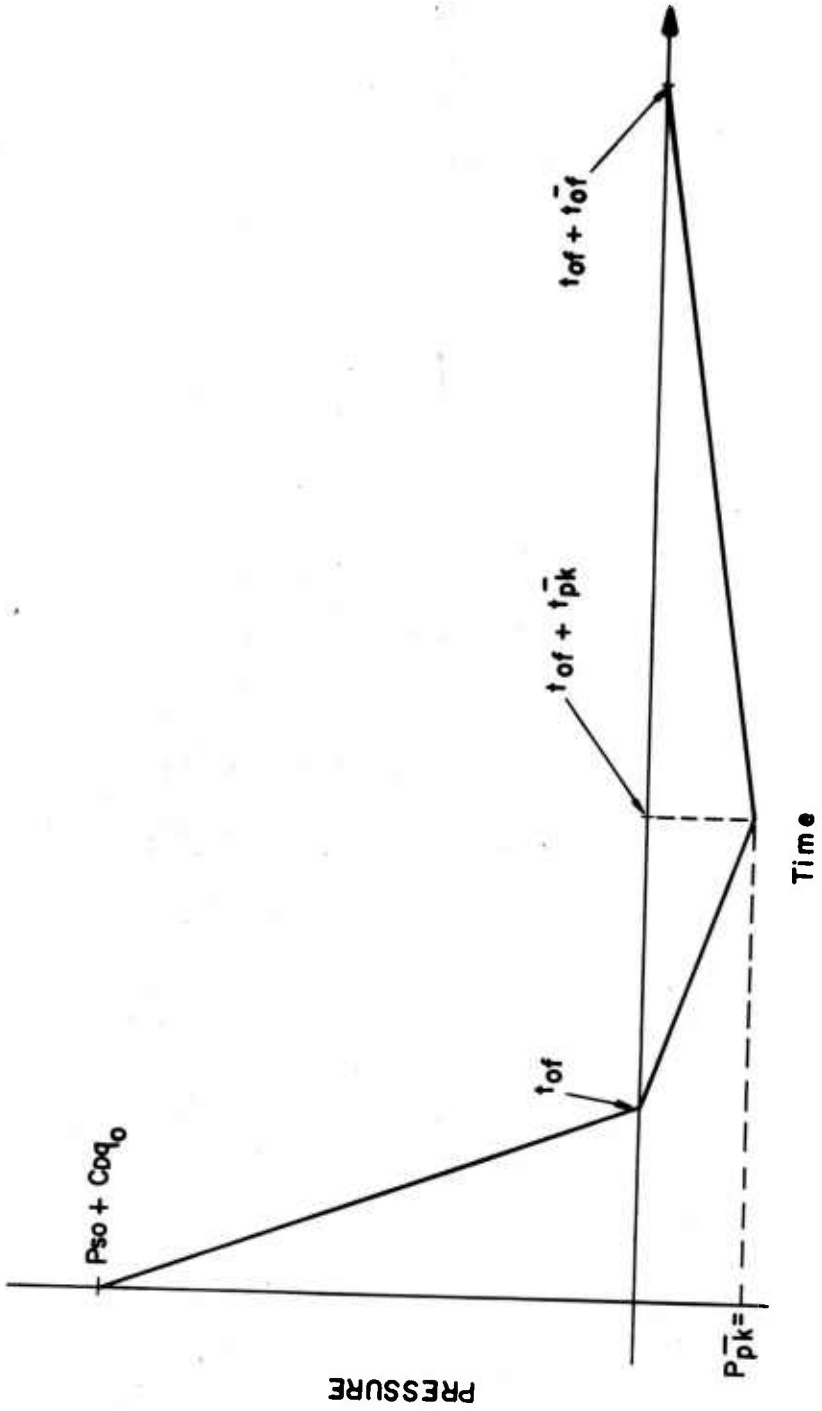

Figure A-2. LOADING ON BLASTWARD END OF ROOF.

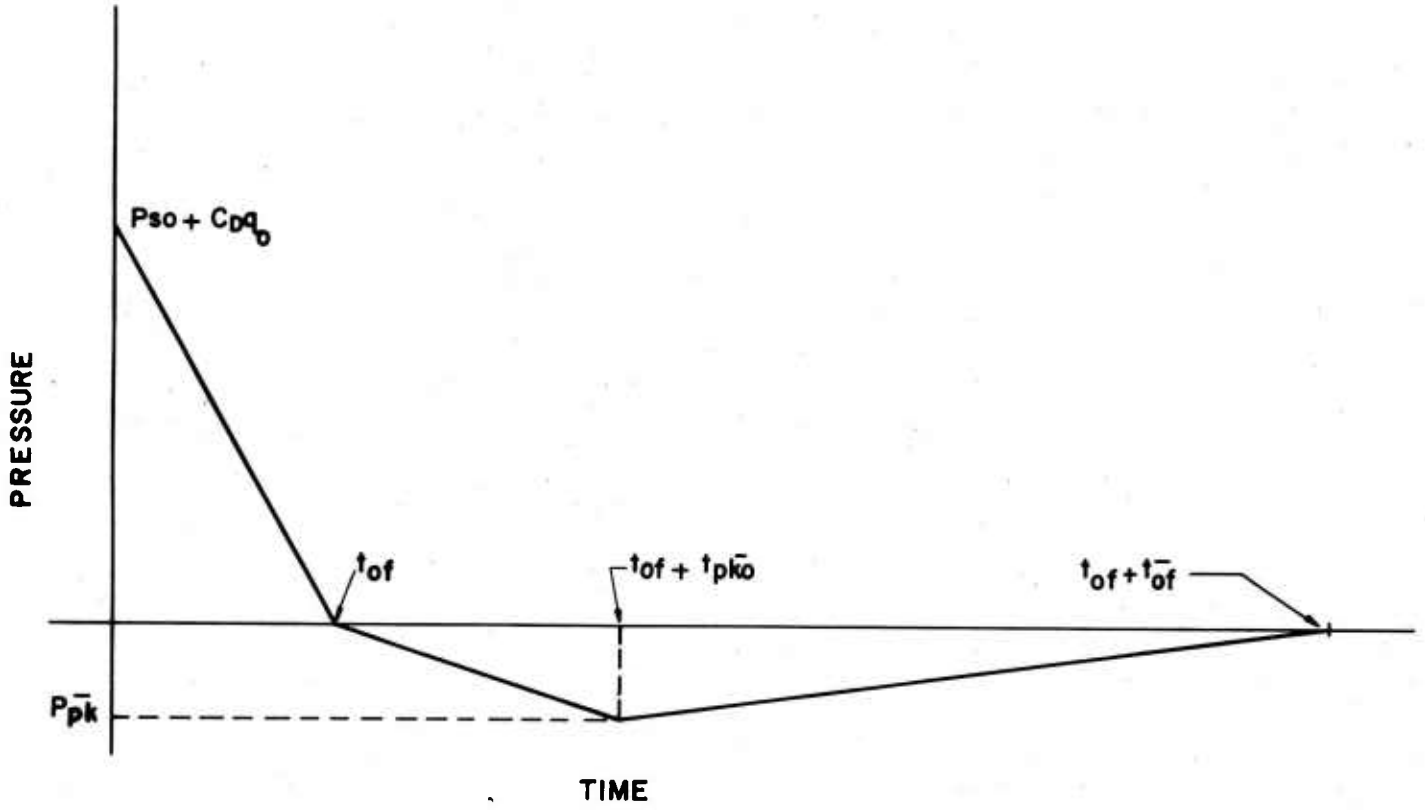

Figure A-3. LOADING ON LEEWARD END OF ROOF.

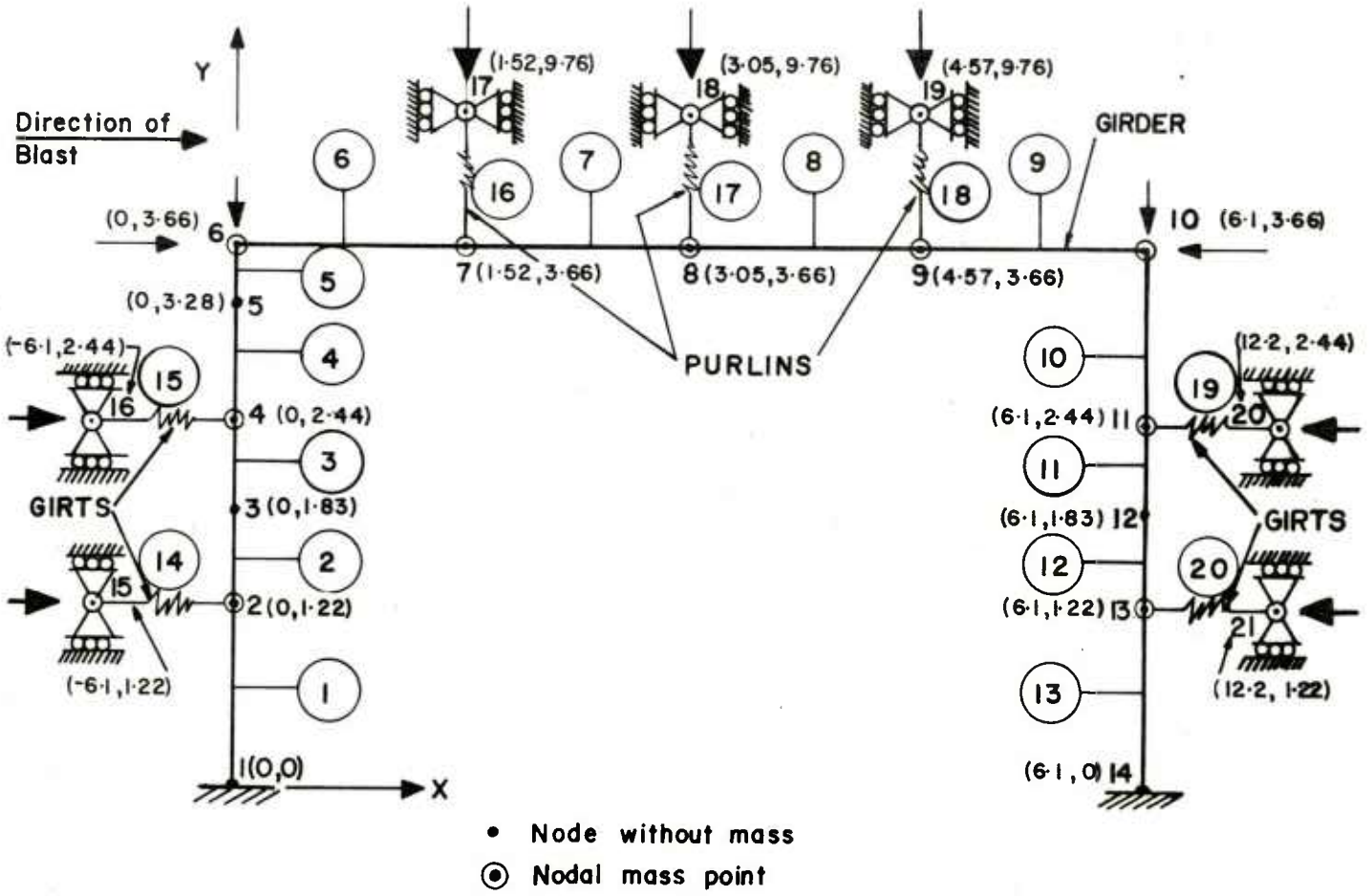

Figure A·4 MODIFIED FRAME MODEL

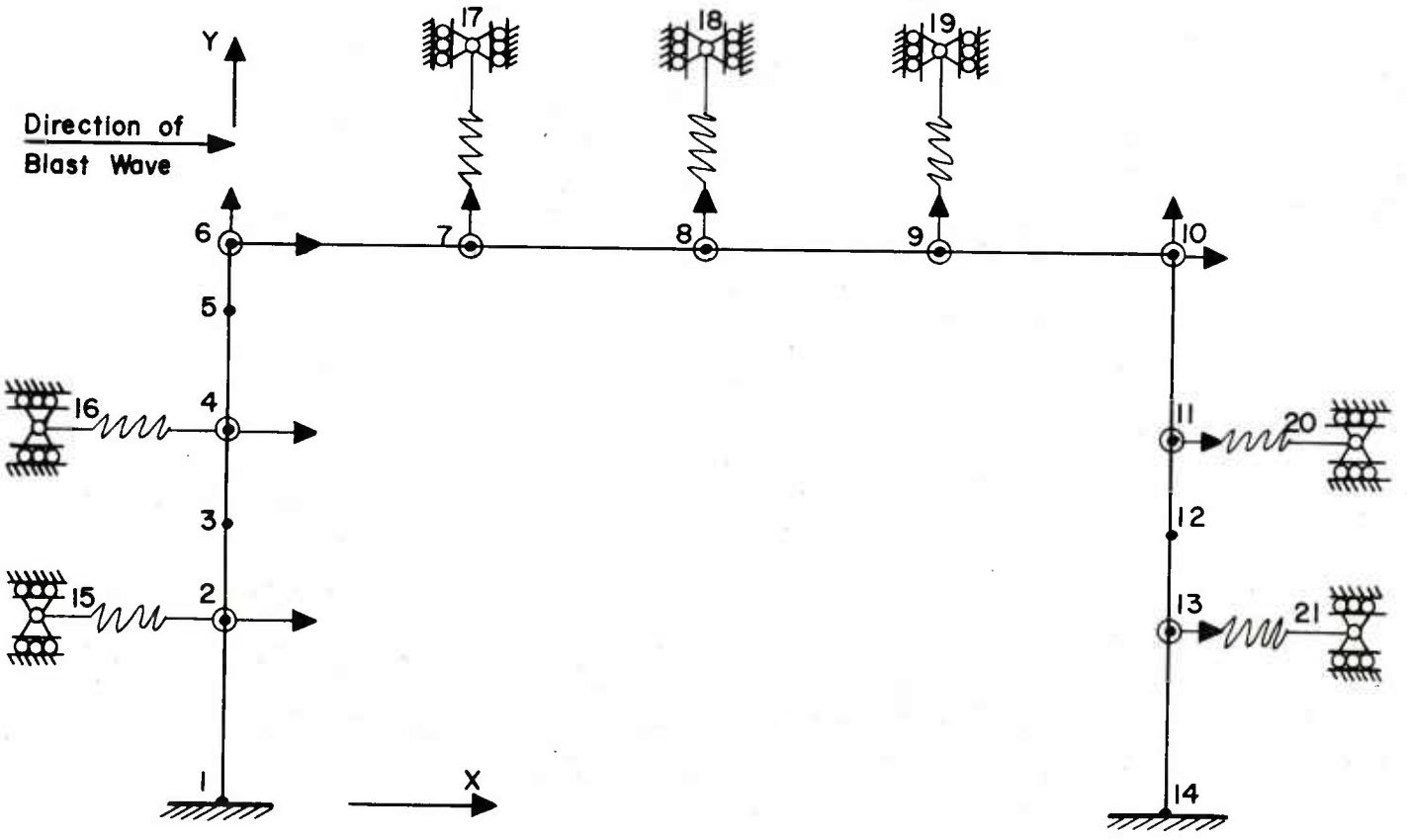

Figure A·5. DYNAMIC DEGREES OF FREEDOM OF MODEL.

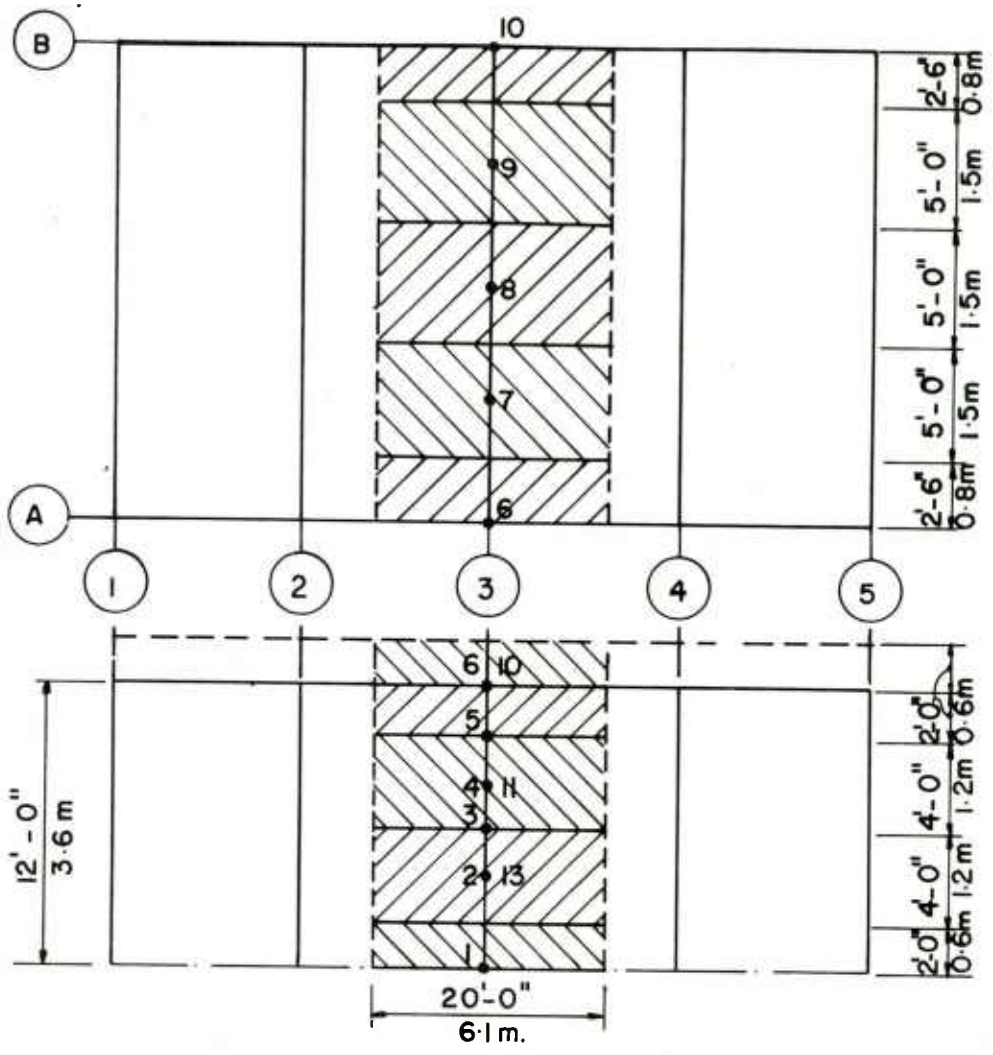

Figure A·6. TRIBUTARY AREAS.

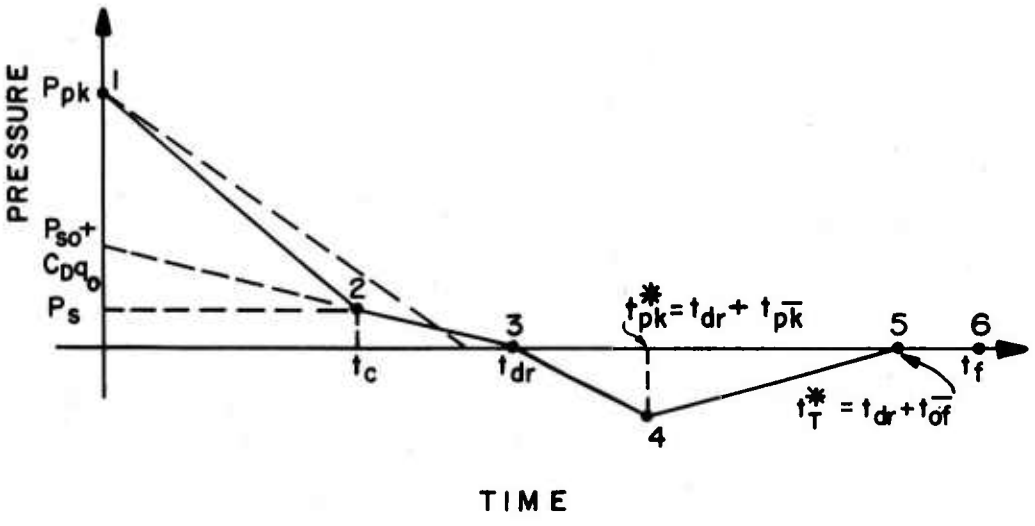

Figure A-7. TYPICAL PRESSURE WAVEFORM FOR BLASTWARD WALL.

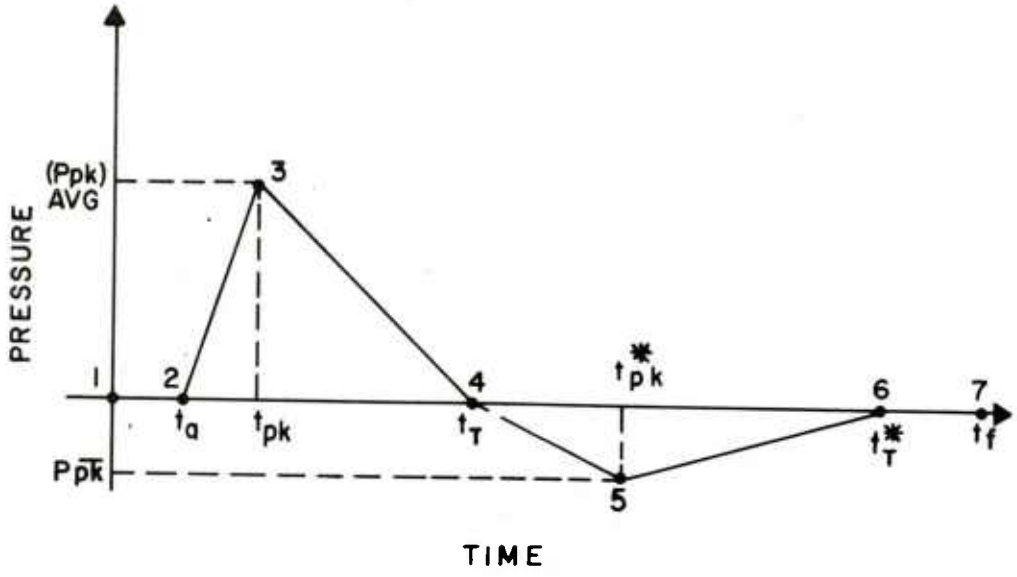

a. TYPICAL PRESSURE WAVEFORM FOR ROOF AND LEEWARD WALL.

b. DIGITIZED PRESSURE TIME DATA.

POINT	PRESSURE	TIME
1	0·0	0·0
2	0·0	t_a
3	(Ppk) AVG.	t_{pk}
4	0·0	t_T
5	$P\bar{pk}$	t^*_{pk}
6	0·0	t^*_T
7	0·0	t_f

FIGURE A·8. DIGITIZED PRESSURE-TIME DATA FOR PRESSURE WAVEFORM WITH LINEAR DECAY.

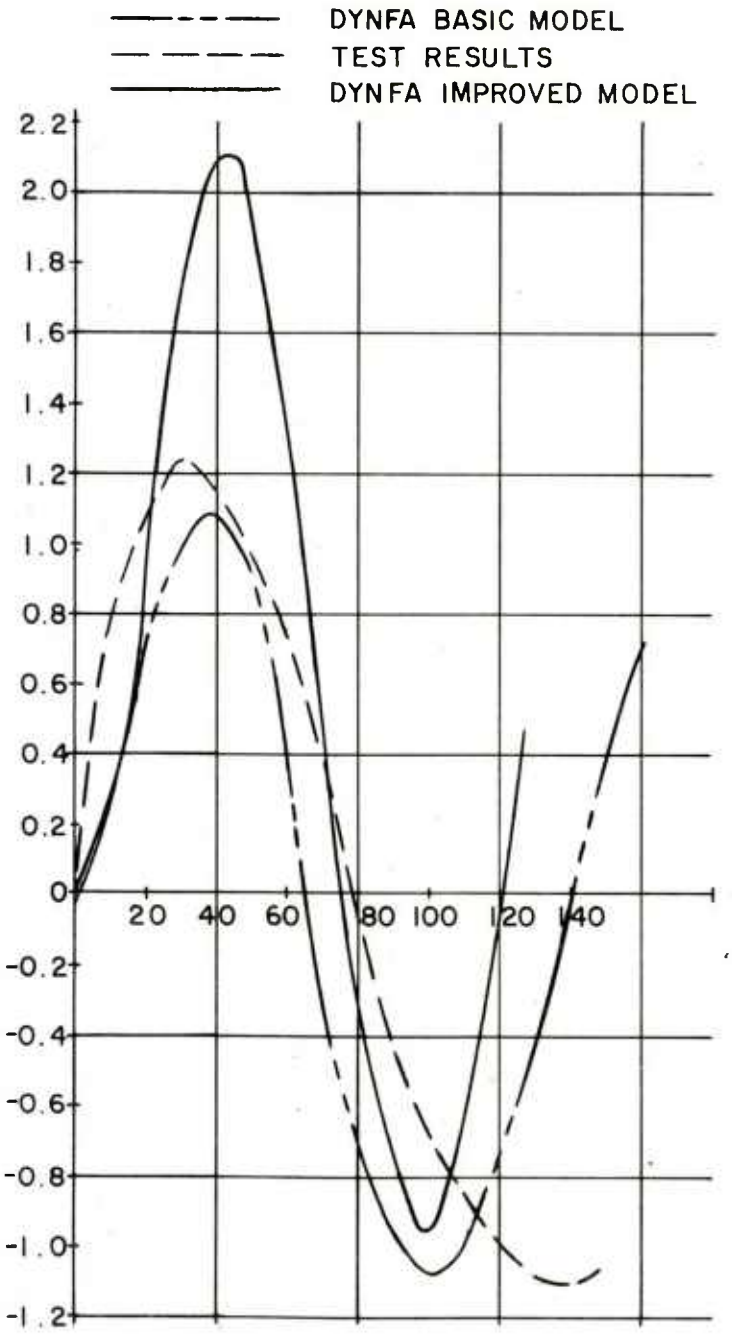

FIGURE A-9. SIDESWAY DISPLACEMENT OF CENTER FRAME

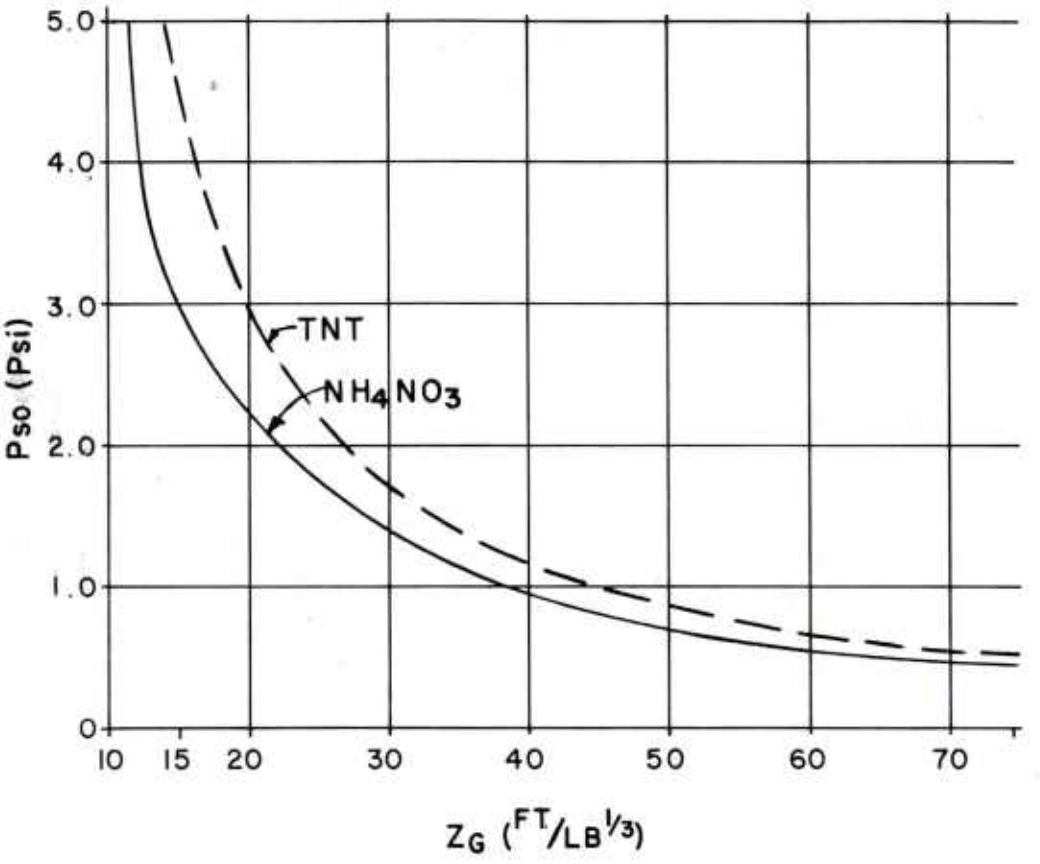

FIGURE A-10. INCIDENT OVERPRESSURE VERSUS SCALED DISTANCE

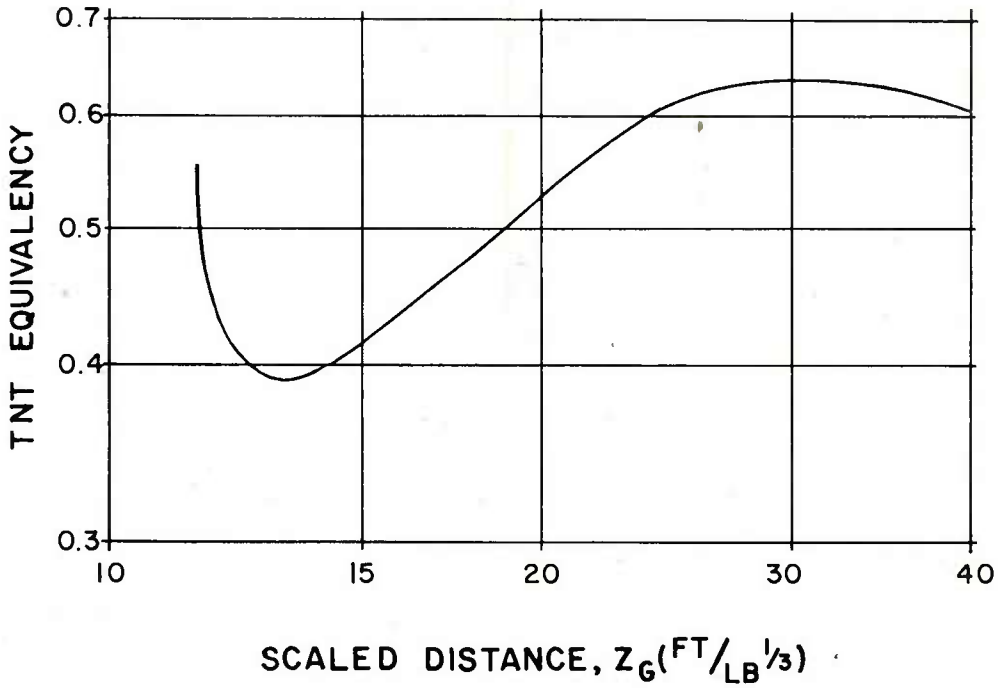

FIGURE A-11. TNT EQUIVALENCY VERSUS SCALED DISTANCE FOR NITRO-CARBO-NITRATE.

APPENDIX B. ENGINEERING DRAWINGS

The following pages contain reduced-size copies of the Engineering Drawings prepared for the construction of the test structure and support framework for the instrumentation used in the dynamic tests. Certain revisions have been made to the drawings but, unfortunately, these are not included in the reduced-size copies.

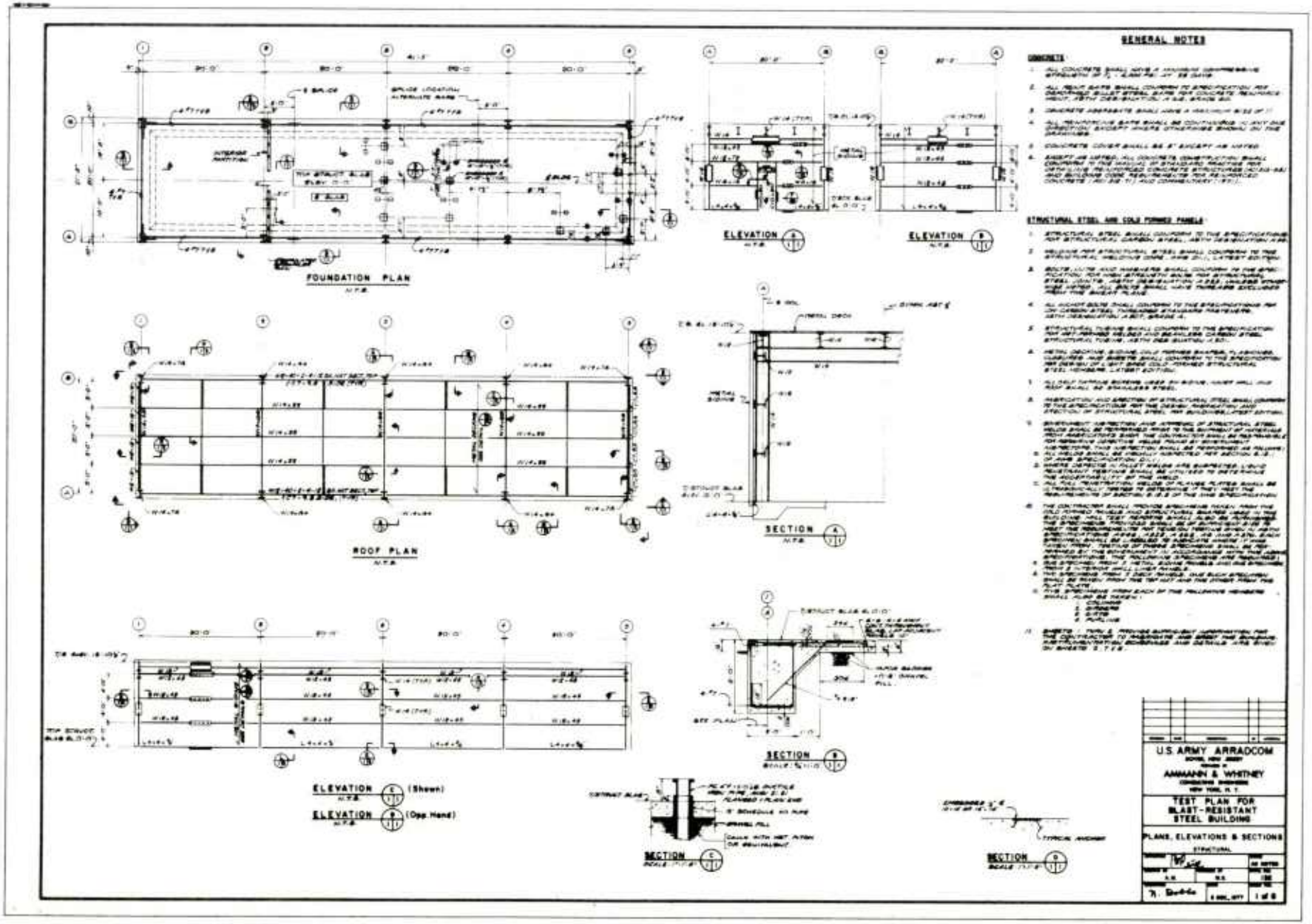
GENERAL NOTES
FOUNDATION PLAN
ROOF PLAN
ELEVATION
ELEVATION
SECTION
SECTION
SECTION
SECTION
ELEVATION (Shown)
ELEVATION (Opp. Hand)
U.S. ARMY ARRADCOM
AMMANN & WHITNEY
TEST PLAN FOR BLAST-RESISTANT STEEL BUILDING
PLANS, ELEVATIONS & SECTIONS
STRUCTURAL

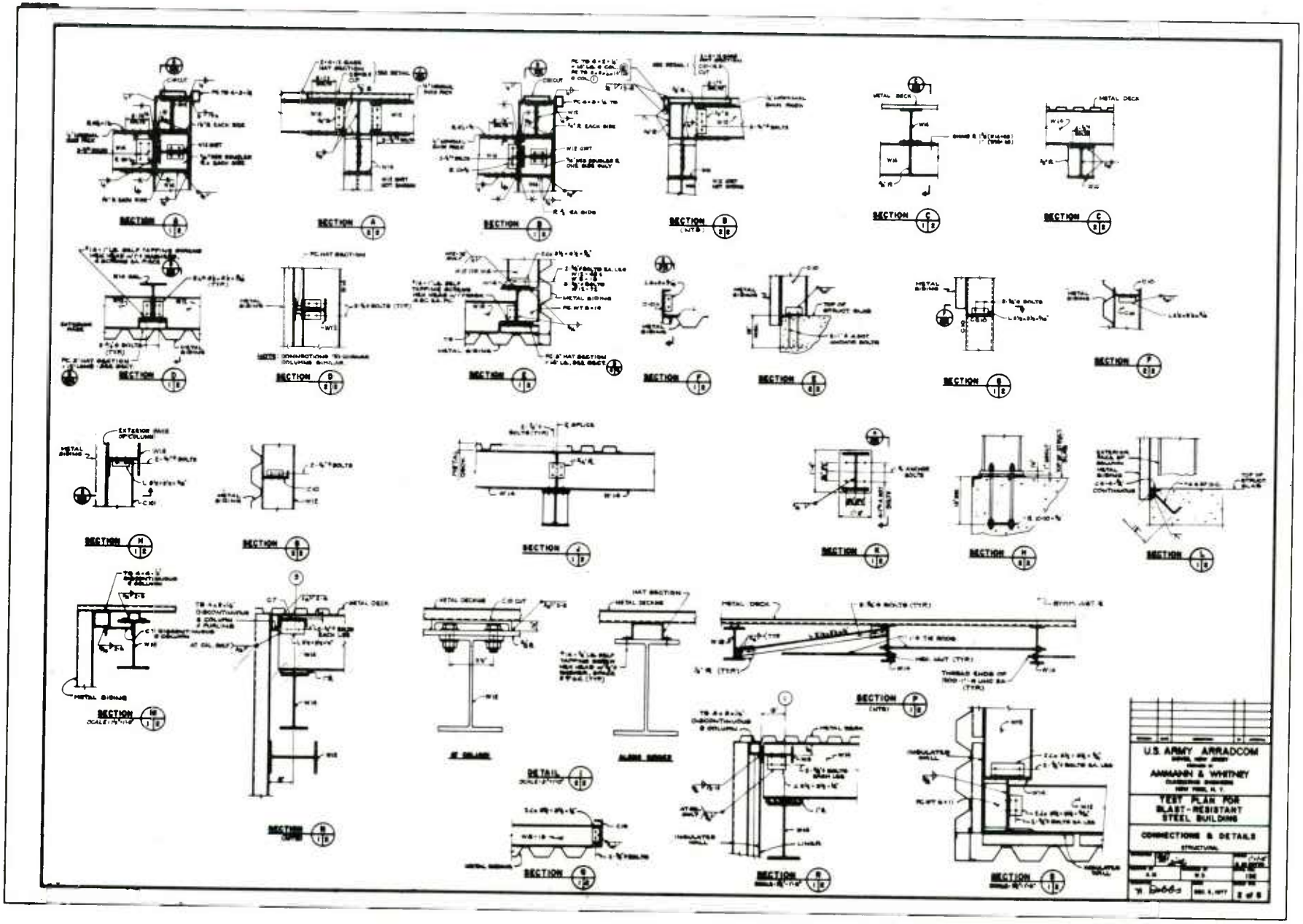
U.S. ARMY ARRADCOM
AMMANN & WHITNEY
YEBT PLAN FOR
BLAST-RESISTANT
STEEL BUILDING
CONNECTIONS & DETAILS
STRUCTURAL

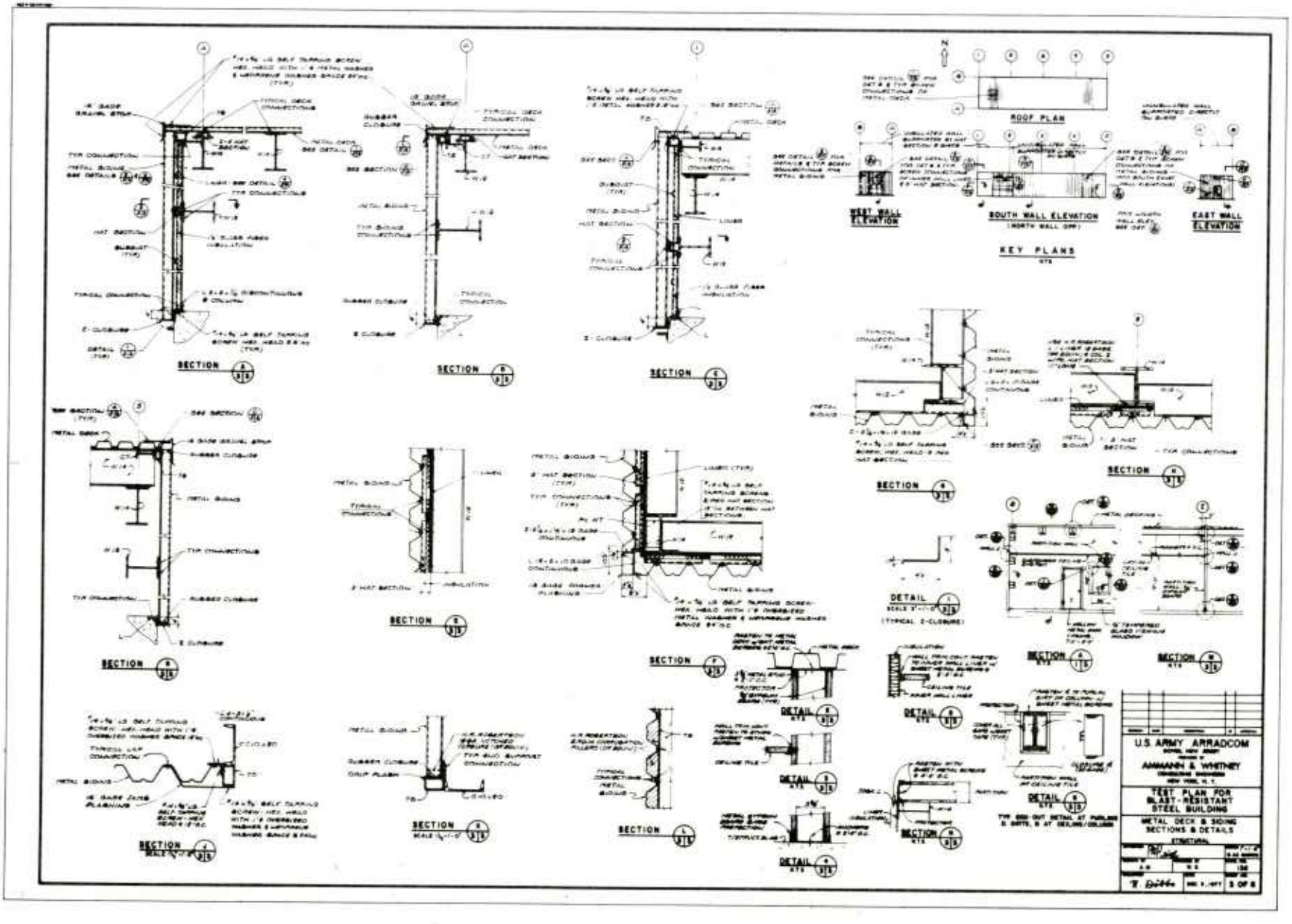
ROOF PLAN
WEST WALL ELEVATION
SOUTH WALL ELEVATION
EAST WALL ELEVATION
KEY PLANS
SECTION
DETAIL
U.S. ARMY ARRADCOM
AMMANN & WHITNEY
TEST PLAN FOR BLAST-RESISTANT STEEL BUILDING
METAL DECK & SIDING SECTIONS & DETAILS
STRUCTURAL

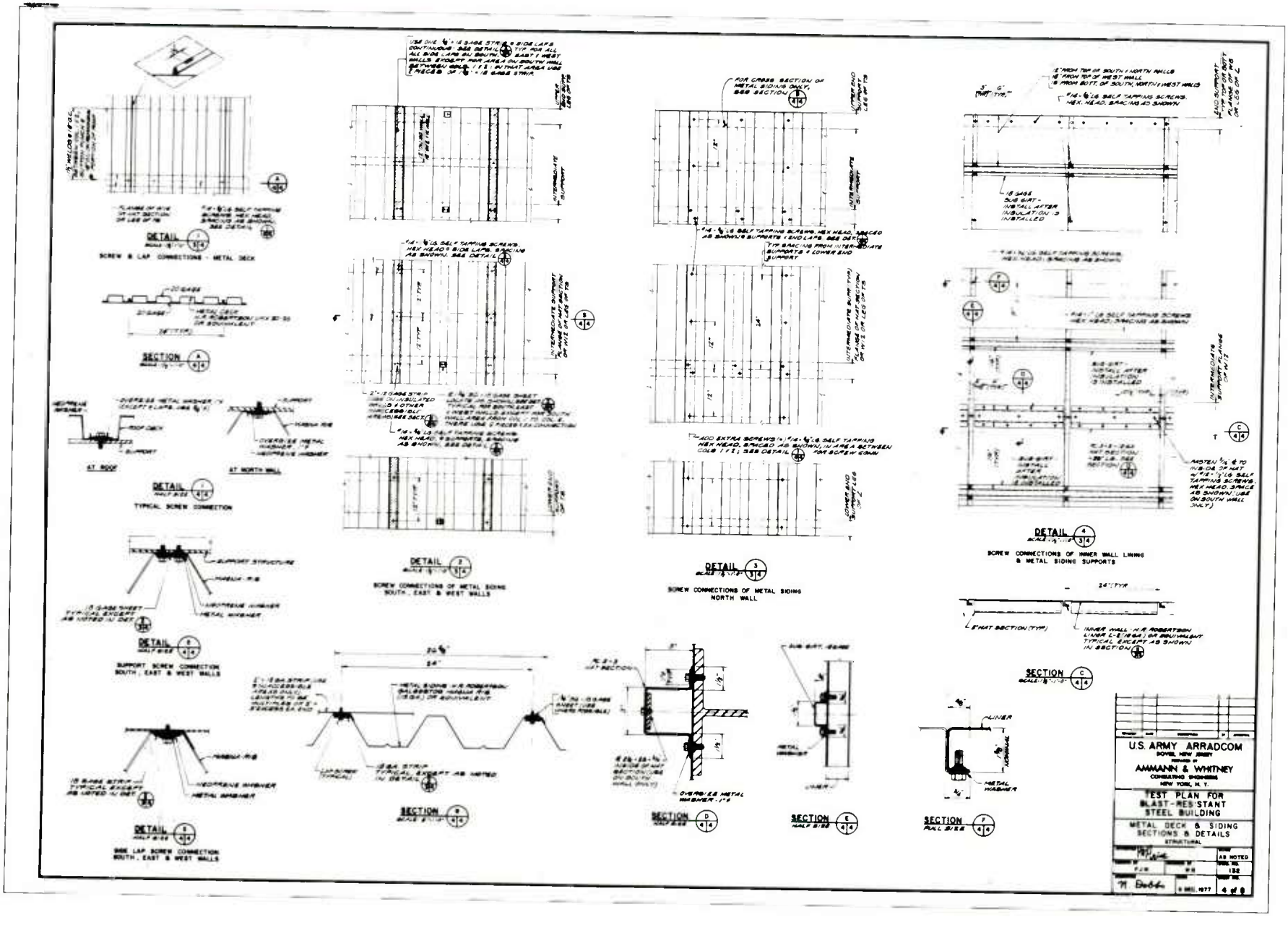
DETAIL
SCREW & LAP CONNECTIONS - METAL DECK
SECTION
DETAIL
TYPICAL SCREW CONNECTION
AT ROOF
AT NORTH WALL
DETAIL
SUPPORT SCREW CONNECTION SOUTH, EAST & WEST WALLS
DETAIL
BASE LAP SCREW CONNECTION SOUTH, EAST & WEST WALLS
DETAIL
SCREW CONNECTIONS OF METAL SIDING SOUTH, EAST & WEST WALLS
DETAIL
SCREW CONNECTIONS OF METAL SIDING NORTH WALL
DETAIL
SCREW CONNECTIONS OF INNER WALL LINING & METAL SIDING SUPPORTS
SECTION
SECTION
SECTION
SECTION
SECTION
U.S. ARMY ARRADCOM
DOVER, NEW JERSEY
PREPARED BY
AMMANN & WHITNEY
CONSULTING ENGINEERS
NEW YORK, N. Y.
TEST PLAN FOR BLAST-RESISTANT STEEL BUILDING
METAL DECK & SIDING SECTIONS & DETAILS
STRUCTURAL
AS NOTED
182
4 of 8

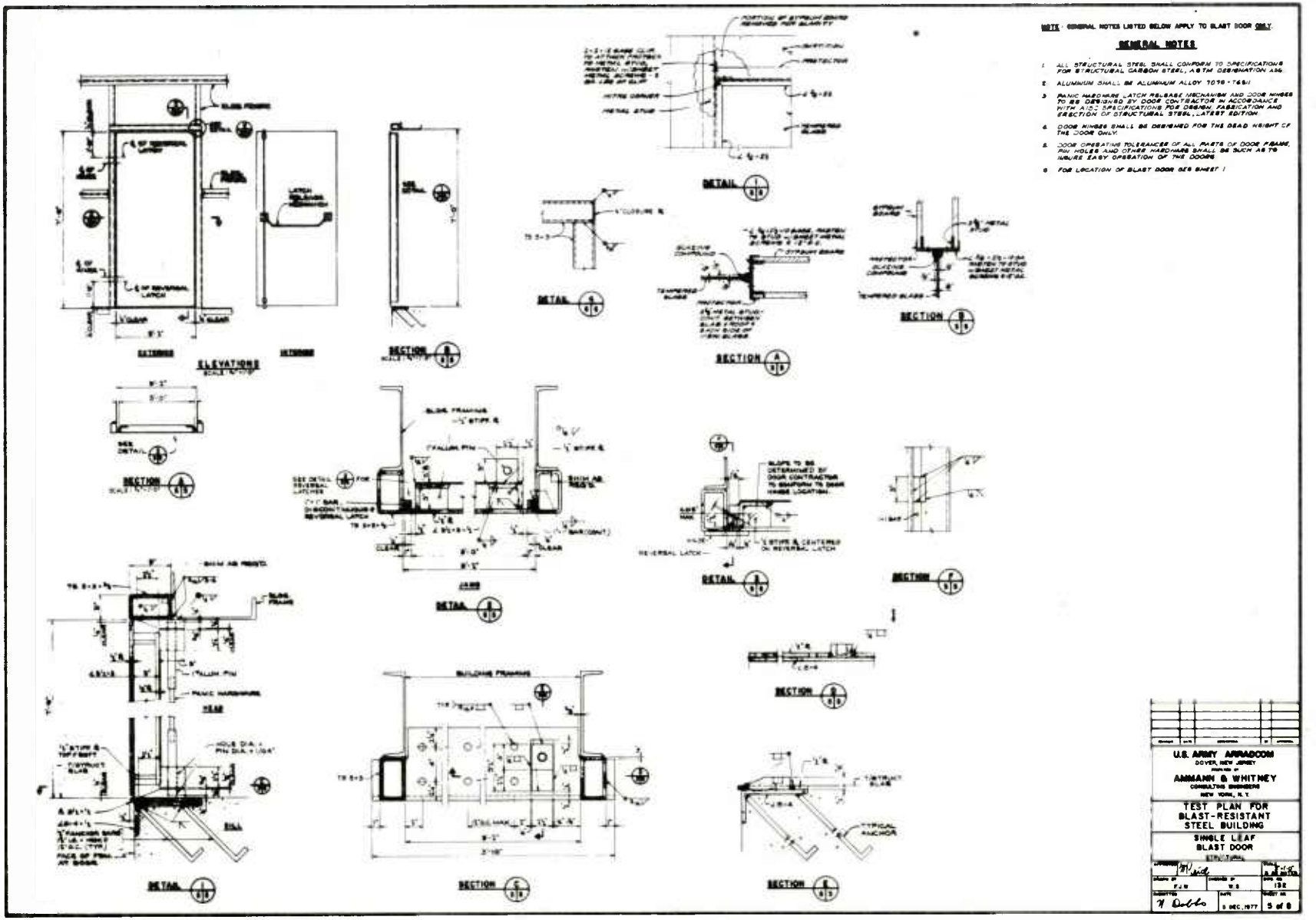
NOTE : GENERAL NOTES LISTED BELOW APPLY TO BLAST DOOR ONLY.
GENERAL NOTES
1. ALL STRUCTURAL STEEL SHALL CONFORM TO SPECIFICATIONS FOR STRUCTURAL CARBON STEEL, ASTM DESIGNATION A36.
2. ALUMINUM SHALL BE ALUMINUM ALLOY 7079 - T6&51
3. PANIC HARDWARE LATCH RELEASE MECHANISM AND DOOR HINGES TO BE DESIGNED BY DOOR CONTRACTOR IN ACCORDANCE WITH A.I.S.C. SPECIFICATIONS FOR DESIGN, FABRICATION AND ERECTION OF STRUCTURAL STEEL, LATEST EDITION.
4. DOOR HINGES SHALL BE DESIGNED FOR THE DEAD WEIGHT OF THE DOOR ONLY.
5. DOOR OPERATING TOLERANCES OF ALL PARTS OF DOOR FRAME, PIN HOLES AND OTHER HARDWARE SHALL BE SUCH AS TO INSURE EASY OPERATION OF THE DOORS.
6. FOR LOCATION OF BLAST DOOR SEE SHEET 1
ELEVATIONS
SECTION
DETAIL
SECTION
DETAIL
SECTION
SECTION
DETAIL
DETAIL
SECTION
SECTION
DETAIL
SECTION
SECTION
U.S. ARMY ARRADCOM
DOVER, NEW JERSEY
AMMANN & WHITNEY
CONSULTING ENGINEERS
NEW YORK, N.Y.
TEST PLAN FOR BLAST-RESISTANT STEEL BUILDING
SINGLE LEAF BLAST DOOR
DRAWN BY F.J.H
DESIGNED BY W.S
DATE 5 DEC. 1977
SHEET NO. 9 of 9

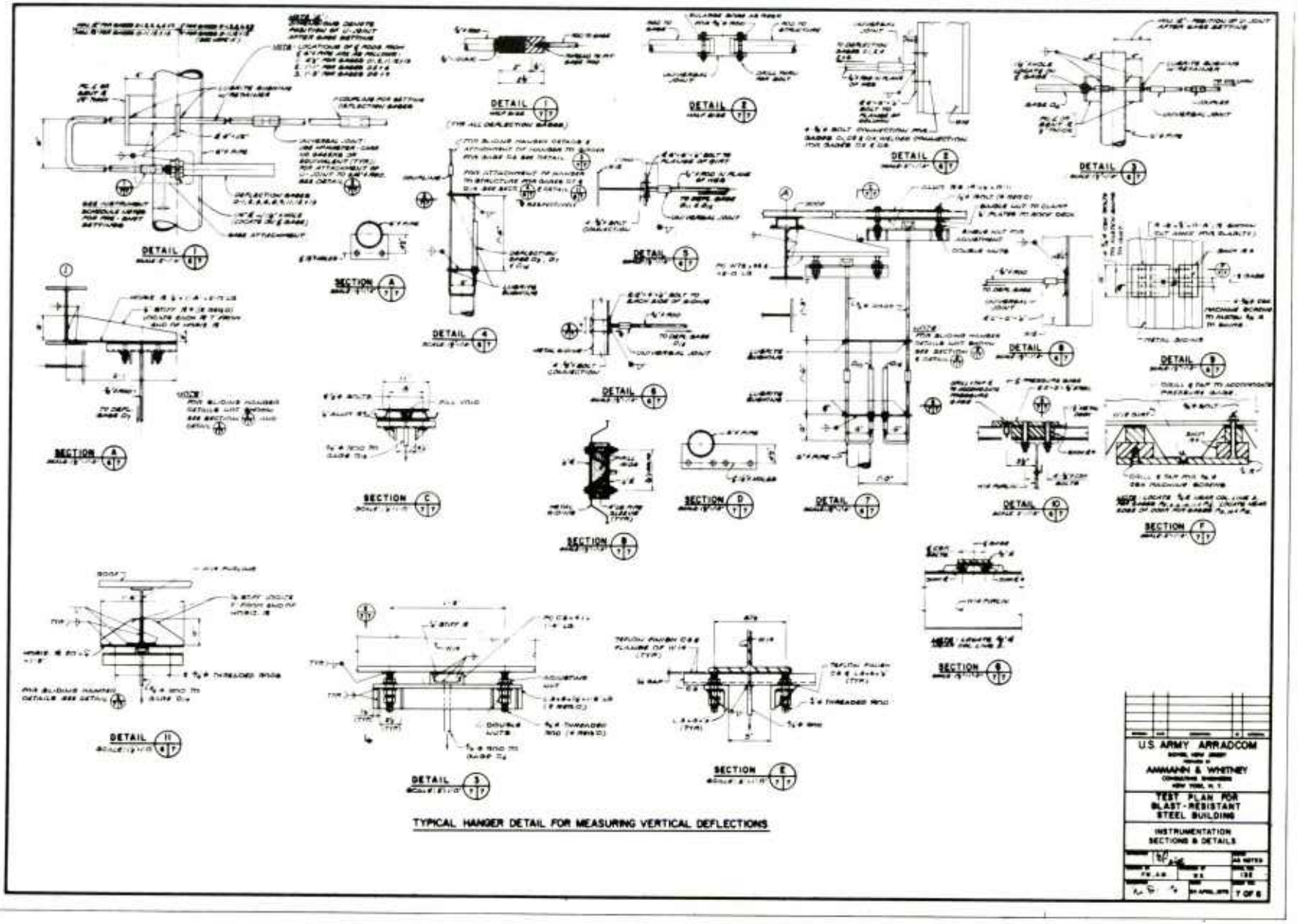

TYPICAL HANGER DETAIL FOR MEASURING VERTICAL DEFLECTIONS

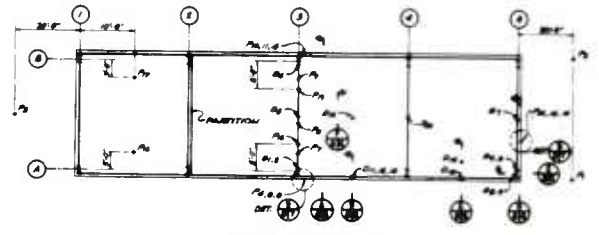

GAGE LOCATION PLAN

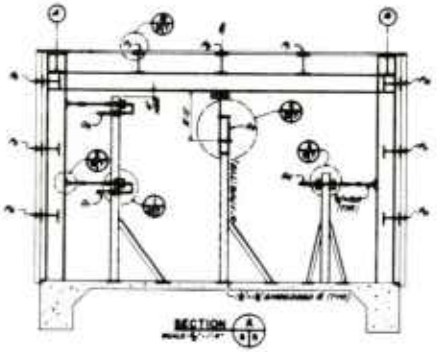

SECTION A

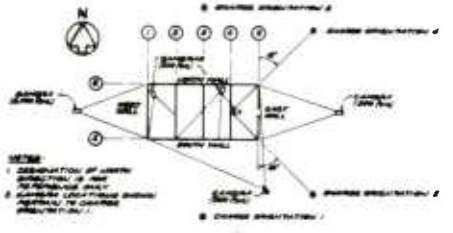

SITE PLAN

INSTRUMENT SCHEDULE

GAGE NO.	TYPE	MEASUREMENT DESCRIPTION	REFLECTED FACE LOCATION REL. LINE	REL. HEIGHT	REMARKS
$P_{1,2,3}$	PRESSURE	FREE FIELD	-	-	
P_{4}		SOUTH WALL (REFLECTED)	S-A	4'-0"	
P_{5}		"	"	8'-0"	
P_{6}		"	"	12'-0"	
P_{7}		ROOF	S	16'-0"	
P_{8}		"	"	"	
P_{9}		"	"	"	
P_{10}		NORTH WALL	S-B	4'-0"	
P_{11}		"	"	8'-0"	
P_{12}		"	"	12'-0"	
P_{13}		EAST WALL	A/B-S	4'-0"	
P_{14}		"	"	8'-0"	
P_{15}		"	"	11'-6"	
P_{16}		INTERIOR	SEE PLAN	7'-0"	SIMILAR TO FREE FIELD GAGES
P_{17}		"	"	"	"
P_{18}		"	"	"	"
P_{19}		"	"	"	"
P_{20}	PRESSURE	"	4	"	"
D_{1}	DEFLECTION	FRAME (N-S DIRECTION)	S-A	6'-0"	10" GAGE
D_{2}		" "	"	10'-9"	"
D_{3}		" (VERT. DIRECTION)	S	11'-6"	6" GAGE
D_{4}		" (N-S DIRECTION)	S-B	6'-0"	10" GAGE
D_{5}		" "	S-A	6'-0"	"
D_{6}		" "	"	9'-9"	"
D_{7}		" (VERT. DIRECTION)	S	11'-6"	6" GAGE
D_{8}		" (E/W DIRECTION)	A-B	6'-0"	10" GAGE
D_{9}		" "	A-B	11'-6"	"
D_{10}		" (VERT. DIRECTION)	A-B/S	16'-7"	6" GAGE
D_{11}		GIRT (N-S DIRECTION)	A-B/S	6'-0"	15" GAGE
D_{12}		"	"	4'-0"	"
D_{13}		DOOR (N-S DIRECTION)	"	6'-0"	"
D_{14}		PURLIN (VERT. DIRECTION)	A/B	15'-7"	10" GAGE
D_{15}	DEFLECTION	ROOF DECK	A-B/S	15'-10½"	10" GAGE

INSTRUMENT SCHEDULE NOTES

1. DESIGNATIONS OF WALLS (N, S, ETC.) & DIRECTIONS ARE EXPLAINED IN SITE PLAN
2. DESIGNATION OF SOUTH WALL (REFLECTED) PRESSURE PERTAINS TO CHARGE ORIENTATION 1 SHOWN IN SITE PLAN.
3. TO ACCOMODATE REBOUND, DEFLECTION GAGES SHALL BE SET AT THE FOLLOWING PRE-SHOT OVERPLACEMENTS:
   - 6" GAGE - 2" SETTING
   - 10" GAGE - 3" SETTING
   - 15" GAGE - 4" SETTING

TEST SCHEDULE

TEST NO.	CHARGE W.E.(lbs)	PRESSURE (psi)	CHARGE ORIENTATION (REFER TO SITE PLAN)	REMARKS
1	2 000	0.80	ORIENTATION 1	
2	"	1.80	"	
3	"	3.0	"	
4	"	TBD	"	
5	"	3.0	ORIENTATION 2	
6	"	TBD	"	
7	"	3.0	ORIENTATION 3	
8	2 000	TBD	ORIENTATION 4	

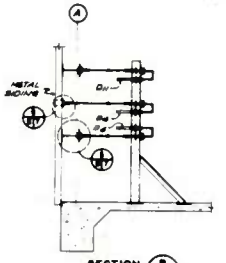

SECTION B

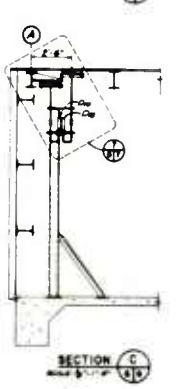

SECTION C

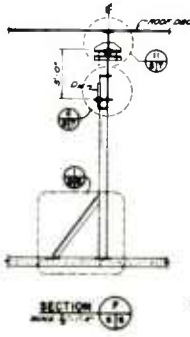

SECTION F

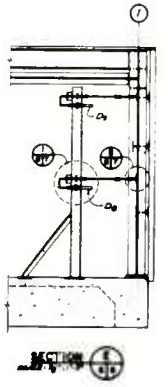

SECTION E

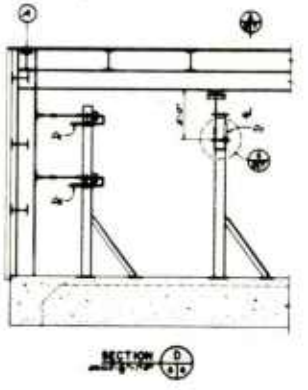

SECTION D

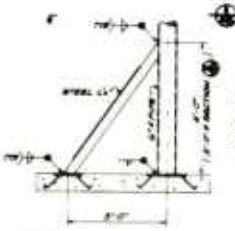

DETAIL

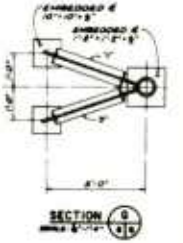

SECTION G

U.S. ARMY ARRADCOM

AMMANN & WHITNEY

TEST PLAN FOR BLAST-RESISTANT STEEL BUILDING

INSTRUMENTATION PLANS & SECTIONS

DISTRIBUTION LIST

Commander
U. S. Army Armament Research and Development Command
ATTN: DRDAR-CG
DRDAR-LCM-M
DRDAR-LCM-SP (25)
DRDAR-SF
DRDAR-TSS (5)
DRDAR-GCL
Dover, NJ 07801

Chairman
Department of Defense Explosive Safety Board (2)
Hoffman Building, No. 1, Room 856C
2461 Eisenhower Avenue
Alexandria, VA 22331

Administrator
Defense Documentation Center
ATTN: Accessions Division (12)
Cameron Station
Alexandria, VA 22314

Commander
Department of the Army
Office, Chief Research Development & Acquisition
ATTN: DAMA-CSM-P
Washington, DC 20310

Office, Chief of Engineers
ATTN: DAEN-MCZ
Washington, DC 20314

Commander
U. S. Army Materiel Development & Readiness Command
ATTN: DRCSF
DRCDE
DRCRP
DRCIS
5001 Eisenhower Avenue
Alexandria, VA 22333

Commander
DARCOM Installations and Services Agency
ATTN: DRCIS-RI
Rock Island, IL 61299

Director
Industrial Base Engineering Activity
ATTN: DRXIB-MT
DRXIB-EN
Rock Island, IL 61299

Commander
U. S. Army Munitions Production Base
Modernization Agency
ATTN: SARPM-PBM
SARPM-PBM-S
SARPM-PBM-L (2)
SARPM-PBM-E
Dover, NJ 07801

Commander
U. S. Army Armament Materiel Readiness Command
ATTN: DRSAR-SF
DRSAR-SC (3)
DRSAR-EN
DRSAR-PPI
DRSAR-PPI-C
DRSAR-RD
DRSAR-IS
DRSAR-ASF
DRSAR-LEP-L
Rock Island, IL 61299

Director
DARCOM Field Safety Activity
ATTN: DRXOS-ES
Charlestown, IN 47111

Commander
U. S. Army Engineer Division
ATTN: HNDED
P. O. Box 1600, West Station
Huntsville, AL 35809

Commander
Radford Army Ammunition Plant
Radford, VA 24141

Commander
Badger Army Ammunition Plant
Baraboo, WI 53913

Commander
Indiana Army Ammunition Plant
Charlestown, IN 47111

Commander
Holston Army Ammunition Plant
Kingsport, TN 37660

Commander
Lone Star Army Ammunition Plant
Texarkana, TX 75501

Commander
Milan Army Ammunition Plant
Milan, TN 38358

Commander
Iowa Army Ammunition Plant
Middletown, IA 52638

Commander
Joliet Army Ammunition Plant
Joliet, IL 60436

Commander
Longhorn Army Ammunition Plant
Marshall, TX 75670

Commander
Louisiana Army Ammunition Plant
Shreveport, LA 71130

Commander
Cornhusker Army Ammunition Plant
Grand Island, NE 68801

Commander
Ravenna Army Ammunition Plant
Ravenna, OH 44266

Commander
Newport Army Ammunition Plant
Newport, IN 47966

Commander
Volunteer Army Ammunition Plant
Chattanooga, TN 37401

Commander
Kansas Army Ammunition Plant
Parsons, KS 67357

District Engineer
U. S. Army Engineering District, Mobile
Corps of Engineers
P. O. Box 2288
Mobile, AL 36628

District Engineer
U. S. Army Engineer District, Ft. Worth
Corps of Engineers
P.O. Box 17300
Fort Worth, TX 76102

District Engineer
U. S. Army Engineering District, Omaha
Corps of Engineers
6014 U.S.P.O. and Courthouse
215 North 17th Street
Omaha, NE 78102

District Engineer
U. S. Army Engineering District, Baltimore
Corps of Engineers
P. O. Box 1715
Baltimore, MD 21203

District Engineer
U. S. Army Engineering District, Norfolk
Corps of Engineers
803 Front Street
Norfolk, VA 23510

Division Engineer
U. S. Army Engineering District, Huntsville
P. O. Box 1600, West Station
Huntsville, AL 35807

Commander
Naval Ordnance Station
Indian Head, MD 20640

Commander
U. S. Army Construction Engineering Research Laboratory
Champaign, IL 61820

Commander
Dugway Proving Ground
Dugway, UT 84022

Commander
Savanna Army Depot
Savanna, IL 61704

Civil Engineering Laboratory
Naval Construction Battalion Center
ATTN: L51
Port Hueneme, CA 93043

Commander
Naval Facilities Engineering Command
200 Stovall Street
(Code 04, J. Tyrell)
Alexandria, VA 22322

Commander
Southern Division
Navel Facilities Engineering Command
ATTN: J. Watts
P. O. Box 10068
Charleston, SC 29411

Commander
Western Division
Naval Facilities Engineering Command
ATTN: W. Moore
San Bruno, CA 94066

Officer in Charge
TRIDENT
Washington, DC 20362

Officer in Charge of Construction
TRIDENT
Bangor, WA 98348

Commander
Atlantic Division
Naval Facilities Engineering Command
Norfolk, VA 23511

Commander
Naval Ammunition Depot
Naval Ammunition Production Engineering Center
Crane, IN 47522

Director
U. S. Army TRADOC Systems Analysis Activity
ATTN: ATAA-SL
White Sands Missile Range, NM 88002

Commander/Director
Chemical Systems Laboratory
U.S. Army Armament Research and Development Command
ATTN: DRDAR-CLJ-L
DRDAR-CLB-PA
Aberdeen Proving Ground, MD 21005

Director
Ballistics Research Laboratory
U.S. Army Armament Research and Development Command
ATTN: DRDAR-TSB-S
Aberdeen Proving Ground, MD 21005

Chief
Benet Weapons Laboratory, LCWSL
U.S. Army Armament Research and Development Command
ATTN: DRDAR-LCB-TL
Watervliet, NY 12189

Ammann & Whitney
Consulting Engineers
Two World Trade Center
ATTN: N. Dobbs (5)
New York, NY 10048

Director
U.S. Army Materiel Systems Analysis Activity
ATTN: DRXSY-MP
Aberdeen Proving Ground, MD 21005